AN INVESTIGATION OF MOLECULAR PATHWAYS TO AID IN THERAPEUTIC DEVELOPMENT FOR NEUROFIBROMATOSIS TYPE 2

Eric Thomas Hawley

Submitted to the faculty of the University Graduate School
in partial fulfillment of the requirements
for the degree
Doctor of Philosophy
in the Department of Biochemistry and Molecular Biology,
Indiana University

May 2019

Accepted by the Graduate Faculty of Indiana University, in partial fulfillment of the requirements for the degree of Doctor of Philosophy.

Doctoral Committee

_____
D. Wade Clapp, M.D., Chair

_____
Mark G. Goebl, Ph.D.

January 23, 2019

_____
Maureen A. Harrington, Ph.D.

_____
Raghu G. Mirmira, M.D.,Ph.D.

DEDICATION

To my family who have provided me with love and encouragement through this training process.

ACKNOWLEDGEMENT

I would like to acknowledge Dr. D. Wade Clapp, M.D., who as my advisor provided me with the support and flexibility to pursue the projects I found most interesting and has been incredibly influential in my development as a future physician scientist. Dr. Clapp went above and beyond the traditional role as a Ph.D. advisor to help build the MSTP at Indiana University and to insure I got the best possible training. Dr. Clapp serves a role model for how to build a successful career as both a clinician and scientist.

I would like to acknowledge and thank members of the Clapp laboratory and in particular Dr. Su-Jung Park for support and training over the past four years. Su-Jung spent significant time teaching me many of the laboratory techniques utilized in this work and provided essential intellectual input in helping to shape these projects and trouble shoot failed experiments. Much of the work presented here would not have been possible without her support.

Conducting experimental therapeutics and preclinical drug trials in mice requires and incredible amount of work and the therapeutic data presented was a team effort that I would not be able to collect had it not been for the work of Waylan Bessler, Xiaohong Li, Li Jang, Qingbo Lu, Abbi Smith, and Bill Dyer along with guidance from the IU Clinical Pharmacology Analytical Core.

I would also like to acknowledge the current and previous graduate, medical, and MSTP students Jeffery Gehlhausen, Julie Mund, Donna Edwards, Benjamin Wahle, and

Ciersten Burks for their support in the lab as well as my MSTP cohort for their friendship and support throughout this process.

Finally I would l would like to acknowledge the IU Simon Cancer Center, the NIH National Institute of Deafness and Communication Disorders, and the Department of Defense NFRP for funding this work.

Some of the text and figures in this dissertation were originally published in the journals Oncotarget and Human Molecular Genetics and are listed as citations 62 and 111.

Eric Thomas Hawley

AN INVESTIGATION OF MOLECULAR PATHWAYS TO AID IN THERAPEUTIC DEVELOPMENT FOR NEUROFIBROMATOSIS TYPE 2

Neurofibromatosis type 2 (NF2) is an autosomal dominant cancer predisposition in which loss of heterozygosity at the *NF2* gene locus leads to the development of tumors of neural crest derived origin, most commonly bilateral vestibular schwannomas. There are currently no FDA approved chemotherapeutic agents for treatment in patients with NF2. Development of therapeutic agents has been hampered by our incomplete knowledge of how Merlin, the protein product of the *NF2* gene, functions as a tumor suppressor. In order develop a deeper understanding for how loss of Merlin leads to oncogenic transformation in Schwann cells we have developed a genetically engineered mouse model (GEMM) of Neurofibromatosis Type 2 in which functional expression of Merlin is lost in Schwann cell precursors. In parallel studies utilizing these mice, we have sought to understand the pathophysiology driving tumor formation in Merlin deficient Schwann cells.

In Chapter 1, we explore the role of Merlin as a negative regulator of the Group A p21 activated kinases, PAK1 and PAK2. We demonstrate that PAK1, a previously well established oncogene in solid tumors and Merlin binding partner, is hyperactivated in Merlin deficient schwannomas. Through therapeutic interventions and genetic manipulations we demonstrate that inhibition of PAK1 was capable of reducing tumor formation and alleviating sensorineural hearing loss in our NF2 GEMM.

In Chapter 2, we investigate the role of NF-κB inducing kinase (NIK) and NF-κB signaling in the formation and growth of Merlin deficient Schwann cell tumors. Prior

work in our lab as well as by others demonstrated elevated NF-κB signaling in Merlin deficient Schwann cell tumors. We observed accumulation of a catalytically active fragment of NF-κB inducing kinase and present data that accumulation of a 55Kd constitutively active fragment of NIK is sufficient trigger wild type Schwann cells to form tumors. *In vivo* however, Schwann cell intrinsic expression of NIK is not required for tumor formation or growth.

D. Wade Clapp, M.D., Chair

TABLE OF CONTENTS

LIST OF FIGURES

LIST OF ABBREVIATIONS

1-ABT	1-aminobenzotriazole
AAALAC	Association for Assessment and Accreditation of Laboratory Animal Care International
ABR	Auditory brainstem response
AIED	Autoimmune inner ear disease
Akt	Protein kinase B
ANOVA	Analysis of variance
BCL	B-cell lymphoma
CD44	Cluster of differentiation 44
Cdc42	Cell division cycle 42
CDK	Cyclin dependent kinase
c-DKO	Conditional double knockout
cKO	Conditional knockout
CN	Cranial nerve
CNS	Central nervous system
COX	Cyclooxygenase
Cre	Causes recombination
CYP	Cytochrome p450 oxidase
DMEM	Dulbecco's modified eagle media
DRG	Dorsal root ganglion
EGFR	Epidermal growth factor receptor
eGFP	Enhanced green fluorescent protein
Erk	Extracellular signal related kinase
ERM	Ezrin Radixin Moesin
FAK	Focal adhesion kinase
FDA	Food and Drug Administration
FERM	4.1 Ezrin Radixin Moesin
GAPDH	Glyceraldehyde 3-phosphate dehydrogenase
gDNA	Genomic deoxyribonucleic acid
GEMM	Genetically engineered mouse model
GGF	Glial growth factor
H&E	Hematoxylin and Eosin
Het	Heterozygous
HIF1	Hypoxia-inducible factor

HIV-HAART	Human immunodeficiency virus highly active antiretroviral therapy
HPV	Human papilloma virus
IACUC	Institutional Animal Care and Use Committee
IC_{50}	Concentration of 50% inhibition
ICAM	Intercellular adhesion molecule
IHC	Immunohistochemistry
IκB	Inhibitor of κB
IKK	Inhibitor of κB kinase
IL-1β	Interleukin-1-beta
IL-1Rα	Interleukin 1 receptor alpha
ILK	Integrin linked protein kinase
IP	Intraperitoneal
IUSM	Indiana University School of Medicine
JNK	c-Jun N-terminal kinase
kD	Kilodalton
kg	Kilogram
K_i	Concentration of ½ V_{max}
LPS	Lipopolysaccharide
MALT	Mucosa-associated lymphoid tissue
MAPK	Mitogen activated protein kinase
Mek	Mitogen-activated protein kinase
mg	Milligram
μM	Micromolar
MMP	Matrix metalloproteinase
MPNST	Malignant peripheral nerve sheath tumor
mRNA	Messenger ribonucleic acid
MST	Mammalian Ste20-like kinases
mTOR	Mammalian target of rapamycin
NEMO	NF-κB essential modulator
NF2	Neurofibromatosis type 2
Nf2-cKO	$Nf2^{flox/flox}$; *Postn*-Cre
Nf2-cKO;*NIK*-Het	$Nf2^{flox/flox}$;$NIK^{flox/+}$;*Postn*-Cre
Nf2;*NIK*-cDKO	$Nf2^{flox/flox}$;$NIK^{flox/flox}$;*Postn*-Cre
NF-κB	Nuclear factor kappa-light-chain-enhancer of activated B cells
NGF	Neural growth factor
NIDCD	National Institute of Deafness and Communication Disorders

NIK	NF-κB inducing kinase
nM	Nanomolar
NOMID	Neonatal-onset multisystem inflammatory disease
p38	p38 mitogen activated protein kinase
PAK	Group A p21 activated kinase
PD	Pharmacodynamics
PDL	Poly-D-lysine
Pen/Strep	Penicillin/Streptomycin
PI3K	Phosphatidylinositol-4,5-bisphosphate 3-kinase
PK	Pharmacokinetics
Plk	Polio like kinase
Postn	Periostin
qd	Daily
Rac1	Ras related C3 botulinum toxin substrate 1
Raf	Rapidly activated fibrosacroma
RB	Retinoblastoma
RNA	Ribonucleic acid
RTK	Receptor tyrosine kinase
Rx	Treatment
S6K	Ribosomal protein S6 kinase beta-1
SEM	Standard error of the mean
shRNA	Small hairpin ribonucleic acid
TNFα	Tumor necrosis factor alpha
USA	United States of America
VEGF	Vascular endothelial growth factor
VS	Vestibular schwannoma
Wnt	Wingless/integrated

THE ROLE OF GROUP A p21 ACTIVATED KINASES IN NEUROFIBROMATOSIS TYPE 2

Introduction

Neurofibromatosis Type 2

Neurofibromatosis Type 2 (NF2) is an autosomal dominant cancer predisposition syndrome which has an incidence of 1/25,000-1/40,000 depending on the population studied [1,2]. Patients with NF2 are born with a single functional copy of the *NF2* gene. Subsequent sporadic loss of heterozygosity in these patients leads to the development of tumors of neural crest derived origin, most commonly bilateral vestibular schwannomas which occur in 90-95% if NF2 patients [1]. These lesions are named as such because they are Schwann cell predominant tumors which grow out of the eighth cranial nerve (CNVIII), also known as the vestibular cochlear nerve. Although generally benign in nature, these tumors are often highly morbid due to their proximity to the CNS and their propensity to grow and compress vital structures. Along with the vestibular schwannomas, 18-58% of patients develop intracranial meningiomas, 29-90% develop spinal schwannomas, 32-67% develop dermal schwannomas, and 2.5-6% develop ependymomas depending on the particular patient population studied [3-6]. In addition to the morbidities associated with the development of solid tumors, the majority of NF2 patients suffer from decreased visual acuity with up to 80% developing cataracts. The most common presenting symptom for NF2 patients is unilateral sensorineural hearing loss [7].

NF2 was first described in 1822 by the J.H. Wishart, a surgeon in Scotland [8]. Even though NF2 is a genetic disease, diagnosis is not based upon patient genotype but instead relies upon the Manchester Criteria which defines NF2 as either the presence of bilateral vestibular or a family history of NF2 along with a unilateral vestibular schwannoma or any two of the following: meningioma, glioma, neurofibroma, schwannoma, or posterior subcapsular lenticular opacities [7]. Biallelic disruption of the *NF2* gene is not limited to tumors in familial NF2 patients. Loss of heterozygosity of *NF2* has been observed in 56% of sporadic vestibular schwannomas (sVS) [9] and 18% of sporadic spinal schwannomas [10]. With more than 3300 vestibular schwannomas diagnosed per year in the USA, there is a significant demand for treatment of *NF2* deficient VS beyond patients diagnosed with NF2 [11]. There are currently no approved chemotherapeutics approved for the treatment of NF2 or *NF2* deficient sporadic tumors. Tumors are treated either via radioablation or surgical resection. Radioablative therapy has yielded mixed success in patients likely because there is no single accepted standard of care. Multiple different approaches including fractional conventional radiotherapy, fractionated stereotactic radiotherapy, stereotactic radiosurgery, and proton therapy have been used by different groups at different institutions. Observational studies for each approach have demonstrated significant variability in achieving local tumor control and hearing preservation without triggering significant facial or trigeminal neuropathy [12]. Surgical resection of these tumors is possible in certain cases but can be limited by their proximity to the central nervous system and their propensity to reoccur and grow into vital structures.

Molecular Biology of *NF2*/Merlin

NF2 is a tumor suppressor gene located on chromosome 22q12 and was named as such when mutations in that locus were discovered to be causative of NF2 [13-15]. *NF2* is a member of the Band FERM (**f**our point 1 protein, **e**zrin, **r**adixin, **m**oesin) gene family and encodes the protein Merlin (**m**oesin-**e**zrin-**r**adixin **l**ike prote**in**). Merlin exists in two isoforms, both of which are 595 amino acids and encoded by 17 exons. Isoform I predominates and includes exons 1-15, and 17 while isoform II in encoded by exons 1-16 [16]. The two isoforms are functionally redundant in their tumor suppressive functions [17-18]. Merlin consists of an N-terminal FERM domain, an α helical coiled coil domain, and a C-terminal hydrophilic tail. Unlike other ERM proteins, the C-terminal domain in Merlin lacks an actin binding site and instead Merlin interacts with actin via N-terminal residues 178-367 [19]. Like other ERM proteins, Merlin acts as a protein scaffold, linking various cell surface receptors and intracellular kinases to the actin cytoskeleton, controlling their cellular localization and function [20]. The cellular localization and activation state of Merlin is controlled via post translational modifications, primarily via phosphorylation. Serine 518 has been the most studied phosphorylation site on Merlin where unphosporylated Merlin appears to adopt a conformational structure necessary for its tumor suppressive function while phosphorylation at S518 blocks Merlin tumor suppressive activity [21,22].

One of the first known functions of Merlin was as a mediator of contact inhibition via directly binding to and suppressing the activity of CD44 and PAK1 [23,24]. Merlin co-localizes with the cytoplasmic tail of CD44 at the cell membrane and inhibits CD44 signaling by preventing activation of Rac1 by CD44 [24]. The interaction between Merlin

and CD44 controlling cell contact inhibition can be dynamically controlled via binding to the Group A p21 activated kinases, PAK1**.** Under normal proliferative conditions, PAK1 interaction with Rac1/Cdc42 leads to PAK1 autophosphorylation, activation, and downstream pro-proliferative signaling [25]. Unphosphorylated Merlin can bind to PAK1 at a site which abrogates the PAK1-Rac1/Cdc42 interactions, preventing PAK1 activation. However, activated PAK1 can in turn phosphorylate Merlin at S518, preventing Merlin from interacting with CD44 thereby shutting off Merlin's tumor suppressive function [26]. Thus under conditions of contact inhibition, unphosphorylated Merlin acts to suppress the Rac1/Cdc42/PAK axis but in a growth permissive state, PAK1 can phosphorylate and inactive Merlin, allowing for activation of the Rac1/Cdc42/PAK signaling axis.

Loss of Merlin can cause alterations in cell signaling beyond the Rac1/Cdc42/PAK axis. In immunocomplexing experiments, Merlin has been shown to pull down in association with variety of cell surface receptors and internal signaling modulators known to play important roles in other cancers (**Figure 1)**. Because expression of many of these receptors and signaling molecules are cell type and context specific, the effects of loss of Merlin may also be cell type and context specific depending on the particular receptors on the cell and ligands in the environment. Upon loss of Merlin, dysregulation and hyperactivation of the EGFR superfamily, Wnt/beta-catenin, hippo, mTOR, NFκB, FAK/Src, and PI3K signaling pathways have all been observed in various different cell types upon loss of Merlin [27-32]. Secondary loss of Merlin connotes a poor prognosis in a variety of solid tumors including breast, colorectal,

and prostate cancer thus there is value in developing a comprehensive knowledge of how Merlin functions in a myriad of different cell types and environments [20].

In the context of NF2, patients are born with germline halpo-insufficiency at the *Nf2* locus and experience global, sporadic loss of heterozygosity across all cell lineages. Yet, the vast majority of tumors in these patients originate from Schwann cells or neural crest derived precursors and occur in predictable, anatomically well defined locations. Therefore, Merlin likely plays a more pivotal role as a tumor suppressor in certain Schwann cell populations or Schwann cell procurers in particular anatomical locations than it does globally in most other cell types. The overarching goal of this work is to advance translational research that will lead to improved therapeutics for NF2 patients and individuals with sporadic *NF2* deficient schwannomas and so the projects presented hereafter will focus on Schwann cells and the specific subset of pathways altered in after cell intrinsic loss of Merlin.

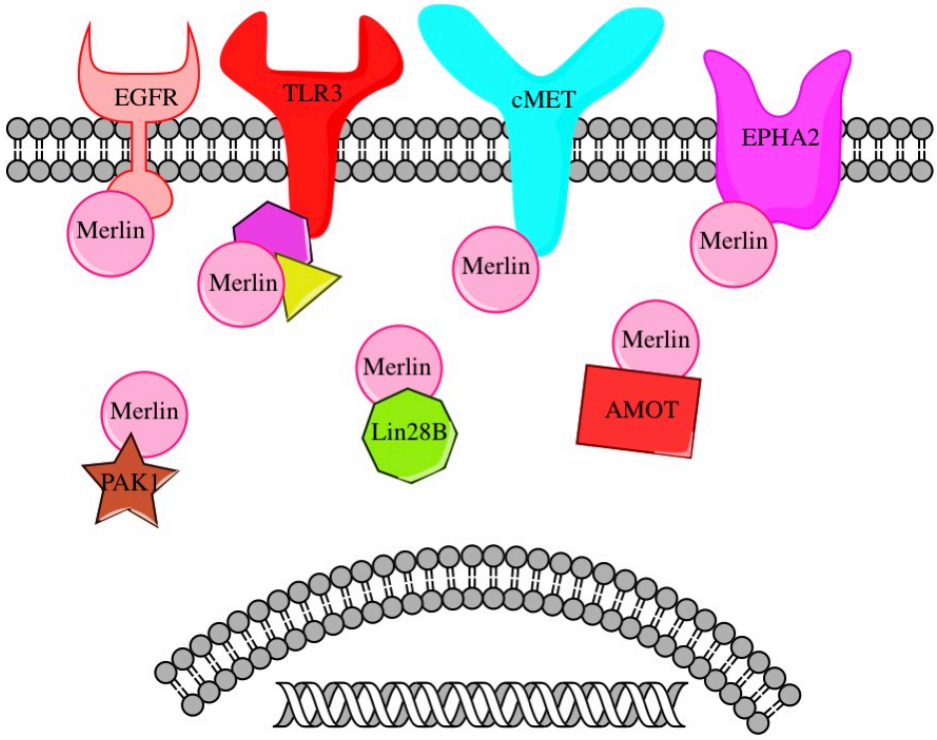

Figure 1. Putative Merlin Binding Partners.

Molecular Biology of the Group A p21 Activated Kinases

The group A p21 activated kinases (PAKs), also known as group I p21 activated kinases, consists of PAK1, PAK2, and PAK3. The PAKs are serine/threonine effector kinases of the Rac/Cdc42 GTPases [33,34]. PAK1 is 545 amino acids in length, PAK2 is 524 amino acids in length, and PAK3 is 544 amino acids in length. The three proteins share a similar structure with a N-terminal p21 binding/autoinhibitory domain and a C-terminal kinase domain [35]. *In vivo*, PAK1 forms homodimers in which the N-terminal autoinhibitory domains of two PAK1 molecules line up in trans and prevent auto phosphorylation and activation [36]. When activated by Rac1/Cdc42, the PAK1 monomers disassociate and autophosphorylation of threonine 423 and serine 144 occurs, leading to activation of downstream signaling [37]. PAK1 is broadly expressed and is detectable in most human tissues. PAK2 expression is more limited and most highly expressed in immune tissues while PAK3 expression is largely limited to the central nervous system, primary in the Purkinje cells in the cerebellum [38].

Of the group A PAKs, PAK1 is the best studied because of its prominent role as an oncogene in solid tumors. *Pak1* is commonly amplified in a variety of malignancies including brain, breast, lung, liver, kidney, bladder, and ovarian cancers [39]. In its role as a potent oncoprotein, PAK1 has been implicated as a gatekeeper kinase which can activate a variety of cellular pathways regulating cell-proliferation, evasion of apoptosis, and DNA damage repair [39-42]. Among its various substrates, PAK1 has been shown to phosphorylate: MEK1 at S298 and Raf-1 at S338 and S339 to activate the Mek/Raf/Erk pathway, ILK at T173 and S246 to activate Akt signaling, Plk1 at S49 to drive the G2/M transition, and Snail1/2 at S246 to activate Wnt/β-catenin signaling [43-46]. *Pak2* has

also more recently been recognized as an oncogene. PAK2 is highly expressed in more than half of lymphoma, colorectal, and ovarian cancers surveyed in the human protein atlas. High levels of *Pak2* expression were found to be a significant, clinically unfavorable prognostic marker in both pancreatic and prostate cancer [38]. Because Merlin has been shown to directly interact with PAK1 and PAK2, PAK1 and PAK2 are expressed in Schwann cells, and Merlin functions as a negative regulator of PAK1, we reasoned that tumor formation in Merlin deficient Schwann cells may be dependent on the loss of inhibition and subsequent constitutive activation of the Group A PAKs 1 or 2 [26, 47].

Schwannoma Biology

The majority of solid tumors which arise in NF2 patients appear to originate from precursor lesions consisting of disorganized overgrowths of Schwann cells often referred to as Schwann cell hyperplasia. Schwann cells are a glial, neural crest derived cell type. In normal, healthy adults, there are two types of mature Schwann cells. One variant of Schwann cells produces myelin and is responsible for wrapping around exons in the peripheral nervous system to aid in Saltatory conduction. They second type does not produce myelin and wraps unmyelinated axons in the peripheral nervous system into Remak bundles [48]. Mature Schwann cells do not replicate in their terminally differentiated state. When proliferation is required, as is the case after nerve injury, both mature Schwann cell types dedifferentiate into a repair or Bungner type Schwann cell. These repair Schwann cells appear to revert to a more primitive Schwann cell state wherein they lose some markers of terminal differentiation and regain their proliferative

potential and aid in axonal growth before re-differentiating into either mature myelinating or non myelinating Schwann cells once the nerve damage is repaired [49].

Multiple lines of evidence support the hypothesis that Schwann cell tumors develop from either repair type Schwann cells or Schwann cell precursors and not directly from mature Schwann cells. First, fully differentiated, mature Schwann cells have minimal if any proliferative potential. Tumors derived from cells with very limited or zero proliferative capacity such as neurons or cardiomyocytes are incredibly rare. Second, in immunohistochemistry studies in primary human vestibular nerve schwannomas as well as in our genetically engineered mouse model (GEMM), tumor forming Schwann cells display a significant reduction in markers of terminal differentiation cells such as myelin basic protein, protein zero glycoprotein, and S100. Additionally we have observed increased levels of stem cell transcription factors Krox 20 and Oct6 in these tumors. So at least by the time there is histologically significant schwannoma formation, the tumorigenic Schwann cells no longer exist in a terminally differentiated state [50]. Third, when Marco Giovannini generated a mouse in which *Nf2* was deleted in mature cells using the mature Schwann cell specific promoter P0, only a small percentage of mice developed Schwann cell tumors and those tumors did not form until very late in life [51]. However when the nerves of those same mice are damaged, they exhibit an aberrant repair process with excessive Schwann cell proliferation and failure to re-myelinate [52]. These data argue that loss of Merlin was not in itself sufficient to drive tumor formation in the mature Schwann cells. But upon a second hit, in this case nerve injury triggering dedifferentiation into repair Schwann cells, Merlin deficiency seems to drive increased and disorganized Schwann cell proliferation and

macrophage infiltration. This disrupted tissue architecture bears some similarity to the Schwann cell hyperplasia we observe in our NF2 GEMM. We know that in certain anatomical locations this hyperplasia does eventually progress into frank Schwannoma. Finally, in our GEMM of NF2, *Nf2* expression is lost in all Schwann cell precursors. These mice develop frank schwannoma with 100% penetrance by 8 months of age. Importantly, the Schwann cell tumors develop in very predictable and well defined anatomical locations. The overwhelming majority of Schwann cells never form tumors in spite of being Merlin deficient. This is consistent with NF2 patients who, despite often being globally *NF2* haploinsufficent, form Schwann cell tumors in predicable anatomical locations. Complete loss of Merlin in these patients is random and sporadic but tumor type and location is not. Loss of heterozygosity must not in itself be sufficient trigger oncogenic transformation in every mature Schwann cell. All of these data support the hypothesis that NF2 deficient schwannomas likely arise either from some yet to be defined, specific, susceptible sub population of Schwann cells or require a very specific microenvironment for growth. This tumor permissive context appears to be anatomically restricted. Identifying and modeling this specific population or cellular context would represent a major step forward in translational research for NF2.

NF2 Schwann Cell Specific *in vitro* and *in vivo* Models

One of the first major cell lines developed for *in vitro* modeling of NF2 was HEI-193. This cell line was generated by immortalizing with HPV E6 and E7, schwannoma cells from a 56 year old NF2 patient [53]. This cell line contains a G to A point mutation in intron 14 at the intron 14/exon 15 splice site. The mutation results in the skipping of

exon 15 and translation of a Merlin splice variant that is strongly hypomorphic compared to the two normal Merlin isoforms [54]. HEI-193 cells have provided significant insight into schwannoma biology. But because these cells were transformed with HPV E6 which inhibits p53 and HPV E7 which targets pRb, this line has in effect lost two major tumor suppressors which we have not observed to be lost in NF2 patients. Dual loss of p53/pRB can cause genomic instability and phenotypic drift in cell lines over time. In order to increase research reproducibility and develop reagents for biochemical assays which more accurately mimic the genetics observed in the formation of Merlin deficient schwannomas, multiple labs have now developed their own murine Merlin deficient Schwann cell lines.

The laboratories of Drs. Macro Giovannini, Cristina Fernandez-Valle, Wade Clapp, and Helen Morrison have all independently generated murine Merlin deficient Schwann cell lines for use in preclinical therapeutics. The Giovannini, Fernandez-Valle, and Morrison laboratories created their respective cell lines via the same general strategy whereby they isolated mature Schwann cells from the sciatic nerve of either *Nf2*$^{ko3/flox2}$ mice in the case of the Giovannini lab or *Nf2*$^{flox2/flox2}$ mice in the case of the Fernandez-Valle and Morrison labs and then induced biallelic loss of *Nf2* via adenoviral transduction with Cre-recombinase. The resultant cells were spontaneously transformed via serial passage. The cell line from the Clapp lab was generated via serial passage of schwannoma cells which were isolated from a spinal schwannoma that occurred in the dorsal root ganglia of one of our *Nf2*$^{flox2/flox2}$;*Periostin*-Cre animals. We believe the signaling within these cell lines, known as SC-4, MS01, MS02, and MS03 from the Giovannini, Fernandez-Valle, Clapp, and Morrison labs respectively, accurately reflect

the signaling of Merlin deficient Schwann cell tumors in NF2. In the Clapp lab we primarily use the MS02 cell line we generated because they were transformed *in vivo* without the need for adenoviral transduction. The SC-4 cells were generated using mice of a different background than the MS01-MS03 cells so for the purposes of reducing variability, the NF2 Synodos consortium chose to use the MS01-MS03 cell lines for an -omics level approach to advance pre-clinical therapeutics. A list of all the cell lines utilized in Chapter 1 and Chapter 2 can be found in the Materials and Methods section and more complete description of all the cells available through Synodos and how they were generated can be found in the primary publication describing the goals of the consortium [55].

The generation of the four cell lines described above represented a step forward in the field, allowing for improved 2D culture models for basic and translational schwannoma research. There are however limitations in using 2D monoculture to model NF2. Cancer cells often behave differently when grown in a homogenous monolayer than they do within the 3D tumor architecture and polycellular microenvironment *in vivo* [56]. We also have an incomplete understanding of how well these cell lines mimic the actual cell of origins in schwannomas. Therefore in order to fully understand the disease etiology and screen compounds for therapeutic potential in NF2, there was a great need for an *in vivo* model which could faithfully and reliably recapitulate the most important pathologies of NF2.

Attempts to generate an NF2 GEMM began with the creation of $Nf2^{-/-}$ mice by Andrea McClatchey and Tyler Jacks [57]. These mice die between E6.6-E7 due to a failure to progress into gastrulation. Follow up studies with $Nf2^{+/-}$ mice demonstrated that

germline heterozygosity of *Nf2* lead to an increased susceptibility for the development of malignant tumors late in life but that the malignancies observed in these mice were not consistent with the tumors that develop in NF2 patients [58]. Marco Giovannini provided a significant step forward with the creation of the *Nf2*$^{flox2/flox2}$ mice [51]. Mutations in exon 2 have been observed to cause disease both in germline NF2 patients and in sporadic schwannomas and meningiomas [51]. Mice were generated in which lox p sites were inserted flanking exon 2 of *Nf2* resulting in excision of exon 2 upon expression of Cre (**c**auses **re**combination) recombinase. Utilizing the P0 promoter to drive expression of Cre recombinase and subsequent deletion in *Nf2* in mature, myelinating Schwann cells, roughly ¼ of the resultant mice developed schwannoma after 10 months of age [51, 59]. Due to the relatively low tumor penetrance at a relatively advanced age, the Clapp lab wondered if a different driver of Cre recombinase could eliminate functional Merlin expression in a broader array of Schwann cell subtypes and push the NF2 pathologies to occur with greater penetrance at an earlier age. To test this hypothesis *Nf2*$^{flox2/flox2}$ mice were crossed with mice expressing Cre recombinase driven by a 3.9kb fragment of the -*periostin* promoter (*Postn*-Cre). This *Postn*-Cre mouse was developed by Simon Conway, who has demonstrated that the *periostin* gene is robustly activated in Schwann cell precursors beginning at day E10 [60]. The resultant *Nf2*$^{flox/flox}$; *Postn*-Cre (*Nf2*-cKO) mice develop a constellation of symptoms including cranial nerve, spinal, and dermal schwannomas along with sensorineural hearing loss and vestibular disturbances with 100% penetrance by 8 months of age [61]. These *Nf2*-cKO mice faithfully develop schwannomas which are histologically comparable and in anatomically similar locations to the tumors in NF2 patients.

The *Nf2*-cKO mice have become the preeminent model for genetically and biochemically evaluating drug targets as well as for the preclinical validation of potential therapeutics. Prior drug trials in NF2 have been marred by toxicity and poor patient response. Both prospective and retrospective therapeutic trials in these *Nf2*-cKO mice have accurately mirrored patient responses to compounds that were moved forward into clinical trials. We therefore have begun to rely on these mice to eliminate toxic or ineffective compounds. This allows us to provide NF2 patients with the assurance that when compounds move from preclinical trials into a Phase I or Phase II trials, evidence suggests these compounds will be well tolerated and effective.

Herein, results from two studies which rely on genetic manipulation in our NF2 GEMM are presented. These experiments were undertaken to advance our understanding of the signaling pathways which control oncogenic transformation and growth in Merlin deficient schwannomas. The outcomes of these studies will help to advance new drug targets and therapies for the treatment of NF2 and sporadic Merlin deficient schwannomas.

Materials and Methods

Animal Study Approval

All animal studies were carried out under the Institutional Animal Care and Use Committee (IACUC) of Indiana University School of Medicine approved protocol #11406 in accordance with the U.S. Department of Agriculture's Animal Welfare Act and the Guide for the Care and Use of Laboratory Animals.

Mice and Genotyping

All mice were housed in an AAALAC accredited facility at the Indiana University School of Medicine. Mice were fed a Teklad Lab Animal Diet and maintained on a 12:12 light/dark photoperiod at 22-24º Celsius. The following primers and thermocycler programs were utilized for PCR based genotyping:

Nf2:

Forward: 5'- CTTCCCAGACAAGCAGGGTTC-3'

Reverse: 5'-GAAGGCAGCTTCCTTAAGTC-3'

Program: 94º C for 3 minutes, 30x (94º C for 30 seconds, 55º C for 30 seconds, 72 º C for 1 minute), 72º C for 2 minutes, hold at 4º C

Expected PCR fragment: FLOX: 442bp WT- 305bp

Periostin-Cre

Forward: 5'-CGA-CCA-CTA-CCA-GCA-GAA-CA-3'

Reverse: 5'-ATG-TTT-AGC-TGG-CCC-AAA-TG-3'

Program: 94º C for 5 minutes, 29x (94º C for 30 seconds, 54º C for 30 seconds, 72º C for 30 seconds), 72º C for 10 minutes, hold at 4º C

Expected PCR fragment: 550bp

Pak1 WT

Forward: 5'-GCC-CTT-CAC-AGG-AGC-TTA-ATG-A-3'

Reverse: 5'-GAA-AGG-ACT-GAA-TCT-AAT-AGC-A-3'

Program: 94º C for 2 minutes, 35x (95º C for 20 seconds, 52º C for 20 seconds, 71º C for 2 minutes), 71º C for 7 minutes, hold at 4º C

Expected PCR fragment: 240 bp

Pak1 KO

Forward: 5'-GCC-CTT-CAC-AGG-AGC-TTA-ATG-A-3'

Reverse: 5'- CAT-TTG-TCA-CGT-CCT-GCA-CGA-3'

Program: 94º C for 2 minutes, 35x (95º C for 20 seconds, 58º C for 20 seconds, 72º C for 2 minutes), 71º C for 7 minutes, hold at 4º C

Expected PCR fragment: 360 bp

Pak2

Forward: 5'-ATC-TTC-CCA-GGC-TCC-TGA-CT-3'

Reverse: 5'-TGA-AGC-TGC-ATC-AAT-CTA-TTC-TG-3'

Program: 95º C for 5 minutes, 30x (95º C for 30 seconds, 57º C for 30 seconds, 72º C for 30 seconds), 72º C for 5 minutes, hold at 4º C

Expected PCR fragment: Flox 391 bp, WT 306 bp

Statistical methods

Statistical analyses were performed using GraphPad Prism 7.02 software. As described in the text, ANOVA or Student's T-test were used to test for differences between samples and the Gehan-Breslow-Wilcoxon test was used to assess for differences in the Kaplan-Meier curve. Specific tests and significance levels can be found in the figures and figure legends.

Preparation of mouse nerve tissues for protein studies

Mice were sacrificed and freshly dissected nerve tissue was placed in PBS on ice. Tissues were washed in cold PBS to remove any residual blood and then placed in 1.5mL Eppendorf tubes containing cold xTractor Lysis buffer (Clontech) with cOmplete Protease inhibitor cocktail (Roche) and PhosSTOP EASYpack Phosphatase inhibitor cocktail (Roche). Tissues were minced with microdissection scissors and left to incubate on ice for 30 minutes. Tissues were then sonicated for 10 seconds and centrifuged at 16,100 RCF at 4° C for 15 minutes. The supernatant was collected and stored at -80° C for future use.

Histology and Immunohistochemistry

Freshly excised tissues were placed in 10% formalin, embedded in paraffin and sectioned according to lab protocol. The slides were deparaffinized in Xylenes and rehydrated through a series of graded alcohols to water. Antigen retrieval was performed in 10mM sodium citrate buffer, pH 6, in a pressure cooker for 3 minutes. Endogenous peroxides were quenched in 0.3% hydrogen peroxide (10 min). Slides were blocked in

5% goat serum (1hr), incubated in primary antibody diluted to the appropriate concentration per manufacturers protocol (overnight at 4°C), and then in the appropriate biotinylated secondary antibody diluted 1:800 (1 hr). Slides were then incubated in VECTASTAIN ABC HRP (PK-4000) (30 min), and then Vector DAB peroxidase substrate (sk-4100) was applied and slides were observed for color development. Slides were counterstained in Hematoxylin QS (Vector H3404), blued, dehydrated, and cover slipped. All wash steps between different reagents applications were done with TBST for 5 min, 3 times.

Western Blot Analysis

Protein concentrations for immunoblots were determined by the use of the Pierce BCA Protein Assay Kit (ThermoFisher). Equal aliquots of 30-40 μg protein were loaded and run on NuPAGE 4-12% Bis-Tris Gels (Invitrogen) and then transferred to a PDVF membranes overnight at 120mA. Membranes were blocked for 5 hours at 4° Celsius in 5% milk and then incubated with primary antibody overnight. Primary antibodies from Cell Signaling were utilized at a concentration of 1:1000. Antibodies from other manufactures were utilized at the manufacturer's suggested concentration. After washing for 15 minutes in PBS-Tween, membranes were incubated with horseradish peroxidase linked anti-mouse IgG or anti-rabbit IgG (GE Healthcare, 1:5000). Membranes were then washed for 1 hour in PBS-Tween and visualized using SuperSignal Chemiluminescence substrate (ThermoFisher) and CL-XPosure Film (Thermo).

Cell Lines

All cell lines utilized were validated for Merlin status via Western Blot and screened upon arrival and every three months thereafter to insure they were mycoplasma free utilizing the MycoAlert Mycoplasma Detection Kit (Lonza).

Cell Line	**Lab Generated**	**Species**	**Genotype**	***Nf2* Expression**
MS02	Wade Clapp	Mouse	*Nf2* exon 2-/-	*Nf2* Null
MS02+*Nf2*	Wade Clapp	Mouse	Nf2 exon 2-/- reconstituted with *Nf2* via lentiviral transduced	*Nf2* Competent
MS12	Hellen Morrison	Mouse	*Nf2* wild type	*Nf2* Competent
HEI-193	David Lim	Human	G to A point mutation at intron 14/Exon 15 border	*Nf2* Hypomorph

Cell culture and Proliferation

MS02 or HEI-193 cells were plated at 5,000 cells/well in a 24 well plate containing 500ul of Dulbecco's Modified Eagle Medium (DMEM, Gibco) supplemented with 10% Fetal Bovine Serum (Sigma) and 2mM L-Glutamine (Lonza) along with the concentrations of FRAX-1036 as indicated in the figure. Cells were placed in ThermoForma Series II cell culture incubator with a 5% CO_2 atmosphere for 72 hours

and proliferation was quantified via the CellTiter-Glo assay (Promega) following the manufacturers protocol.

Frax-1036 Treatment

Mice at 8 months of age were treated with 30 mg/kg Frax-1036 in 20% (2-hydroxypropyl)-β-cyclodextrin in 50mM citrate buffer pH 3.0 daily for 12 weeks via oral gavage.

ABR Analysis

Auditory brainstem responses were measured at prior to enrollment, at the study midpoint, and just prior to sacrifice. Mice were anesthetized with Ketamine/Xylezene (100mg/kg ketamine and 10mg/kg xylazine IP) and placed into a custom apparatus with Faraday cage shielding and sound-dampening acoustic foam to attenuate electrical and sound interference. Click stimuli were presented at a rate of 21/second with stimuli presented in decreasing 10dB increments from 90-30dB via a closed-field speaker. Subdermal electrodes connected to a RA4PA Medusa Preamplifier and RZ6 auditory processor (Tucker Davis Technologies) performed the digital-audio conversions which were analyzed in the BioSigRZ application. Biological signals were band pass filtered above 3Hz and below 3,000 Hz. For mice in which no response was identified, a 90dB threshold was recorded.

Dorsal Root Ganglia Quantification

At the conclusion of the 12 week drug treatment, mice were sacrificed and then fixed for 48 hours in 10% formalin. Carcasses were then transferred to 5% formalin/5% formic acid for decalcification for 48 hours. Whole nerve trees were then dissected out under a stereoscopic microscope. Four anatomically matched dorsal root ganglion were measured using the approximate volume of a spheroid, $0.52x\ (width)^2 x$ length.

High Performance Liquid Chromatography and Mass Spectrometry

High performance liquid chromatography (HPLC) and Mass Spectrometry (MS) were performed by the IU Simon Cancer Center's Clinical Pharmacology Analytical Core. Samples were acidified and extracted in hexane:ethyl acetate (50:50, v/v). After solvent evaporation, mobile phase (acetonitrile:5mM ammonium acetate; 70:30, v/v) was mixed with residual sample and injected into an Agilent 1290 HPLC system with an Eskigent Autosampler. Mass spectrometry was performed using an ABSciex 5500 Q-TRAP.

NVS-PAK1-1 Treatment

For the initial PK data (**Figure 13**) mice were treated with 100 mg/kg 1-ABT followed two hours later by 100 mg/kg Frax-1036 in 60% PEG400/ 40% water via oral gavage. For the initial PD data (**Figure 14**) mice were treated in a 6 week dose escalation where they received 100mg/kg 1-ABT followed two hours later by 10 mg/kg Frax-1036 in 60% PEG400/ 40% water for the first week with an increase of 10mg/kg/week resulting in a final concentration of 100mg/kg 1-ABT followed two hours later by 60

mg/kg Frax-1036 in 60% PEG400/ 40% water via oral gavage prior to sacrifice. For the 12 week drug treatment and subsequent PK/PD data (**Figures 15-18**) mice were treated starting at 3 months of age with 100mg/kg 1-ABT followed two hours later by 30 mg/kg Frax-1036 in 60% PEG400/ 40% water via oral gavage.

Primary Antibody List for Western Blots

cMYC (Cell Signaling 5605), GAPDH (Cell Signaling #5174), PAK1 (Cell Signaling #2602), PAK2 (Cell Signaling #2608), PAK1/2 (ThermoFisher PA5-38693**),** PAK3 (Cell Signaling #2609), pPAK1/2 (S144/141) (Cell Signaling #2606), pPAK1/2 (T423) (Santa Cruz #12925-R), pPAK1/2 (T423) (ThermoFisher PA-38693), pAKT 473 (Cell Signaling #9271), pERK1/2 (Cell Signaling #9102), pGSK3β (Cell Signaling #9323), Merlin (Cell Signaling #12888), MEK (Cell Signaling #4694), AKT (Cell Signaling #4685), pMEK1/2 217/221 (Cell Signaling #9154), pMEK 298 (Cell Signaling #98195), pERK1/2 (Cell Signaling #4370), pGSK3B S9 (Cell Signaling #9323), pp38 (Cell Signaling #4511), pJNK (Cell Signaling #9251), p70S6K 389 (Cell Signaling #9234), pMTOR 2448 (Cell Signaling #5536).

Primary Antibody List for IHC

pPAK1/2 (T423) (Santa Cruz #12925-R), Ki67 (Abcam ab16667)

Results

PAK1/2 are Hyperactivated in Merlin Deficient Murine Schwannoma

Given the prior work undertaken by Drs. Joe Kissil and Tyler Jacks demonstrating Merlin's function as a negative regulator of PAK1/2, we were interested to investigate whether PAK1/2 were hyperactivated in the Merlin deficient Schwann cell tumors in our *Nf2*-cKO mice [26,47]. Using immunofluorescence based deconvolution microscopy to probe for activated PAK1/2 with a pPAK1(Thr423)/pPAK2 (Thr402) antibody, we found significantly increased activated PAK1/2 in the trigeminal nerves of 10 month old *Nf2*-cKO mice as compared with Cre negative controls (**Figure 2**). Confirming this finding, immunoblotting demonstrated significantly increased activated PAK1/2 in tissues lysates from 10 month old *Nf2*-cKO along with increased levels of cMYC, pAKT, and pGSK3β, proteins all known to be downstream of PAK1 (**Figure 3**). These data confirmed constitutive activation of PAK1/2 in Merlin deficient schwannomas in our *Nf2*-cKO mice. Because of the potent role PAK1 has been shown to play as an oncogene in solid tumors we hypothesized that the constitutive activation of PAK1 could be critical for the growth of schwannomas in our mice.

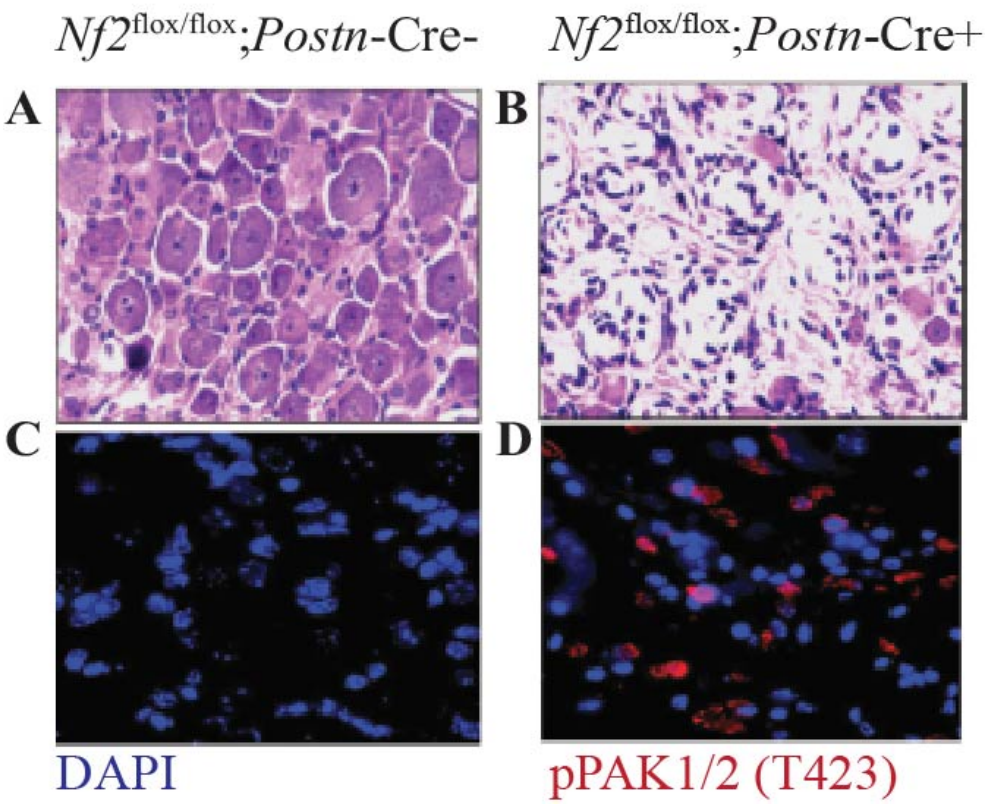

Figure 2. PAK1/2 are hyperactivated in murine Merlin deficient schwannoma *in vivo*. Hematoxylin and Eosin (H&E) staining of trigeminal nerves from **(A)** Cre negative and (**B**) Cre positive 10 month old *Nf2*-cKO animals demonstrating schwannoma formation in Cre positive animals. (**C**) Immunofluorescence of DAPI (Blue) and pPAK1/2 (Red) of Cre negative and (**D**) Cre positive 10 month old *Nf2*-cKO animals demonstrating increased pPAK1/2 in the Cre positive *Nf2*-cKO animals. Original magnification 60x.

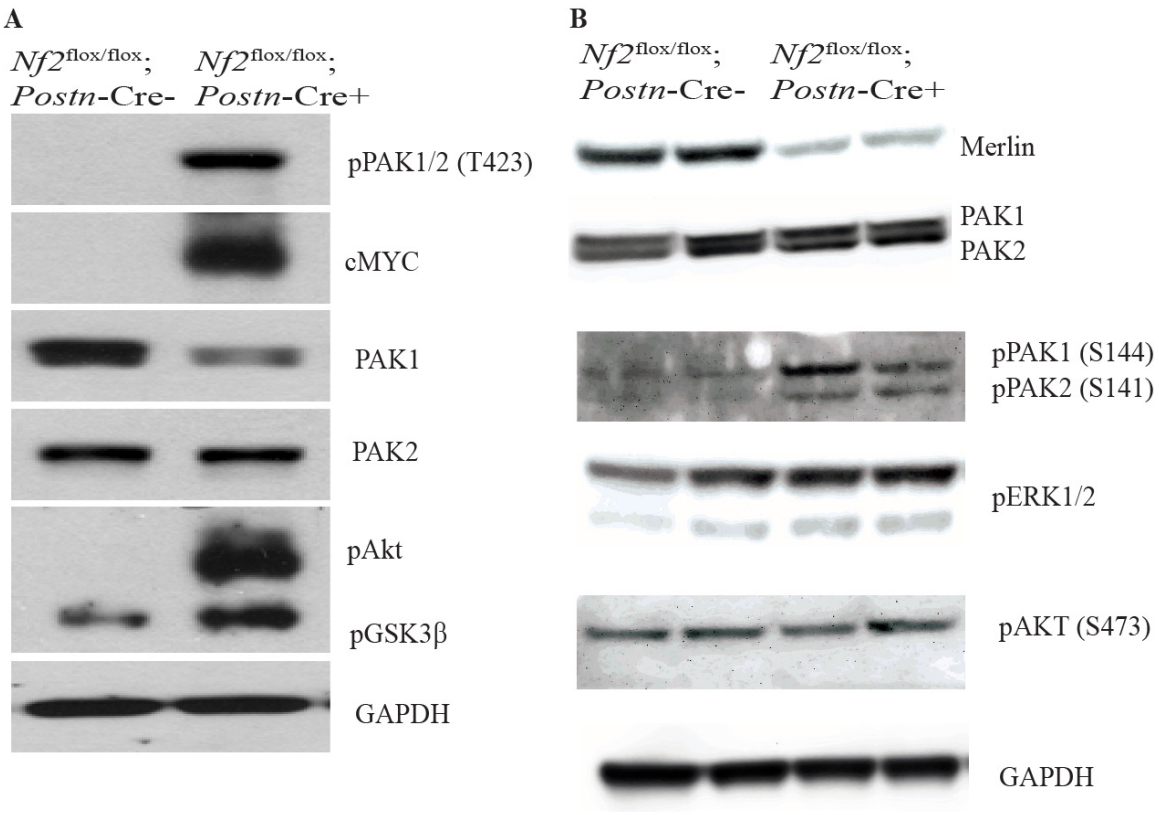

Figure 3. PAK1/2 signaling is hyperactivated in murine Merlin deficient schwannoma *in vivo*. (A) Western blot of trigeminal nerve lysates from 10 month old mice demonstrating phosphorylation of PAK1/2 (S423) with hyperactive signaling in tumor bearing mice. (B) Western blot of trigeminal nerve lysates from 10-12 month old mice demonstrating phosphorylation of PAK1/2 (S144/141).

PAK1/2 Competitive Small Molecule Inhibitor FRAX-1036 Reduces PAK1/2 Activation in Merlin Deficient Schwann Cells *in vitro*

To test the hypothesis that the activation of PAK1/2 was responsible for the growth of Merlin deficient schwannoma, we acquired the PAK1/2 potent and selective small molecule inhibitor FRAX-1036 [62]. FRAX-1036 has a published Ki of 23.3nM against PAK1 and 72.4nM against PAK2. Incubation for 24 hours with sub-micromolar concentrations of FRAX-1036 significantly reduced the basal PAK1 activation in our *Nf2* deficient MS02 cell line and human NF2 patient derived HEI-193 cell line. A reduction in pERK1/2 was also observed in treated cells suggesting a reduction in pro-proliferative signaling (**Figure 4**). Furthermore, in a 72 hour CellTiter-Glo® assay which measures [ATP] as a surrogate for cell number, FRAX-1036 significantly reduced the proliferation of MS02 cells with an IC_{50} of 162nM and HEI-193 cells with an IC_{50} of 1.6μM (**Figure 5**). These data demonstrate a central role for PAK1/2 activation in the proliferation of Merlin deficient schwannoma cells and support a possible therapeutic potential for targeting PAK1/2 as a mechanism for slowing tumor growth.

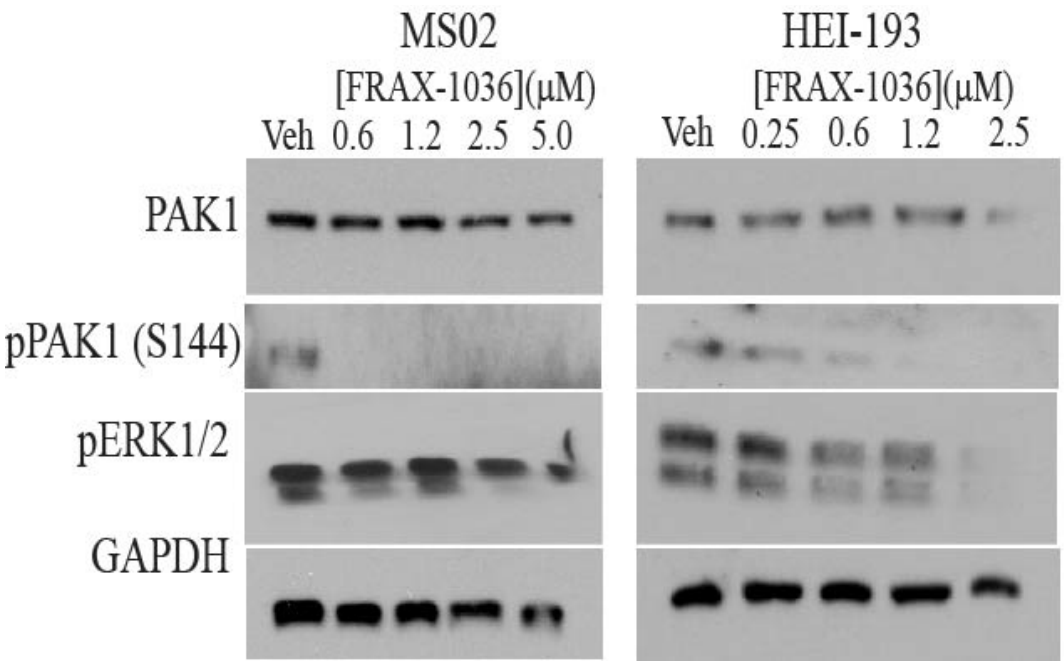

Figure 4. FRAX-1036 inhibits PAK1 autophosphorylation and downstream signaling in MS02 and HEI-193 cells. 24 hour treatment of MS02 and HEI-193 cells with varying concentrations of FRAX-1036 demonstrating potent inhibition of PAK1 autophoshorylation and concentration dependent inhibition of ERK phosphorylation.

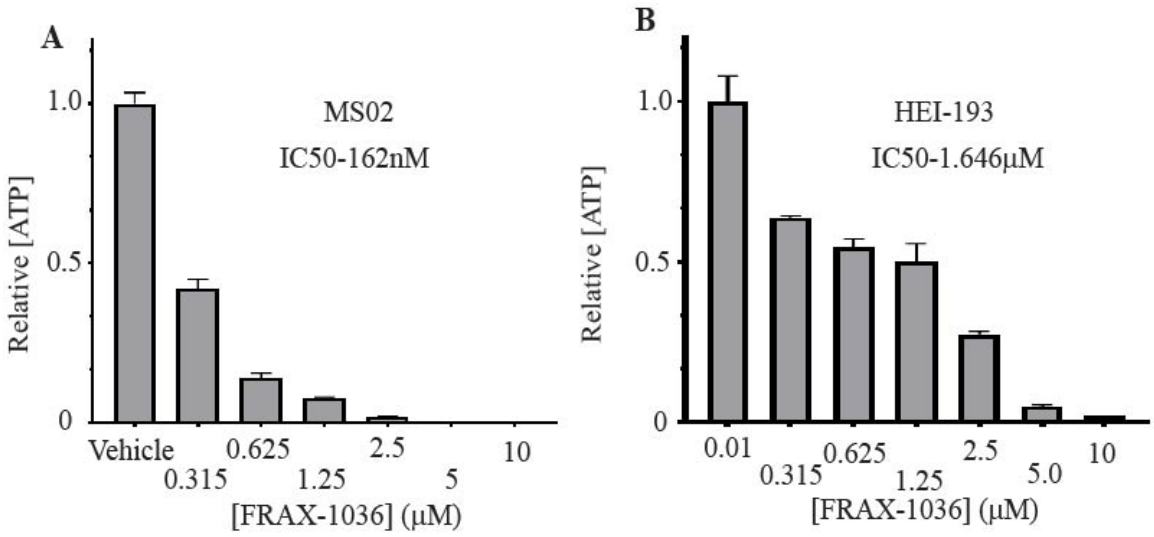

Figure 5. FRAX-1036 inhibits proliferation of both MS02 and HEI-193 cells. (A) 72 proliferation assay with MS02 cells showing concentration dependent inhibition of cell proliferation, IC_{50} =162nM, error bars represent SD (**B**) 72 proliferation assay with HEI-193 cells showing concentration dependent inhibition of cell proliferation, IC_{50} =1.6μM, error bars represent SD. IC_{50} values calculated in GraphPad Prism via [inhibitor] vs normalized response nonlinear fit algorithm.

Treatment with FRAX-1036 Fails to Reduce the Growth of Tumors in our NF2 GEMM

Having validated FRAX-1036 as a potent PAK1/2 inhibitor of human and murine schwannoma cells *in vitro*, we chose to set up a preclinical trial in our *Nf2*-cKO mice to determine whether or not the compound showed efficacy against the growth of Schwann cell tumors *in vivo*. Our *Nf2*-cKO mice develop frank schwannomas with 100% penetrance by 8 months of age and being to die around 10 months of age from tumor burden [58]. We treated 8 month old *Nf2*-cKO animals with a previously established maximum tolerated dose of 30mg/kg/qd FRAX-1036 formulated in 20% (2-hydroxypropyl)-β-cyclodextrin in 50mM citrate buffer with a pH 3.0 for 12 weeks. The drug regimen was well tolerated in the mice and after 3 months of treatment the mice were sacrificed. ABR testing was conducted prior to enrollment on study, at the halfway point of treatment, and just prior to sacrifice to track any changes in sensorineural hearing loss. After 12 weeks on therapy, we observed no difference between vehicle and FRAX treated mice in tumor size, histology, or cell proliferation as measured by IHC of Ki76+ Schwann cells in the Schwann cells tumors (**Figure 6A**). We also did not see any reduction in the average size of the spinal dorsal root ganglia of drug treated mice compared to vehicle treated controls (**Figure 6B**). We also did not detect not see any significant protection in the magnitude or progression of the sensorineural hearing loss between the two groups (**Figure 6C**). In total, treatment with FRAX-1036 did not appear to significantly reduce the growth of the Schwann cell tumors in our *Nf2*-cKO animals.

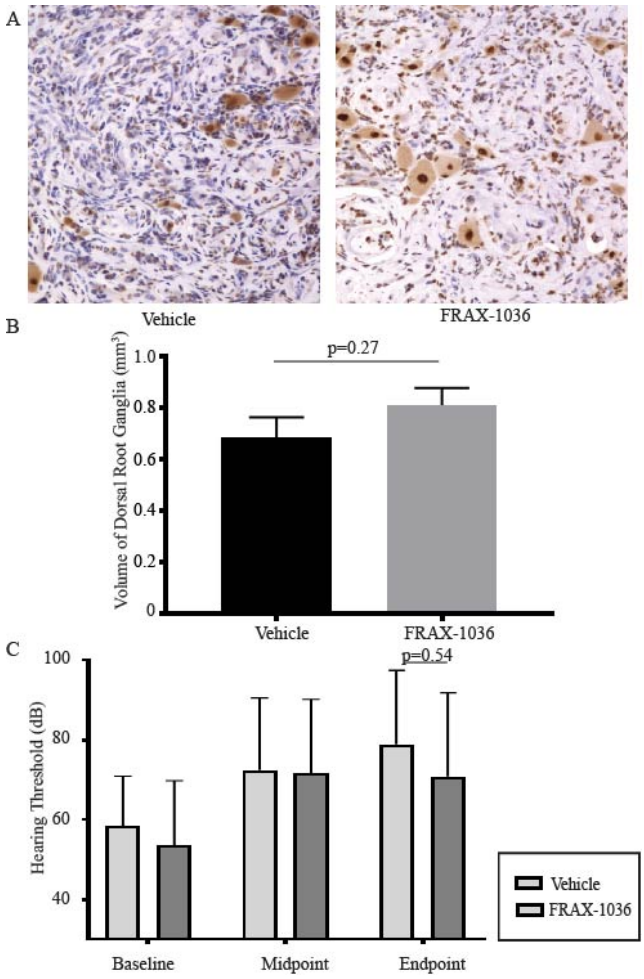

Figure 6. Treatment with FRAX-1036 fails to reduce the growth of tumors in our NF2 GEMM. (A) Representative IHC sections of DRG from vehicle and FRAX-1036 treated mice stained for Ki67. Original magnification 20x. **(B)** Quantification of average size of spinal DRG. Four anatomically DRG were measured per mouse, n=5 mice for vehicle group and n=12 mice for FRAX-1036 treatment group. p=0.27, students t-test error bars represent SEM. **(C)** ABR thresholds of vehicle and FRAX-1036 mice. Both ears in each animal were scored individually, n=6 mice for Vehicle treated, n=15 mice FRAX treated, p=0.54, Two way ANOVA with multiple comparisons, error bars represent SEM.

Maximum Tolerated Dose of FRAX-1036 Demonstrated Suboptimal Pharmacodynamics *in vivo*

We reasoned that failure of FRAX-1036 to slow the growth the Schwann cell tumors *in vivo* was likely either due to limitation of PAK1/2 as a drug target in NF2 or limitations of FRAX-1036 in inhibiting PAK1/2 activation in tumor tissue *in vivo*. To distinguish between these two possibilities we evaluated the pharmacodynamics of FRAX-1036 in tumor bearing tissues of the treated mice. When the 12 FRAX-1036 treated mice were sacrificed, they were randomly separated them into 3 groups of 4 mice which were euthanized either 2, 6, or 24 hours after receiving the final dose of drug. Staining for pPAK1/2 (Thr423/402) in trigeminal nerve sections demonstrated a trend in the reduction of PAK1/2 phosphorylation over the first 6 hours which fully rebounded by 24 hours (**Figure 7A&B**). Immunoblotting in tumor bearing nerve tissues further confirmed a decrease in PAK1/2 phosphorylation over the first 6 hours which waned by 24 hours. Downstream pro-proliferative targets of PAK1, phospho-p38 MAPK, and phospho-MEK1/2 were reduced by FRAX-1036 treatment at 2 hours but had been restored by 6 hours post treatment. pERK1/2 and pAKT appear to not be reduced by treatment at any time point (**Figure 7C**). It therefore appears that we failed to achieve the necessary concentration of FRAX-1036 *in vivo* to adequately inhibit PAK1/2 activation and signaling in the Schwann cell tumors.

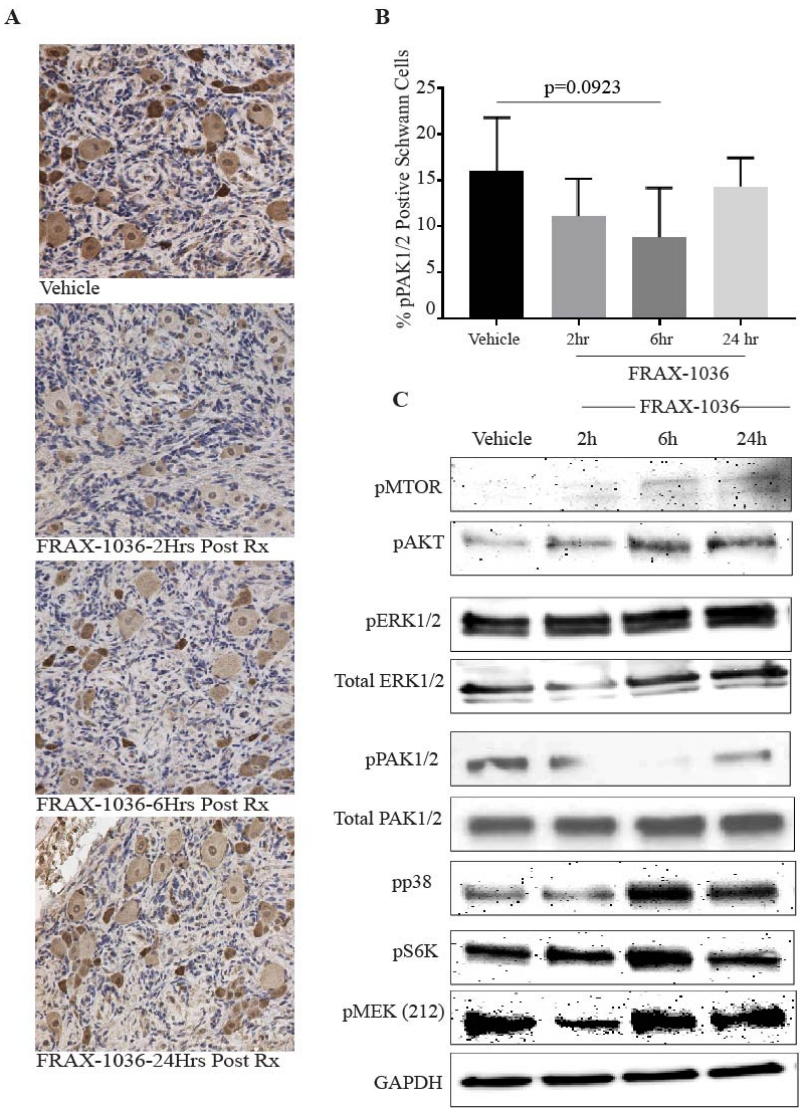

Figure 7. Treatment with FRAX-1036 demonstrated suboptimal pharmacodynamics *in vivo*. (A) Representative images of immunohistochemistry of pPAK1/2 (Thr423/402) in the DRG of treated mice at the specified time point. Original magnification 20x. **(B)** Quantification of pPAK1/2^{+} Schwann cells in DRG schwannomas as measured by IHC. n=4 mice at 2, 6, and 24 hours post treatment. n=5 mice for vehicle treatment. p=0.0923, One way ANOVA with Tukey's test, error bars represent SD. **(C)** Immunoblotting of trigeminal nerve lysates from treated mice.

Simply increasing the dosing of FRAX-1036 seemed ill advised because our collaborator had demonstrated in a different mouse model, doses exceeding 45mg/kg were very poorly tolerated over a 14 day treatment [63]. We predicted that we would need to meet or exceed that 45mg/kg threshold to achieve sustained PAK1/2 inhibition in tumor tissue *in situ*. We attempted *in vivo* inhibition of PAK1/2 with G-5555, a small molecule inhibitor that Genentech proposed as an optimized, second generation competitive PAK inhibitor that was in preclinical development [64]. G-5555 reduced basal PAK1 phosphorylation to undetectable levels in our MS02 cells at concentrations as low as 100nM and inhibited proliferation with an IC_{50} of 200nM in these cells. However, this compound was poorly tolerated in our mice. Single doses as low as 30mg/kg were acutely lethal within 4 hours. After reducing the dose down to 15mg/kg/qd most of our mice died within 14 days, often becoming moribund and developing agonal breathing shortly after drug dosing. Basic necropsy was uninformative. Using echocardiography we determined that at doses as low as 10mg/kg/qd, the mice were developing significant, progressive, left ventricular hypertrophy with pronounced arrhythmias in 7-10 days. It appears that the cardiotoxicity with FRAX-1036 and G-5555 was due to on target inhibition of PAK2 in cardiomyocytes. The cardiotoxicity of G-5555 is likely more profound at lower doses than that of FRAX-1036 due to G-5555 being a significantly more potent inhibitor of both PAK1 and PAK2. PAK2 function may be absolutely required for normal cardiac function and therefore pan-Group A PAK inhibitors are unlikely to be a viable therapeutic for NF2 *in vivo*.

Selective, non-competitive PAK1 inhibition however, may still be of value. PAK1 is larger than PAK2 and so the two proteins run differently on a denaturing gel. PAK1

appears slightly higher in the gel, around 68kD and PAK2 runs lower, around 61kD. The phosphorylation epitopes are so similar that the phospho-antibodies detect both PAK proteins. If both PAK1 and PAK2 were equally expressed and activated, then two bands should appear on Western blots utilizing the phospho specific antibodies. As expected, PAK1 and PAK2 are both expressed in Schwann cells as shown in **Figure 3**. When we probed for PAK activation, a band correlating with pPAK1 was observed but no lower band correlating to pPAK2 was detected (**Figure 3** and **Figure 4)**. This result may indicate that PAK1 and PAK2 are either not functionally redundant or have separate mechanisms controlling their activation in Schwann cells. PAK1 activation may be more important than PAK2 in the formation or growth of tumors in our *Nf2*-cKO mice. Therefore PAK1 may be a viable drug target in NF2 if it could be inhibited independently of the other Group A PAKs.

Germline Deletion of *Pak1* but not Conditional Deletion of *Pak2* is Partially Protective Against the Development of Schwann Cell Tumors in our NF2 GEMM

To dissect out the separate roles of PAK1 and PAK2 in the development of Merlin deficient Schwann cell tumors and to test whether or not inhibition of PAK1 alone could prevent or slow the development and growth of tumors in our NF2 GEMM we crossed our *Nf2*-cKO mice with either *Pak1*$^{-/-}$ (*Pak1*-KO) or *Pak2*$^{flox/flox}$ (*Pak2*-cKO) mice. *Pak1*$^{-/-}$ mice were created by deleting a 2kB region of gDNA that encodes the p21 binding domain of PAK1 [65]. Germline deletion of *Pak2* utilizing a similar approach yields mice which die *in utero*. For ablation of PAK2, a *Pak2* conditional deletion wherein exon 2 of *Pak2* was floxed leading to exon excision and functional loss of PAK2 protein in cells expressing Cre recombinase was employed [66,67].

Nf2$^{flox/flox}$;*Pak1*$^{-/-}$;*Postn*-Cre (*Pak1*-DKO) and *Nf2*$^{flox/flox}$;*Pak2*$^{flox/flox}$;*Postn*-Cre (*Pak2*-cDKO) mice were grown to 10 months of age. At the time of sacrifice, the *Nf2*-cKO and *Pak2*-cDKO mice had all developed frank schwannoma in the trigeminal nerves and dorsal root ganglia. Tissue from the *Pak1*-DKO animals however exhibited Schwann cell hyperplasia without the clear presence of Antoni A and Antoni B histology, the hallmarks of true schwannoma (**Figure 8A)**. The average DRG size of *Pak1*-DKO but not *Pak2*-cDKO mice was also significantly reduced compared to *Nf2*-cKO controls. This result indicated that *Pak1* deletion could slow the growth of Merlin deficient Schwann cell tumors even in the presence of functional PAK2 and activated PAK3 (**Figure 8B**). Lending further support to a critical role of *Pak1* in the NF2 like phenotype, deletion of *Pak1* significantly extended the lifespan and restored the sensorineural hearing loss in the *Nf2*-cKO animals (**Figure 9A&B**). Tissues from the *Pak1*-DKO animals displayed a

significant reduction in Mek, ERK, p38, tumor bearing and β-catenin non-tumor bearing nerve tissues we observed that deletion of *Pak1* reduced downstream PAK signaling **(Figure 10)**. Due to the epitope similarity, the phospho-specific antibodies are not Group A PAK selective and bind PAK1,pMST1/2. Since PAK2, and PAK3. PAK1 and are still present, this result demonstrated that in Merlin deficient Schwann cells, neither PAK2 are different molecular weights and can be separated after electrophoresis on a denaturing gel. PAK1 and PAK3 are only one amino acid different in length and are not distinguishable from each other on immunoblots. This accounts for the high levels of PAK phosphorylation observed in the trigeminal and brachial nerve plexi in PAK1 deficient animals. These data argue that even in the presence of PAK2 and PAK3, deletion of *Pak1* reduces oncogenic signaling and tumor formation in Merlin deficient Schwann cells.

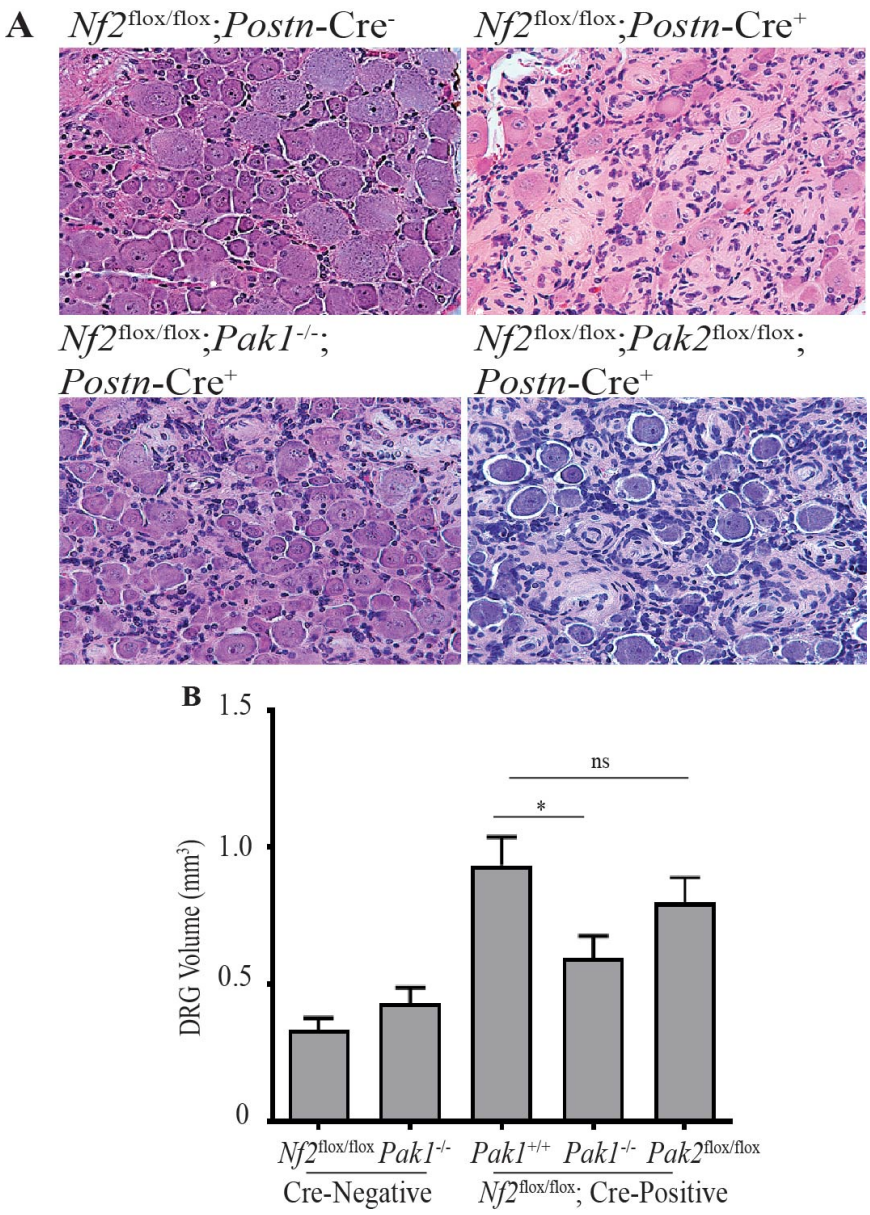

Figure 8. Deletion of *Pak1* slows the development and growth of Schwann cell tumors in *Nf2*-cKO animals. (A) Representative H&E sections of spinal DRG from 10 month old mice. Original magnification 20x. **(B)** Quantification of average DRG volume. 4 anatomically matched DRG were measured from each mouse. n= 5 mice/group for all groups except *Pak2* cDKO mice, n=6 for *Pak2* cDKO mice. $p<0.05$, one-way ANOVA with Tukey's test, error bars represent SEM.

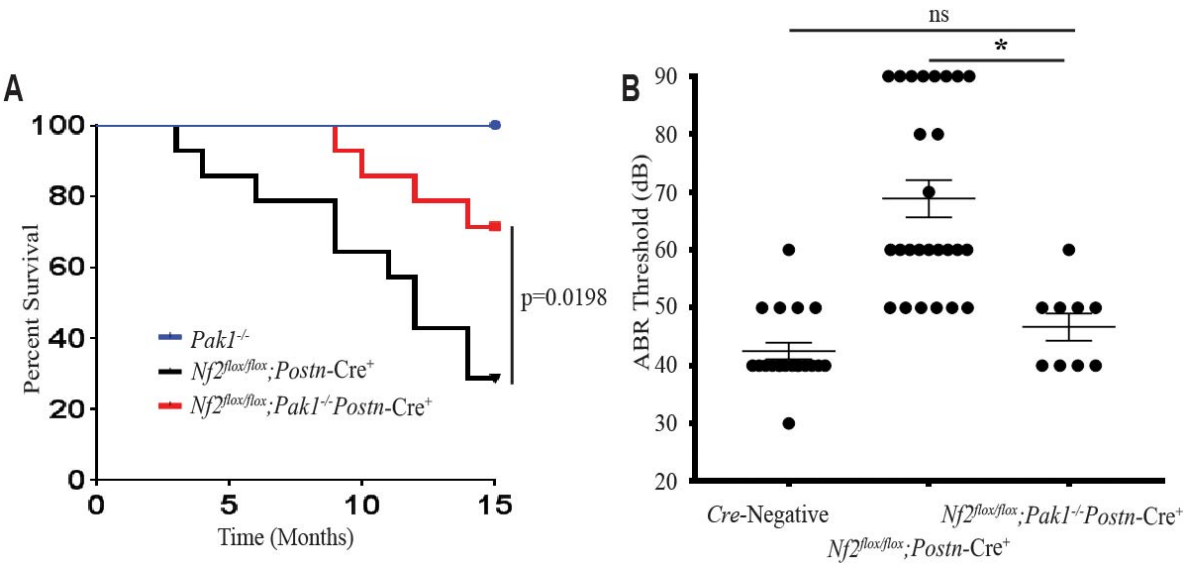

Figure 9. Deletion of *Pak1* extends the lifespan of and is protective against the sensorineural hearing loss in *Nf2*-cKO mice. (A) Kaplan-Meier Curve, n=14 mice/group, p=0.0198, Gehan-Breslow-Wilcoxon test. **(B)** ABR Thresholds at 8 months of age, both ears were tested independently on each mouse, Cre-Negatives n=10 mice, *Nf2*$^{flox/flox}$; *Postn*-Cre^{+} n=13 mice, *Nf2*$^{flox/flox}$;*Pak1*$^{-/-}$;*Postn*-Cre^{+} n=5 mice. $p<0.05$, one way ANOVA with Tukey's test, error bars represent SEM.

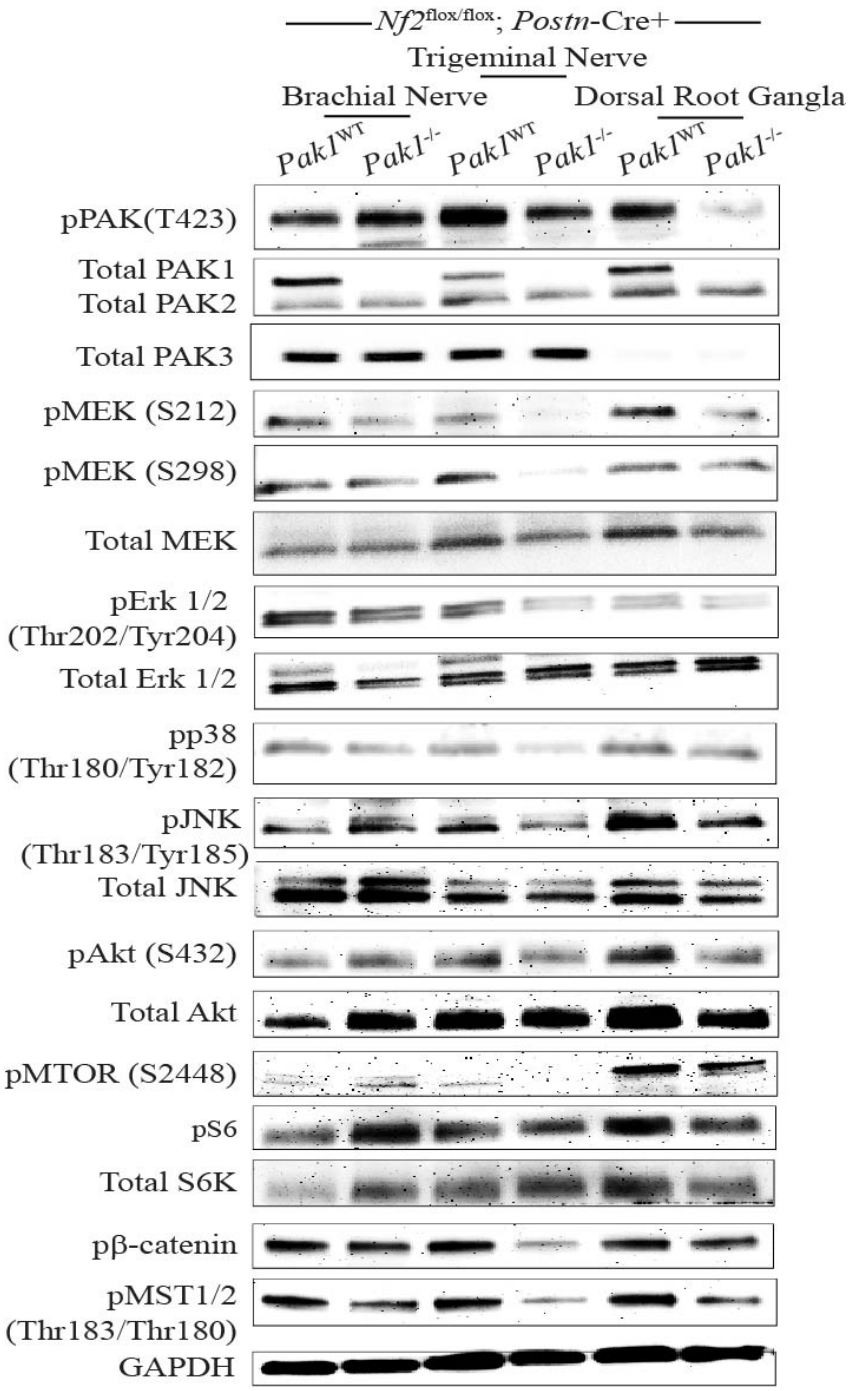

Figure 10. Deletion of *Pak1* reduces PAK signaling in tumor and non-tumor bearing nerve tissues. Tissue lysates from 10 month old mice from the trigeminal nerve, brachial nerve plexus, and spinal DRG.

The PAK1 Allosteric Inhibitor NVS-PAK1-1 Potently Inhibits PAK1 Activation and Proliferation in Merlin Deficient Schwann Cells *in vitro*

During our work with G-5555, Genentech made us aware of a novel, potent, allosteric inhibitor of PAK1 which they had recently acquired from Novartis, NVS-PAK1-1 [68]. As shown in **Figure 11**, NVS-PAK1-1 is structurally distinct from FRAX-1036 and G-5555. Acting through allosteric as opposed to competitive inhibition, NVS-PAK1-1 is 75x more selective for PAK1 than PAK2. Theoretically this compound could allow us to inhibit PAK1 in Schwann cell tumors without the cardiac toxicity. Novartis did not pursue this compound further into preclinical development because although it demonstrated excellent PAK1 selective inhibition *in vitro*, it appeared to have no biological effect *in vivo* due poor bioavailability attributed to rapid degradation by the cytochrome P450 oxidase system.

In our Schwann cells *in vitro*. NVS-PAK1-1 potently inhibited PAK1 autophosphorylation in MS02 cells and reduced the proliferation of MS02 and HEI-193 cells with an IC_{50} of 4.7μM and 6.2 μM respectively (**Figure 12A&B**). These IC_{50} value were much higher than what we had observed with FRAX-1036 in the same cell lines but the effects of NVS-PAK1-1, as compared to FRAX-1036, suggested a cytostatic and not cytotoxic mechanism of action. Treatment slowed the expansion of the two cell lines without triggering significant cell death. The cytostatic phenotype is similar to what was observed when the MS02 cells were reconstituted with functional Merlin. If our hypothesis about Merlin as a negative regulator of PAK1 is correct, this result is more in line with what we would expect for a true PAK1 inhibitor.

FRAX-1036
K_i PAK1=23.3nM
K_i PAK2=72.4nM

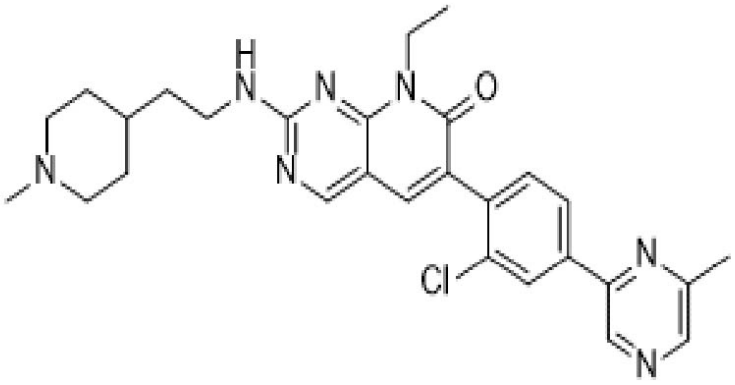

G-5555
K_i PAK1=3.7nM
K_i PAK2=11nM

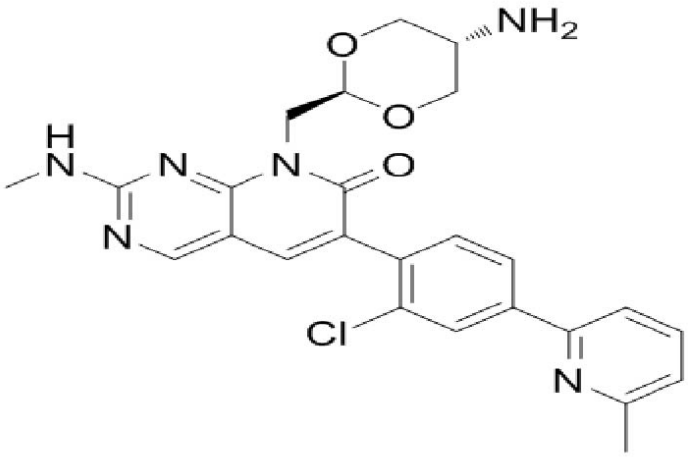

NVS-PAK1-1
K_i PAK1=5.2nM
K_i PAK2=400nM

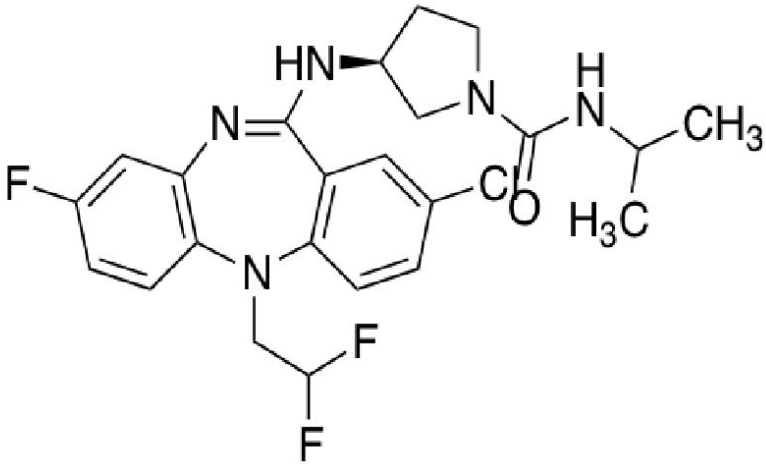

Figure 11. Chemical structures and biological activity of PAK inhibitors as published by the manufactures from which they were purchased.

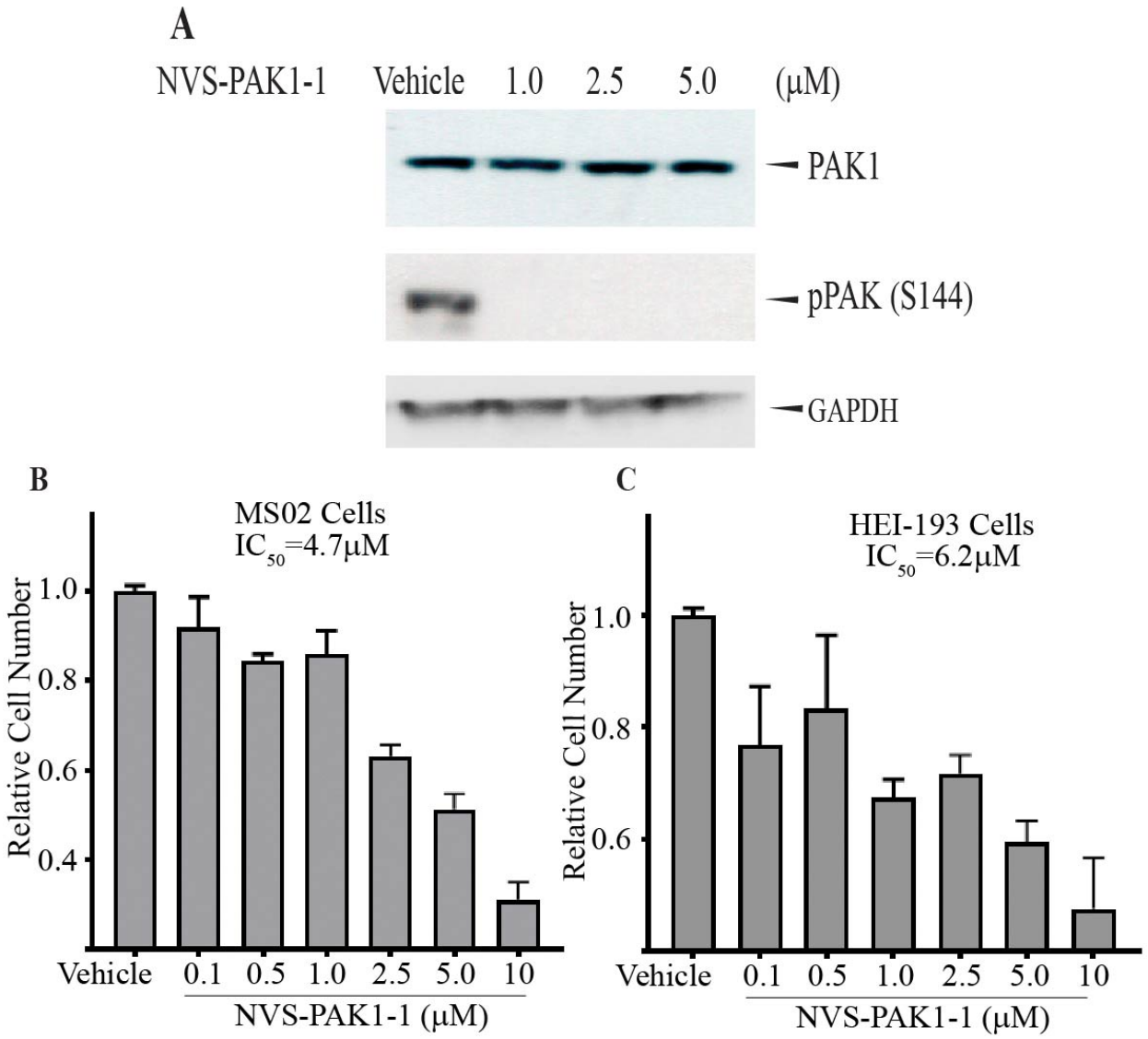

Figure 12. NVS-PAK1-1 inhibits PAK1 autophosphorylation and Merlin deficient Schwann cell proliferation *in vitro*. (A) 2 hour treatment with NVS-PAK1-1 in MS02 cells. **(B)** 72 hour proliferation assay in murine and **(C)** human Merlin deficient schwannoma cell lines with IC_{50}s of 4.7μM and 6.2μM respectively, error bars represent SEM. IC_{50} values calculated in GraphPad Prism via the [inhibitor] vs normalized response nonlinear fit algorithm.

Inhibition of the Cytochrome P450 Oxidase System Prevents the Degradation of NVS-PAK1-1

NVS-PAK1-1 was created through chemical modification and optimization of a basic dibenzodiazepine structure [68]. Pharmaceutical benzodiazepines are some of the most commonly used drugs in the United States and in general are rapidly metabolized via oxidized by the hepatic CYP450 (CYP) system, predominantly by CYP3A4 [69].We therefore hypothesized that the half-life of NVS-PAK1-1 in humans is likely dependent upon the rate of oxidation by CYP3A4.

More than half of all drugs used clinically are metabolized by CYP3A4. There are FDA approved compounds which act as CYP3A4 inhibitors and can be given to delay the degradation of other co-administered compounds. These so call pharmacokinetic inhibitors serve to prolong the half-life of the other bioactive active compounds [70]. The most commonly used pharmacokinetic inhibitor is ritonavir. Ritonavir was originally developed as an HIV protease inhibitor but is largely though to function primarily as a CYP3A4 /CYP2D6 inhibitor to prolong the half-life of the antivirals saquinavir and indinavir given as standard of care for HIV-HAART [71].

To test the rate of NVS-PAK1-1 was metabolism by hepatic P450 enzymes and to investigate if a pharmacokinetic inhibitors could be useful for prolonging the compound's half-life, we partnered with the Clinical Pharmacology Analytical Core (IUSM). NVS-PAK1-1 was incubated with either murine or human liver microsomes for 10 minutes and then mass spectroscopy was used to quantify degradation of the parent compound. NVS-PAK1-1 was rapidly metabolized by the human liver microsomes its degradation was strongly inhibited by ritonavir, as well as by the murine pan-cytochrome P450 inhibitor

1-aminobenzotriazole (1-ABT) and Ketoconazole, another potent CYP inhibitor in humans (**Figure 13A**).

NVS-PAK1-1 was metabolized at a lower basal rate in the murine liver microsomes and the addition of ritonavir increased drug oxidation. This result was not what we had predicted but predicting drug metabolism is much more difficult in mice than it is in humans. Mice have 102 functional *Cyp* genes compared to only 57 in humans [72]. This gene expansion creates greater functional overlap between the murine Group 1-3 Cyps. Cyp3A11 is the closest murine homologue to CYP3A4 but it would likely be necessary to inhibit a combination of murine Cyps to achieve the same effect as inhibiting CYP3A4 in humans [72,73]. We decided not to try and dissect out the precise enzymes required for degradation of NVS-PAK1-1 in mice due to this disconnect between mouse and human biochemistry. Instead, we chose to utilize the pan-Cyp inhibitor, 1-ABT for further studies. 1-ABT is a well-tolerated, nonspecific CYP inhibitor in mice and did appear to prolong the half-life of NVS-PAK1-1 *in vitro* [74] (**Figure 13A**). Utilizing a single oral dose administration of NVS-PAK1-1 at 100 mg/kg with or without 1-ABT at 100 mg/kg dosed 2 hours prior, we found that the addition of 1-ABT more than tripled the *in vivo* half-life of NVS-PAK1-1 from 4.9 hours up to 15.4 hours (**Figure 13B**).

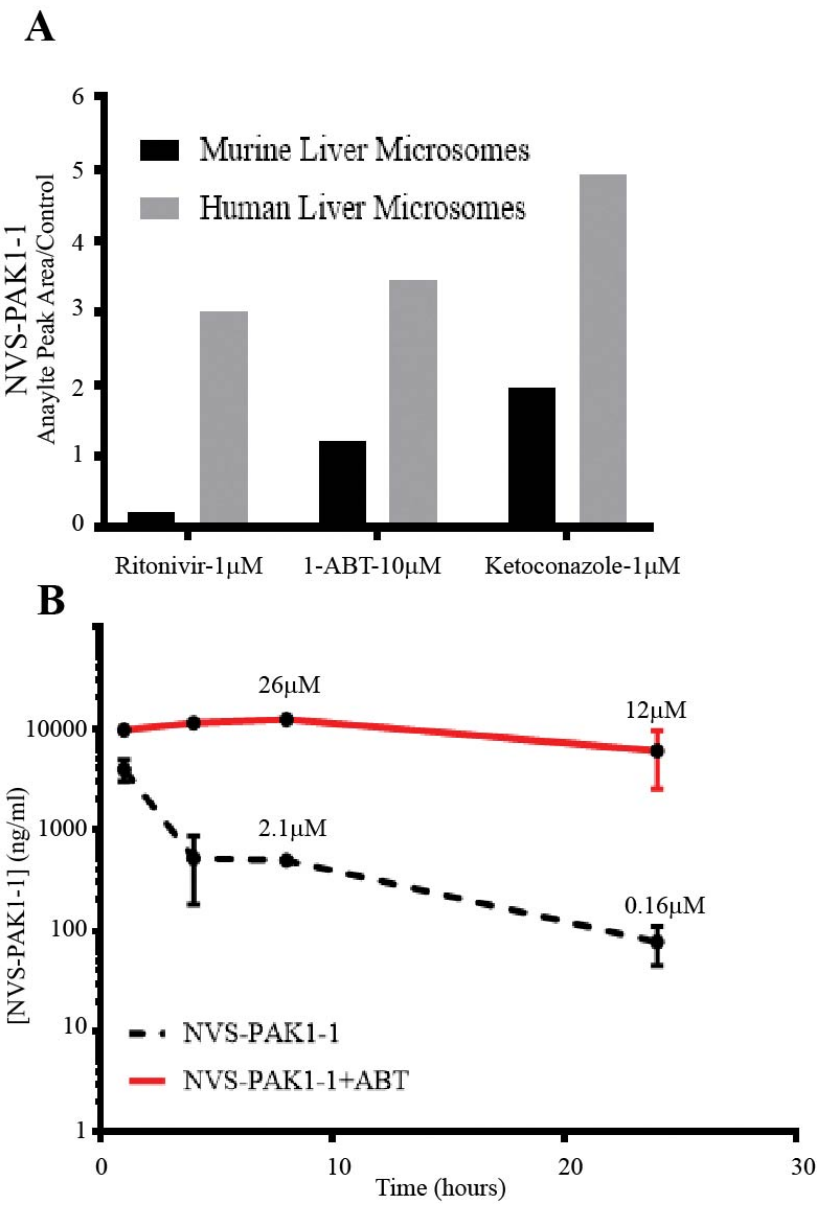

Figure 13. 1-ABT prolongs the half-life of NVS-PAK1-1 *in vitro* and *in vivo*. (A) Levels of NVS-PAK1-1 remaining after 10 minutes of co-incubation in murine or human liver microsomes normalized to amount of compound remaining after 10 minutes without the addition of CYP inhibitors. (**B**) Serum concentrations of NVS-PAK1-1 measured at 1,4,8 and 24 hours after a single dose administration of 100 mg/kg NVS-PAK1-1 with or without 2 hour pretreatment with 100 mg/kg 1-ABT. 3 mice/group/time point. $T_{1/2}$ NVS Alone=4.9 hours, $T_{1/2}$ NVS+ABT =15.4 hours, error bars represent SD.

Inhibition of PAK1 Phosphorylation in Tumor Bearing Tissue *in vivo* can be Achieved via Oral Dosing of NVS-PAK1-1

In order to establish a maximum tolerated dose of NVS-PAK1-1 for preclinical therapeutic trials, we conducted a 6 week dose escalation experiment in which mice were treated daily with 1-ABT at 100 mg/kg followed two hours later by NVS-PAK1-1 at 10 mg/kg. The dose of NVS-PAK1-1 was then subsequently increased by 10mg/kg each week to achieve a final dosing of 60 mg/kg. Two hours after the final administration of NVS-PAK1-1, mice were sacrificed and trigeminal nerves were removed. PAK1 and PAK2 phosphorylation were significantly reduced in the tumor bearing tissues of mice treated with NVS-PAK1-1 as compared to that observed in tissues from control mice which just received the 1-ABT alone (**Figure 14**). Treatment with NVS-PAK1-1 also lead to a significant reduction in pS6RP and pSRC, indicating that the compound was truly inhibiting pro-proliferative signaling.

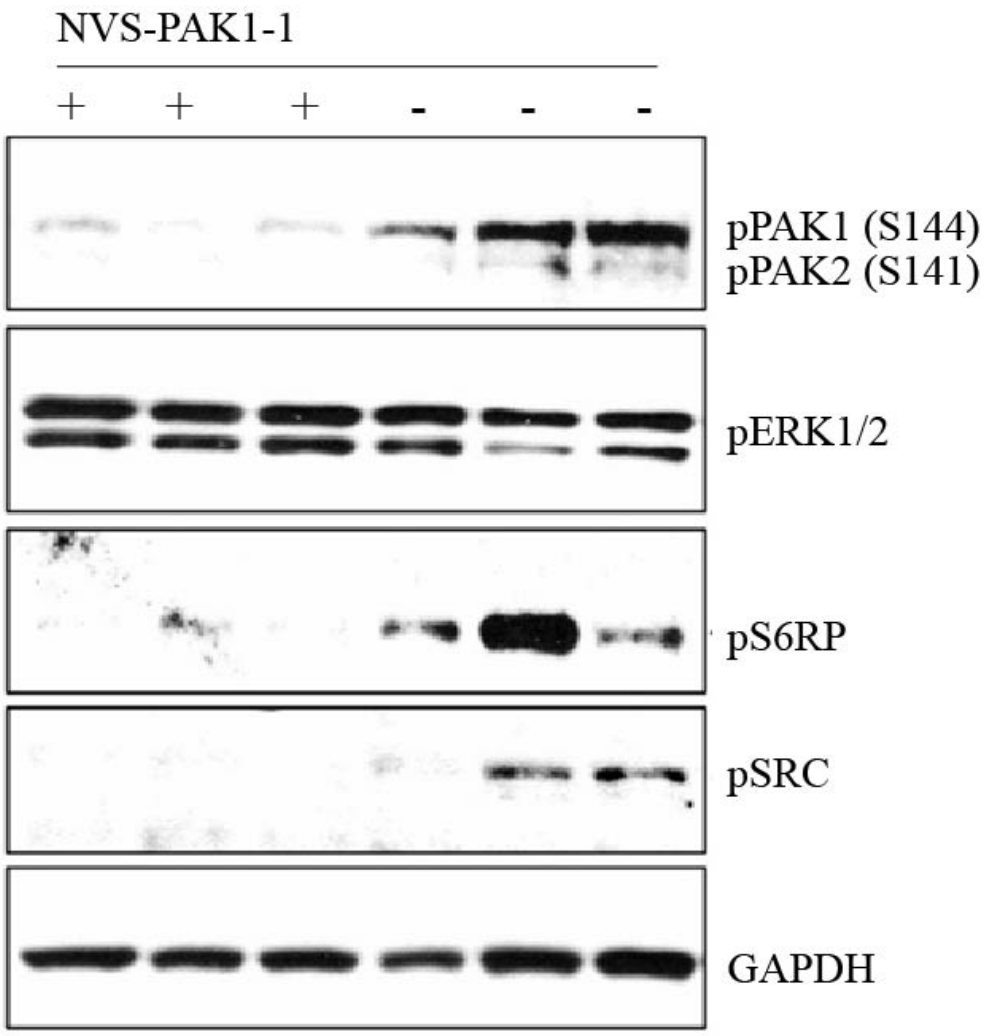

Figure 14. Oral administration of NVS-PAK1-1 can reduce PAK phosphorylation and pro-proliferative signaling in tumor tissue *in vivo*. Trigeminal nerve lysates from 10 month old *Nf2*-cKO mice treated in a 6 weeks dose escalation experiment and sacrificed two hours after their final dose of 60 mg/kg NVS-PAK1-1.

NVS-PAK1-1 Treatment does not Reduce the Magnitude of Sensorineural Hearing Loss in *Nf2*-cKO Mice

At 60 mg/kg, NVS-PAK1-1 was poorly tolerated in our mice. Based upon those data, we decided to treat mice with half maximal tolerated dose. Mice were treated daily for 12 weeks with 100 mg/kg of 1-ABT followed 2 hours later with 30 mg/kg of 1-ABT. With the FRAX-1036 trial, preclinical studies were designed to examine the effects of pan-PAK inhibition on slowing the growth of established tumors. In the *Nf2*-cKO mice, PAK1 appeared to function early in tumor formation. PAK1 inhibition may exert a protective effect against the development of Schwann cell tumors and sensorineural hearing loss if initiated early in life so for this study we decided to treat mice starting at 4 months of age.

A 3 month time course with NVS-PAK1-1 provided no reduction in the magnitude of sensorineural hearing loss (**Figure 15A**). Of note we believe the sensorineural hearing loss in the mouse model to be permanent as we have never observed normal hearing rescued in mice that previously exhibited elevated ABR thresholds and at the 4 month baseline ABR, the majority of the mice utilized for both the vehicle control and NVS-ABT groups exhibited significantly elevated hearing thresholds (**Figure 15B&C**). It is unusual to have such a high percentage of *Nf2*-cKO mice in any cohort which demonstrate significant hearing loss at that age and we may have missed the critical window in which PAK1 inhibition may act to prevent the onset of hearing loss. We have a very incomplete understanding of the mechanisms which control the progression of hearing loss both in NF2 patients and in our *Nf2*-cKO mice and with the cohorts as generated, we had insufficient numbers of mice with normal hearing at

baseline to be powered to test whether treatment with NVS-PAK1-1 could delay or prevent the initiation of sensorineural hearing loss in this trial.

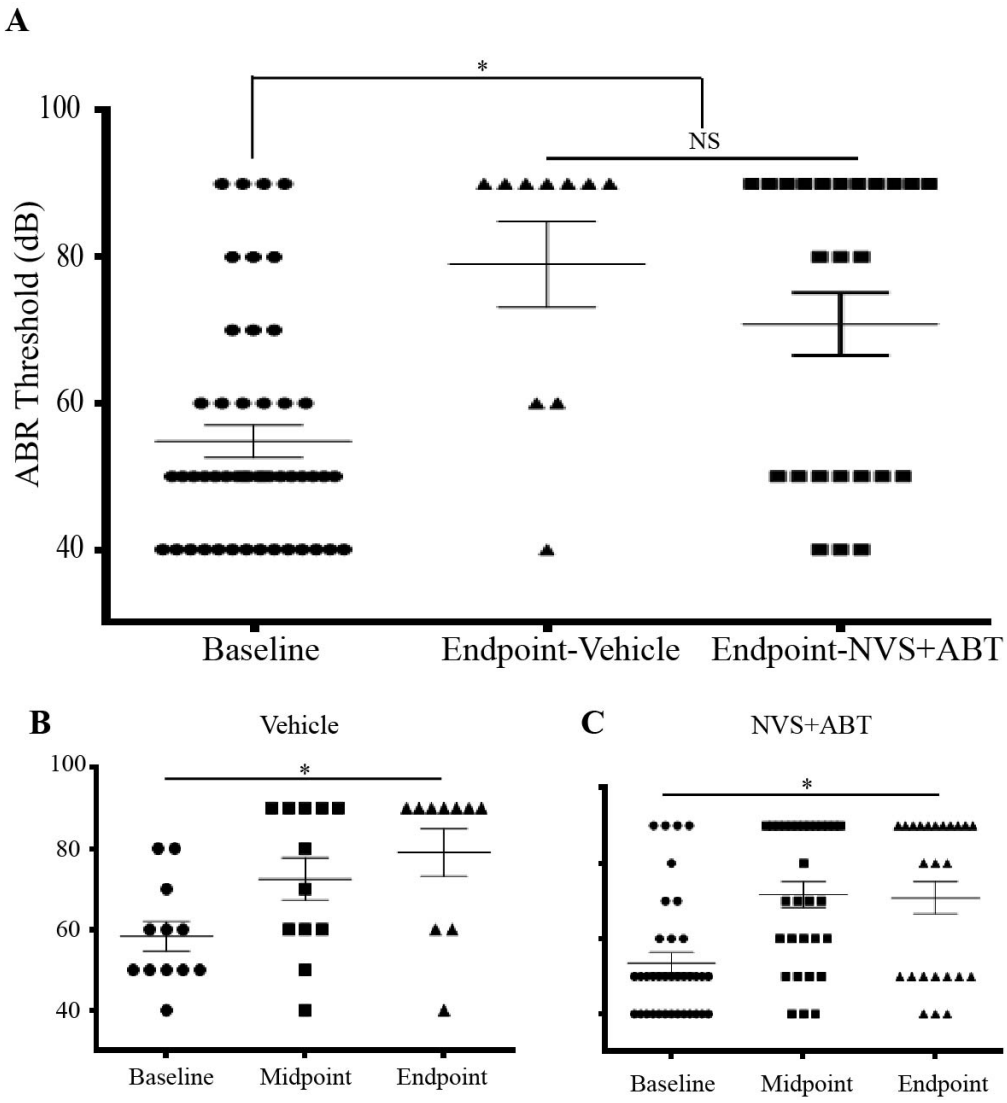

Figure 15. ABR Thresholds in NVS-PAK1-1 treated mice. (A) ABR thresholds in mice treated for 12 weeks with 30mg/kg NVS-PAK1-1+1-ABT or the vehicle along with measurements at 4 months prior to initiation of therapy. Error bars represent SEM. Ears tested independently, baseline n=19 mice, vehicle n=6, NVS n=13, $p<0.05$, one way ANOVA with Tukey's test. (**B**) Mice from vehicle treatment in A, separated out with midpoint ABR numbers. Error bars represent SEM, $p<0.05$, one way ANOVA with Tukey's test. (**C**) Mice from NVS+ABT treatment in A, separated out with midpoint ABR numbers. Error bars represent SEM, $p<0.05$, one way ANOVA with Tukey's test.

NVS-PAK1-1 Treatment does not Prevent Tumor Formation but does Reduce the Average DRG Size of *Nf2*-cKO Mice

After 3 months of treatment, histologic schwannomas were observed in all of the vehicle, 1-ABT only, and NVS-PAK1-1+1-ABT mice. Schwannomas in the vehicle and 1-ABT treated mice were indistinguishable from one another in morphology. In comparison, the histology in the NVS-PAK1-1+1-ABT treated mice was more variable (**Figure 16A**). Specifically, about half of the DRG contained schwannomas which appeared similar in histology to the tumor in mice treated with 1-ABT alone while the other half appeared smaller and less developed. One of the mice treated with 1-ABT alone also developed a subdermal axillary mass with histology consistent with that of an advanced schwannoma (**Figure 16B**).

Consistent with histologic observations, the average DRG size of vehicle and 1-ABT alone treated mice were similar while mice treated with NVS-PAK1-1+1-ABT had significantly smaller average DRG volume (**Figure 17**). This difference appears to be driven by the fact that while 15 of the 32 DRG in the NVS-PAK1-1+1-ABT group appeared very similar in volume to the two control groups, the remaining 17 DRGs in the NVS-PAK1-1+1-ABT group were much smaller in size. The unusually high percentage of mice with elevated ABR thresholds at baseline leads us to believe that some percentage these mice already had tumors prior to therapy. The tumor quantification data therefore may further indication that PAK1 inhibition prevent tumor formation in Merlin deficient Schwann cells but does not strongly inhibit the growth of established Schwannomas.

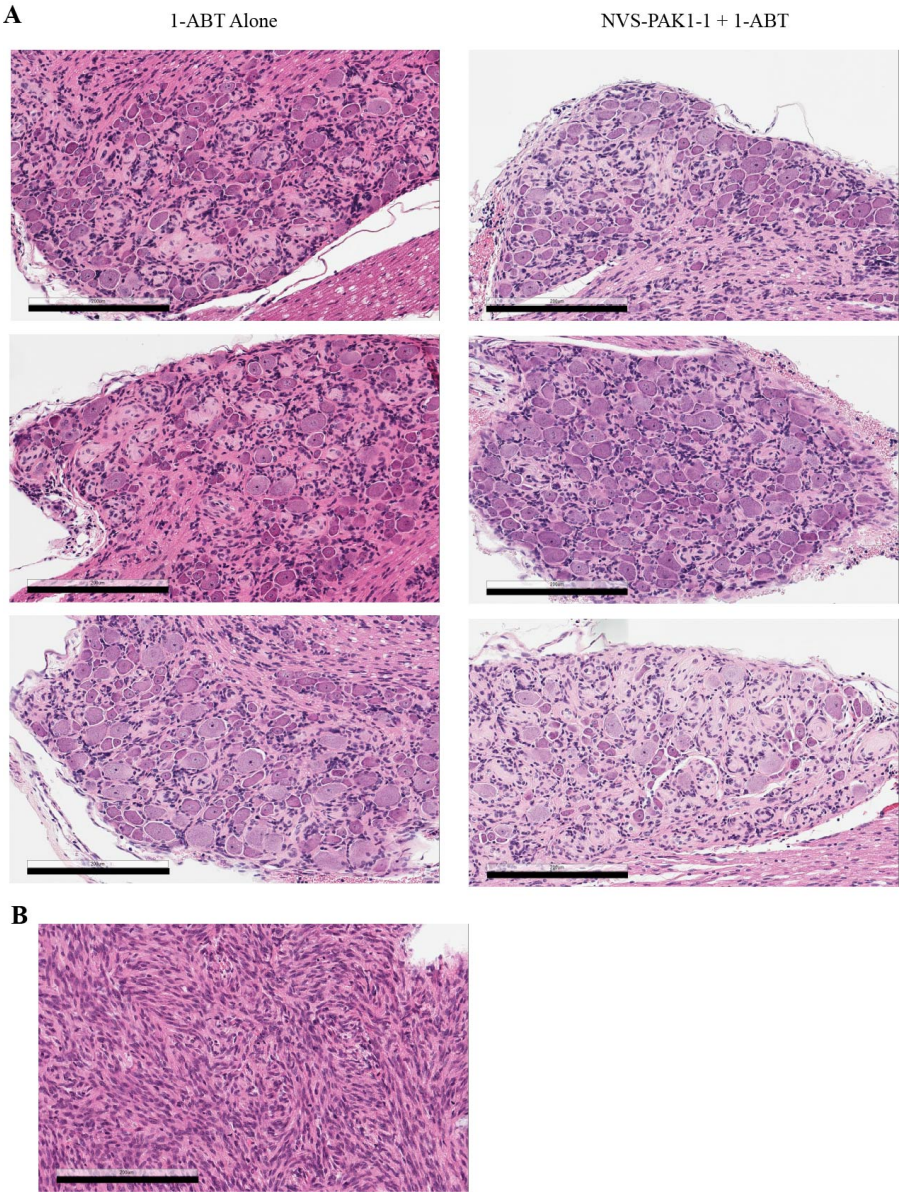

Figure 16. DRG Histology in 1-ABT alone and NVS-PAK1-1 + 1-ABT treated mice. **(A)** Representative H&E sections from 3 different 1-ABT alone and NVS-PAK1-1+1-ABT treated animals. Original magnification 20x. Scale bars= 200μM. (**B**) Subdermal schwannoma in a 1-ABT alone treated animal. Original magnification 20x. Scale bars= 200μM.

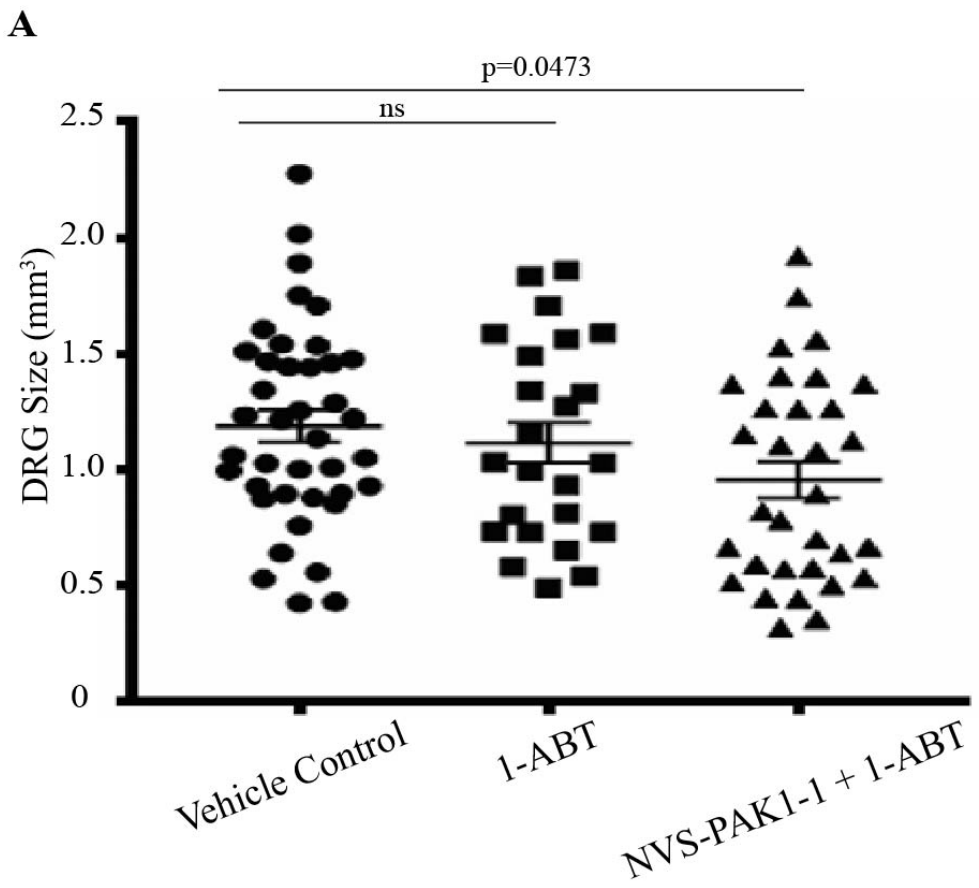

Figure 17. Average DRG volume in the NVS-PAK-1 cohort. Quantification of average volume of spinal DRG. Four anatomically DRG were measured per mouse, n=10 mice for vehicle group, n=6 mice for 1-ABT alone treatment group, n=8 mice for NVS-PAK1-1+1-ABT. p=0.0473, one way ANOVA with Tukey's test, error bars represent SEM.

Pharmacokinetics and Pharmacodynamics of 30mg/kg/qd NVS-PAK1-1 +100mg/kg 1-ABT

One quarter of the NVS-PAK1-1+1-ABT treated mice died during the 12 week drug course. These mice did not exhibit any noticeable GI toxicity. Both the vehicle and 1-ABT alone drug regimens were very well tolerated. We wondered if the deaths in the NVS-PAK1-1 treatment cohort could again be attributed to cardiotoxicity associated with inhibition of PAK2. We collected cardiac and hepatic tissues for histologic sectioning from the mice that survived the 12 weeks and did not observe any overt pathologies. We had anticipated that but cutting the NVS-PAK1-1 dosing by 1/3 compared with the original 100mg/kg we used for the primary PK data, the serum concentrations would also drop by at least 1/3. At the 30mg/kg NVS +1-ABT dosing over 12 weeks, peak concentrations of NVS-PAK1-1 were found to be higher than we anticipated at 17μM in serum and 4.3μg/g in DRG tissues (**Figure 18A&B**). These peak serum and tissue concentrations were still elevated above the ideal therapeutic window where we would expect selective PAK1 inhibition without blocking activating of PAK2.

To assess whether the 30 mg/kg/qd NVS-PAK1-1 was sufficient to inhibit PAK1 in tumor tissue *in vivo*, trigeminal nerves were extracted from mice after the 12 weeks of treatment. Relative to the total expression of PAK1, the mice treated with NVS-PAK1-1+1-ABT demonstrated reduced levels of pPAK1/2 (**Figure 18C**). Erk and p38 phosphorylation were not reduced. At 7 months of age we would expect relatively small schwannomas, making up less than 5% of the trigeminal nerve volume. The uniformly low levels of pERK1/2 and phosho-p38 may reflect normal signaling in healthy trigeminal nerve and are not reflective of the changes occurring the tumor.

We are currently evaluating the PK and PD from 12 month old tumor bearing mice treated with 10 mg/kg NVS-PAK1-1+100 mg/kg 1-ABT. We anticipate that by dropping the NVS-PAK1-1 concentration again by 3 fold we will substantially increase long term tolerability. At the time of sacrifice we will collect cardiac tissues to experimentally measure left ventricular concentrations of NVS-PAK1-1 and probe for PAK2 activation status via Western blot so we can directly assess whether NVS-PAK1-1 is inhibiting PAK2 activation in the heart at the measured concentration. The larger tumors in these older mice will make it much easier to evaluate whether the 10mg/kg/qd NVS-PAK1-1+1-ABT is sufficient for inhibition of PAK1 in the schwannomas. If we can establish a drug dose inhibits PAK1 in schwannomas but does not inhibit PAK2 in cardiomyocytes we will proceed with another 12 week preclinical trial with this optimized dosing regimen.

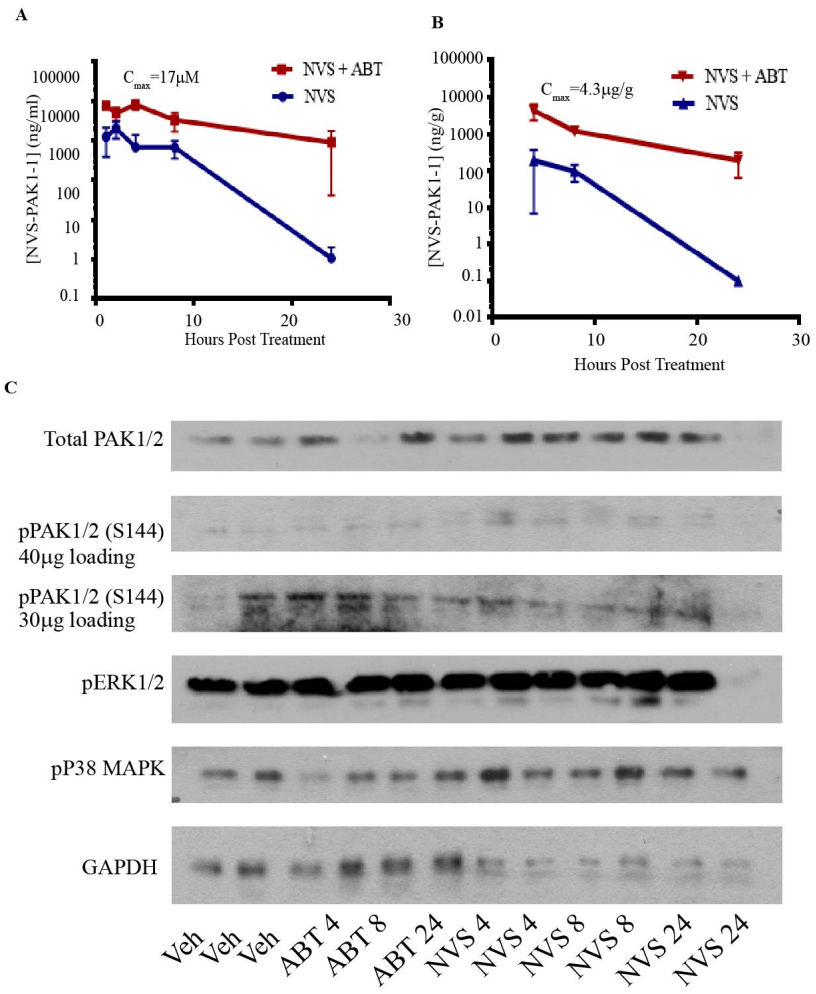

Figure 18. Pharmacokinetics and pharmacodynamics of 30mg/kg/qd NVS-PAK1-1 +100mg/kg 1-ABT. (A) Serum concentrations of NVS-PAK1-1 after 12 weeks of treatment with 30 mg/kg/qd NVS-PAK1-1+100 mg/kg 1-ABT along with a control of mice treated with a dose of NVS-PAK1-1 alone. Error bars represent SD. (**B**) Tissue concentrations of NVS-PAK1-1 after 12 weeks of treatment with 30mg/kg/qd NVS-PAK1-1+100 mg/kg 1-ABT along with a control of mice treated with a dose of NVS-PAK1-1 alone. Error bars represent SD. (**C**) Western blot analysis from trigeminal nerve lysates of mice treated for 12 weeks as indicated. Numbers on x-axis represent the number of hours post treatment.

Discussion

To investigate the physiological role of PAK1/2 activation in schwannoma formation *in vitro* and *in vivo* experiments were conducted. The results demonstrate increased PAK1/2 phosphorylation and downstream PAK1 signaling in both human and murine Merlin deficient schwannomas. There is strong evidence to suggest that Merlin is a direct, negative regulator of PAK1. Blocking PAK1 activation can reduce the hyper-proliferative phenotype of Merlin deficient Schwann cells *in vitro*. Due to the direct link between loss of Merlin and PAK1/2 activation, the known role of PAK1 as a potent oncogene, and the commercial availability of Group A selective PAK inhibitors, we hypothesized that inhibiting PAK1 could be a viable strategy for reducing tumor growth and tumor related morbidities in NF2 and is worth continued exploration.

The PAK1/2 inhibitor FRAX-1036 demonstrated significant efficacy *in vitro*, blocking PAK1 phosphorylation and inhibiting the proliferation of Merlin deficient schwannomas at sub micromolar concentrations. *In vivo*, however, mice treated for 3 months starting at 8 months of age with 30mg/kg/dq FRAX-1036 showed no reduction the progression or magnitude of their sensorineural hearing loss or in their average DRG volume. There are three major factors which may account for the apparent lack of efficacy of FRAX-1036 in the *Nf2*-cKO mice. First, although there appears to be a connection between the presence of vestibular schwannoma and the presence of sensorineural hearing loss in NF2, the physiology linking the two is unknown. In serial MRI scans of NF2 patients, individuals with larger tumors were found to be more likely to have some degree of hearing loss, but neither the absolute size of the vestibular

schwannoma nor the rate of schwannoma growth had predictive value when estimating the magnitude or progression of sensorineural hearing loss in patients [75]. Sensorineural hearing loss is the most common presenting symptom of individuals with a vestibular schwannoma. Therefore it is reasonable to argue that preventing tumor formation may prevent the hearing loss but current data does not support the hypothesis that slowing tumor growth will necessarily be otoprotective [7]. Preventing sensorineural hearing loss would be a desirable outcome for a NF2 therapeutic. However otoprotection may not be observed with a compound that slows the growth of but does not prevent the formation of schwannomas. Second, if inhibition of PAK1 primarily served to prevent tumor formation, the age range at which these mice were treated would have prevented us from seeing that effect in this study. For most of our therapeutic trials we treat mice for 12 weeks starting a 5 months of age. For the FRAX-1036 study we treated older mice in order to investigate the effects of PAK1 inhibition in established tumors. It is possible the primary oncogenic effects of PAK1 hyperactivation occur earlier and we missed the ideal window of treatment by not starting therapy until 8 months of age. Third and most importantly, PAK2 inhibition is toxic and FRAX-1036 demonstrated only mild selectivity for PAK1 over PAK2. The PAK competitive inhibitors, FRAX-1036 and G-5555, at concentrations required to inhibit PAK1 in tumor tissue *in vivo* also inhibited PAK2 in the cardiac tissue. Therefore there are unlikely to be doses of either compound that both effectively inhibit PAK1 and are well tolerated *in vivo*.

Merlin can interact with both PAK1 and PAK2. If PAK1 and PAK2 were functionally redundant as oncogenes in Merlin deficient schwannomas, then we would no longer consider PAK1 to be a viable drug target. The genetic intercross between the *Nf2*-

cKO and *Pak1*$^{-/-}$ animals clearly demonstrated that global, prolonged inhibition of PAK1 could be both well tolerated and a successful in reducing NF2 like pathologies in our *Nf2*-cKO animals. The prolonged lifespan, the protection from sensorineural hearing loss, and the reduction in average DRG volume were all profound and argue for a central role of PAK1 activation in this disease.

The tissue histology supported the hypothesis that the deletion of *Pak1* is at least partially protective against tumor formation. The prevention of tumors in these animals may explain both the otoprotection we observed as well as the failure of FRAX-1036 as *Pak1* may play a more important role in initial tumor formation and less of a role in the growth of established schwannomas. The anti-tumor effects of PAK1 inhibition appear independent of PAK2 function as the *Pak1*-DKO mice maintained fully functional *Pak2*. We had not anticipated that PAK3 would be so highly expressed or activated in the brachial plexus and trigeminal nerve of our *Nf2*-cKO animals but high levels of activated PAK3 did not appear to functionally mimic activated PAK1 in the *Pak1*-DKO animals.

The *Nf2;Pak2*-cDKO had to be excluded from our survival analysis because of additional abnormalities of the peripheral nervous system associated with Schwann cell deletion of *Pak2*. Approximately 20% *Pak2* floxed, Cre positive mice from each litter had to be sacrificed prior to one month of age due to hind limb paralysis with accompanying inability to ambulate or feed. None of the mice born with normal ambulation appear to develop paralysis later in life. We have previously observed this phenotype in other mice which were *Nf2* wild type but had genetic deletions upstream of *Pak2*. The sciatic nerve is the longest nerve in the body and contains neurons that have the longest axons in the body and thus requires the most time to grow and myelinate. We

have prior data that loss of *Pak2* can lead to a disruption in the actin cytoskeleton. We believe that in some percentage of mice, the nerve isn't fully developed and hasn't established mature synapses with the muscle bodies in the anterior compartment of the leg prior to *Periostin* expression and Schwann cell maturation at day 13.5. In the floxed *Pak2* animals, once *Pak2* gets disrupted, the resultant cytoskeletal aberrations may prevent the nerve from further maturing resulting in the paralysis. These data from the genetic intercross further support the hypothesis that PAK1 may be a valuable therapeutic target for the treatment of NF2 while inhibition of PAK2 is not only unnecessary but unadvisable.

Allosteric inhibition of PAK1 through the use of NVS-PAK1-1 greatly increased our ability to selectively target PAK1. 12 weeks of treatment with 30mg/kg/qd NVS-PAK1-1 plus 100mg/kg 1-ABT significantly reduced the average DRG volume of 7 month old mice. This treatment however was not well tolerated and did not protect against sensorineural hearing loss. The drug toxicity likely is a result of the very high serum and tissue concentrations of NVS-PAK1-1 leading to cardiac inhibition of PAK2. We have relied on the use of 1-ABT as a CYP450 inhibitor because we know NVS-PAK1-1 is rapidly metabolized by humans and that rapid breakdown will necessitate the use of pharmacokinetic inhibitors if it is translated into human trials. As the data in **Figure 13** demonstrates, and has borne out *in vivo*, the mice metabolize the compound much slower than humans. Given our PK data, pharmacokinetic inhibition isn't essential in the mice and the addition of the pan CYP450 inhibitor is blocking the metabolism of NVS-PAK1-1 so potently that we are overshooting our intended therapeutic window and experiencing toxicities as a result.

The development of sensorineural hearing loss in spite of the very high concentrations of NVS-PAK1-1 is interesting. Clearly by histology, these mice are still developing tumors, many of which are similar in size and architecture to the tumors in vehicle treated animals. But the histology and average DRG volume supports the hypothesis that the treatment appears to have stalled or prevented some subset of Schwann cells from forming tumors. There may be some critical role for PAK1 for tumor initiation in Merlin deficient Schwann cells. We know that some of the mice already had elevated ABR thresholds at baseline and in starting to treat these mice when we did, there may have already been a subset of Schwann cells that had passed the transition point where PAK1 is critical and were in a state where subsequent PAK1 inhibition had no effect. But in Merlin deficient Schwann cells which had not yet progressed to that stage, we may have blocked that transition into tumor formation.

There are two confounding factors in this NVS study which may have limited the observed efficacy of the compound. The first was been severity of the pathology in this particular co-hort. DRG volume tends to expand and ABR thresholds tend to increase over time in our *Nf2*-cKO mice. At 11 months of age, the average DRG volume in our FRAX-vehicle treated mice was 0.686 mm^3, at 7 months of age, the average DRG volume in our NVS-PAK1-1 vehicle treated mice was 1.255mm^3. For the average DRG volume to be 1.8x larger in mice that were 4 months younger, many of the mice in the NVS cohort must have either developed tumors unusually early or had tumor that grew unusually rapidly. We may have been treating the mice in the NVS cohort at a later stage in tumor progression than we had anticipated. The second limiting factor with the NVS study was the elevated drug concentration. At 30mg/kg the mice were sick. They had

serum concentration of NVS-PAK1-1 far exceeding the ranges in which the compound has been shown to be PAK1 selective and we need to be at a lower serum dose to be certain that any effects we see are truly specific to the inhibition of PAK1. The observed reduction in average DRG size is encouraging but the studies need to be repeated at a lower drug dose that is better tolerated and less likely to have off target effects in the tumor tissue.

Introduction

The NF-κB Signaling Pathway

The NF-κB signaling pathway was first described by David Baltimore and Ranjan Sen in 1986 as a class of 3 transcription factors which bound to κ chain enhancers in B cells [76]. Since that time, the class of NF-κB transcription factors has expanded to 5 and these proteins along with the signaling pathways which control their activation have been among the most studied in all of molecular biology. Although originally described for its role in B cell maturation and activation, the NF-κB pathway has now been shown to be critical in both the innate and adaptive immune response, controlling cell survival, cell proliferation, and activation [77]. The intense interest in the NF-κB pathway over the past 30 years has largely been driven by the fact that this pathway appears to be the nexus which controls the inflammatory response in humans. Inflammation plays a pivotal role in the pathology observed in most the of major causes of death in the United States including but not limited to cardiovascular disease, cancer, obesity, type 2 diabetes, neurodegenerative disorders, COPD, chronic kidney disease, and sepsis [78]. So, developing therapeutics modulate and control NF-κB has become a holy grail in treating modern disease.

The NF-κB family of transcription factors includes RelA (p65), RelB, c-Rel, p50, and p52. These transcription factors have been shown to act via homo and hetero dimerization. Thirteen of the 15 possible dimeric complexes have been described in the

literature but primarily, NF-κB signaling appears to terminate in nuclear translocation and activation of a heterodimer of either RelA/p50 or RelB/p52 [79]. The signaling cascades leading to the activation of these two heterodimers are generally divided into two distinct pathways: canonical and non-canonical. The canonical pathway terminates in nuclear translocation of RelA/p50 and the non-canonical pathway ends in the nuclear translocation of RelB/p52. There are multiple extensive reviews detailing the precise proteins and control mechanisms involved in NF-κB signaling [80,81]. In short, canonical NF-κB can be initiated by a variety of Toll Like, TNF superfamily receptors and cytokine receptors resulting in phosphorylation of the IKK complex consisting of NEMO, IKKα, and IKKβ. The activated IKK complex in turn phosphorylates an IκB family member, leading to its degradation, and the release and nuclear translocation of the RelA/p50 heterodimer. Non-canonical signaling is initiated via a subset of TNF superfamily receptors which activate NF-κB inducing kinase (NIK). NIK in turn phosphorylates IKKα homodimers leading to the processing of p100 into p52 and the nuclear translocation of the RelB/p52 heterodimer. With over 150 experimentally validated genes shown to be bound by and activated by the RelA/p50 heterodimer, activation of the NF-κB pathway has the ability to fundamentally alter the phenotype of a cell [82].

NF-κB in Cancer

As it pertains directly to cancer, the NF-κB signaling pathway has a very complex role. NF-κB signaling seems to influence different cell types in different ways in

different microenvironments such that depending on the precise context and genetics of the malignancy, NF-κB activation can either help or harm tumor growth.

The phenotypic variability associated with NF-κB activation in cancer can be exemplified by prototypic activator of the NF-κB canonical singling pathway, tumor necrosis factor alpha (TNFα). Originally isolated in 1975, TNFα was named tumor necrosis factor because it was found to trigger necrosis of tumor xenographs when injected into mice which had been transplanted with subcutaneous sarcomas [83]. Based up this observation, more than 4 multi center and 20 single center trials were undertaken to study the efficacy of localized perfusion of TNFα in combination with the chemotherapeutic melphalan for the treatment of non resectable, isolated soft tissue sarcomas and malignant melanomas. Eighty-90% of patients in these trials exhibited a significant clinical response after treatment, indicating that in this particular context, activation of NF-κB signaling is potently tumoricidal [84,85]. Consistent with the role of NF-κB activation restricting local tumor growth, adalimumub, the human monoclonal antibody targeted against TNFα, carries a black box warning that it may increase the prevalence of certain malignancies.

In other contexts, endogenous expression of TNFα seem to have the opposite effects where *in vivo*, TNFα expression has been shown to promote tumor growth [86-88]. Cancer cell intrinsic NF-κB signaling is generally characterized as a tumorigenic, where it can promote tumor growth, drug resistance, and metastasis [89,90]. NF-κB transcription factors were first characterized for their role in controlling the exponential, clonal expansion of B and T cells during a normal immune response and appear to be able to promote this same type of growth in many cancers [91]. Cancer cell intrinsic

activation of NF-κB been shown to induce gene expression of Cyclin D1, Cyclin E, and CDK2 to promote proliferation, BCL-XL and BCL-2 to promote survival, VEGF and HIF1α to promote angiogenesis, and MMP2/9 and ICAM1 to promote metastasis [92].

Experimentally, inhibitors of NF-κB signaling have been shown to act in a synergistic manner to improve cytotoxicity of chemotherapeutics *in vitro* [93,94]. Therapeutic development of NF-κB inhibitors has led to the identification of 700 compounds of varied potency and selectivity. Translation of these molecules into the clinic has been complicated both by the dual role these compounds have in either inhibiting or promoting tumor growth depending on context and by significant *in vivo* toxicity [95].

NF-κB Activation in our GEMM

NF-κB activation appears to play a critical role in the growth of many different types of solid tumors. When an Ingenuity Pathway Analysis was conducted on a data set of previously published microarray data from sporadic human vestibular schwannoma (sHVS), 32 genes annotated for an involvement in NF-κB signaling and 61 genes annotated as NF-κB transcription targets were significantly differentially expressed in the sHVS as compared to control tissue [96]. Merlin has previously been demonstrated as a suppressor of NF-κB signaling and PAK1 can act as a potent inducer of NF-κB. Therefore we reasoned that activation of NF-κB signaling by PAK1 could be responsible for oncogenic transformation in Merlin deficient Schwann cells [97,98].

The NF-κB signaling pathway is hyperactivated in our murine Merlin deficient schwannomas [96]. We discovered that NIK, the initiator kinase of the NF-κB non-

canonical signaling pathway, accumulated both as a full length protein and a 55kD catalytically active fragment in the Schwann cell tumors in our mice and in human VS. PAK1 has previously been shown to activate NIK directly and a similar NIK cleavage fragment has also been shown to play a pathogenic role in MALT lymphoma [98,99]. These data led us to hypothesize that the accumulation of NIK may be of physiological significant in Schwann cell tumors.

The 55kD fragment appeared to be an internal cleavage product which had an intact kinase domain but had lost the negative regulatory domain putatively rendering it constitutively active. We confirmed the presence of the kinase domain in the fragment through mass spectroscopy and demonstrated that both the full length NIK protein and this 55kD fragment were capable of binding to and phosphorylating IKKα. We then demonstrated that the endogenous levels of NIK which accumulated in Merlin deficient schwannomas were sufficient to cause significant phosphorylation of IKKα and drive NF-κB non-canonical signaling in the tumor cells [96].

Many different mouse models have been generated in an attempt to develop a more complete understanding of role of each of the proteins involved in NF-κB signaling. Unlike other murine knockouts of many of the other critical signaling proteins in the NF-κB signaling pathway including IKKα, IKKβ, and NEMO (IKKγ) which are embryonic lethal, germline biallelic disruption of NIK is viable in both mice and man [100-104]. In particular, the clinical presentation of the two patients described with total loss of functional NIK supports a hypothesis that NIK specific inhibition may have less systemic toxicity than what has previously been observed with other NF-κB inhibitors [104]. Based upon these data, a team at Genentech has developed a NIK small molecule

inhibitor which they are investigating as a potential therapeutic for systemic lupus erythematosus [105,106].

The studies in the chapter seek to investigate NIK as a potential therapeutic target for the treatment of NF2. We demonstrate that overexpression of NIK is sufficient to drive Schwann cell transformation and schwannoma development but that Schwann cell intrinsic endogenous expression of *NIK* (*Map3k14*) is not essential for tumor formation in Merlin deficient Schwann cells *in vivo*. These data support the hypothesis that NF-κB signaling is critical for the growth and development of Merlin deficient schwannoma but that NIK is not an essential protein in this process. Drug development may need to target the upstream pathways which connect loss of Merlin to the activation of NF-κB.

Materials and Methods

Animal Study Approval

All animal studies were carried out under the Institutional Animal Care and Use Committee (IACUC) of Indiana University School of Medicine approved protocol #11406 in accordance with the U.S. Department of Agriculture's Animal Welfare Act and the Guide for the Care and Use of Laboratory Animals.

Mice and Genotyping

NIK:

Forward: 5'- ATCAAGCTGGCCCTTAACCT-3'

Reverse: 5'-CAAGGAGTTCTTGTTTCCCAG-3'

Program: 94º C for 5 minutes, 34x (94º C for 60 seconds, 64º C for 30 seconds, 72 º C for 1 minute), 72º C for 10 minutes, hold at 4º C

Expected PCR fragment: FLOX: 303bp WT- 247bp

Statistical Methods

Statistical analyses were performed in GraphPad Prism 7.02. As described in the text, ANOVA or Student's T-test were used to test for differences between samples. Chi-squared analysis was used for the genetics analysis. Specific tests and significance levels can be found in the figures and figure legends.

Celecoxib Treatment.

Upon weaning, mice were fed with chow manufactured by ResearchDiets designed to deliver 300mg/kg/qd celecoxib or a control diet lacking celecoxib but identical in every other way.

COX-2 Activity Eliza

8-month-old *Nf2*$^{flox/flox}$*;PostnCre-* mice were separated into two groups of 5 mice and fed either celecoxib or vehicle diet for 5 days. On day 5, the mice were injected intraperitoneally with 100ng of tissue culture grade *Escherichia coli* O111:B4 derived LPS in 100ul of sterile PBS. Mice were sacrificed 2 hours later. The left cerebral hemisphere was harvested from each mouse. Tissues were processed and samples were run as described following the factory protocol using the Cayman Chemical COX Activity Assay Kit (760151).

Embryonic DRG Harvest and Culture

Wild type breeders were set up in the evening and left together for 24 hours. 14 days later in the morning, pregnant dams were sacrificed and embryos were removed. Embryos were placed in cold PBS+1% Pen/Strep (Lonza 10K/10K) and the dorsal root ganglion (DRG) were dissected from each embryo with the aid of a dissecting microscope. All DRGs isolated from an individual were pooled and placed into a tube containing 500µl of DMEM + 10%FBS and placed on ice. The DRGs were then digested in 0.05% trypsin-EDTA (Gibco) and dissociated with syringes. DRGs pooled from a single embryo were then plated on Poly-D-Lysine (PDL, .1mg/mL)/Laminin (.25mg/mL,

Sigma) coated 12-well plates at one embryo per well in SC Media I (SCM-I) comprised of DMEM with 50 U/mL penicillin, 50 μg/mL streptomycin, 2mM L-Glutamine (Lonza), 1X N2 supplement (Life Technologies), and 250 ng/mL Nerve Growth Factor (NGF, Harlan Bioproducts). The following day, the media was changed to SC Media II (SCM-II), which was identical to SCM-I except for the substitution of 2 μM Forskolin and 10 ng/mL Glial Growth Factor (GGF, Sigma) for NGF. The cells grow to confluence in 5-7 days at which point they are passaged in standard serum containing media (DMEM+10%FBS+1%L-glutamine+1% Pen/Strep) and re-plated onto PDL/Laminin plates. 12-22 hours after passage the media is replaced and the cells are maintained in SCM-II.

Orthotopic Transplant Studies

One million primary Schwann cells (P1 – P2) were transduced with IRES-eGFP or 309-801 NIK lentivirus. Transduction efficiency was measured after 24 hours using flow cytometry. 48 hours post transduction, cells were transplanted into the sciatic nerves of female B6.Cg-Foxn1/J (nude) mice purchased from Jackson labs. Mice were roughly 8-12 weeks old at the time of experimentation. Each mouse was anesthetized with isofluorane and a small incision was made using an 11 blade surgical scalpel. The sciatic nerve was then exposed with blunt dissection using scissors under a dissecting microscope. A 1:1 admixture of suspended Schwann cells and Culture® basement membrane extract (Trevigen) totaling 20 μl was injected into the right sciatic nerve of each mouse using a 33 gauge syringe (Hamilton). The wound was then closed with 5-0 prolene suture. Mice were monitored daily and buprenorphine was administered subQ at

the site of the incision for pain management.

RNA Extraction and qPCR Analysis

For extraction of RNA, trigeminal nerves were isolated from freshly sacrificed animals, washed in ice cold PBS, and then flash frozen in TRIzol Reagent (Thermo). RNA was then extracted from the samples using the PureLink RNA mini kit (Thermo) per manufacturer's protocol for phenol/chloroform extractions. RNA concentrations were measured on a NanoDrop and then cDNA synthesis was conducted utilizing the QuantiTect Reverse Transcription Kit (Qiagen). cDNA quantification was done using the Fast SYBR Green Real-Time PCR Master Mix (Life Technologies) with validated TaqMan gene probes (ABI) (Mm00478375_g1 for Ptgs2, Mm00444166_m1 for NIK, Mm99999915_g1 for GAPDH), and an ABI 7500 Fast Thermal Cycler.

Primary Antibody List Western Blot

COX-2 (Santa Cruz #1745), RelA (Cell Signaling #8242), RelB (Cell Signaling #10544), NIK (Cell Signaling #4994)

Primary Antibody List IHC

RelA (Santa Cruz sc-109), RelB (Santa Cruz sc-226), NIK (Cell Signaling #4994), GFP (Abcam ab1218)

Results

Targeting Proteins Downstream of NF-κB Activation May be Insufficient to Prevent the Formation and Growth of Schwann Cell Tumors

Clinical interest in targeting NF-κB in vestibular schwannoma was sparked in 2014 following a retrospective case review of 347 patients with vestibular schwannoma. Patients whom happened to be taking aspirin were less likely to experience tumor growth than those patients who did not take aspirin [107]. Aspirin is a COX-1/2 (cyclooxygenase 1/2) inhibitor. The observed tumorostatic effect observed was attributed to the ability of aspirin to inhibit COX-2. COX-2 catalyzes the first reaction in the pathway which converts arachidonic acid into prostaglandins and thromboxane. COX-2 has been previously well studied for its role in driving inflammation and supporting tumor growth [108]. Expression of *PTGS2,* the gene which encodes COX-2, is induced by NF-κB. As measured by immunoblotting and immunohistochemistry, COX-2 expression has been directly correlated with Schwann cell tumor growth *in vivo* [109]. Based upon this data, a Phase II double blind trial (NCT03079999), is currently ongoing to test the efficacy of aspirin in slowing tumor growth in patients with vestibular schwannoma.

We were interested to determine if we could prevent the formation of tumors in our *Nf2*-cKO mice via inhibition of COX-2. In order to separate the potential effects of COX-1 inhibition vs COX-2 inhibition, we chose to treat our mice with the potent, COX-2 selective inhibitor, celecoxib. We allowed newly weaned *Nf*2-cKO mice to feed on a diet infused with celecoxib at a concentration designed deliver 300mg/kg/qd of the inhibitor to each mouse. We found that although *PTGS2* was highly expressed in

schwannoma bearing tissues in our mice, the COX-2 inhibitor celecoxib had no therapeutic benefit in preventing tumors in our *Nf2*-cKO mice (**Figure 19**) [110]. We did not treat mice beyond 6 months to test whether COX-2 inhibition could slow the growth of the developing tumors.

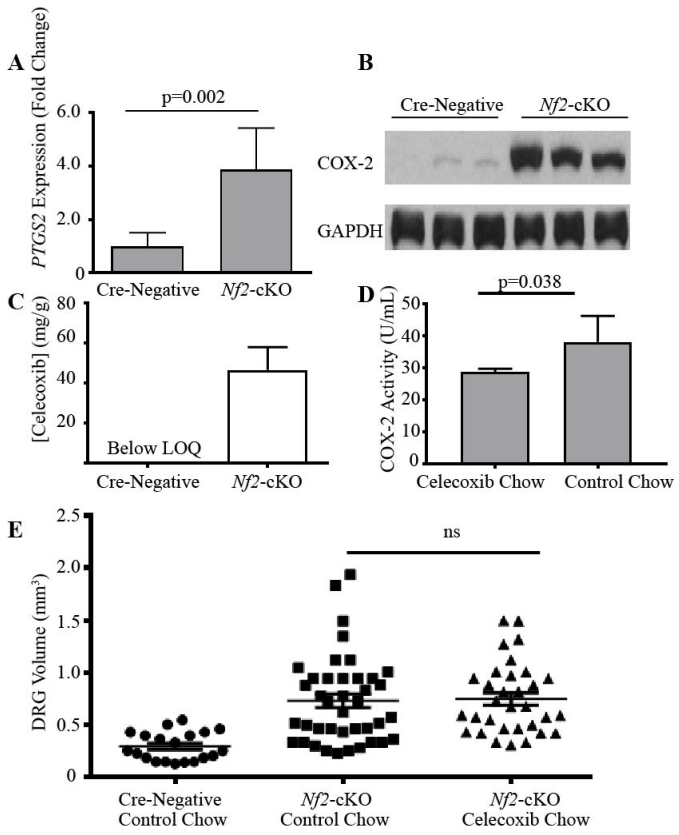

Figure 19. Celecoxib fails to prevent schwannoma formation in *Nf2*-cKO mice. (A) *PTGS2* gene expression in the trigeminal nerve of 6-8 month old mice normalized to levels in Cre-Negative mice. Six mice/group, p=0.002, students t test, error bars represent SEM. **(B)** Western blot analysis of trigeminal nerve lysates from 6 month old mice. **(C)** Mass spectroscopy measuring concentrations of celecoxib present in the DRG of mice treated for 6 months, error bars represent SEM **(D)** Eliza measuring COX-2 activity in the brain 8 month old mice fed Celecoxib infused or control chow for 5 days and then injected with 100ng LPS to induce COX-2 expression. 3 mice/group, p=0.038, students t-test, error bars represent SD (**E**) Quantification of average DRG volume at 6 months of age. 4 anatomically matched DRG were measured from each mouse. Cre-Negative n= 5 mice, control chow, n=10 mice, celecoxib chow, n=8 mice, one-way ANOVA with Tukey's test, error bars represent SEM.

Overexpression of Constitutively Active NIK can Induce the Formation of Schwannomas

Both the canonical and non-canonical NF-κB signaling pathways are upregulated in Merlin deficient Schwann cells. One mechanism previously shown in HEK-293 and HeLa cell lines to simultaneously activate both pathways is the accumulation of NF-κB inducing kinase (NIK) [111-113]. Under basal conditions, NIK phosphorylates IKKα at low levels to drive non-canonical signaling. When NIK accumulates in cells, the resultant high levels of pIKKα promote phosphorylation of IKKβ within the IKK complex to activate the canonical signaling pathway. Given NIKs ability to activate both the canonical and non-canonical NF-κB pathways, NIK accumulation could explain the NF-κB activation in Merlin deficient Schwann cells.

To probe the physiologic changes induced by NIK accumulation in Schwann cells, a transducible construct of the 55kD NIK fragment containing an eGFP reporter was generated. Lentiviral transduction of the 55kD-NIK-eGFP construct activated both canonical and non-canonical signaling in primary Schwann cells. Transduction of NIK increased the proliferation of primary murine Schwann cells and knockdown of the protein with an shRNA reduced the proliferation of MS02 and HEI-193 cells [96]. Overall, many of the changes observed in the Schwann cells transduced with the 55kD-NIK fragment appeared to mimic changes observed in Schwann cells upon loss of Merlin.

We next conducted a Schwann cell transfer experiment to test whether NIK accumulation could cause the Schwann cells to form tumors *in vivo*. Primary embryonic Schwann cells were harvested from the DRGs of E13.5 old mice and expanded in culture

for two weeks. Cell were then transduced with either lentivirus harboring a 55kD-NIK-eGFP construct or control IRES-eGFP construct. Forty eight hours after transduction, the cells were checked for eGFP positivity via flow cytometry and 1 million $eGFP^+$ cells were injected into the sciatic nerve of nude, athymic (*Foxn1*^{nu}) mice (**Figure 20A**). After 5 months the mice were sacrificed and the sciatic nerves were serially sectioned at the site of injection. Schwann cell tumors were present in 11/13 of the sciatic nerves injected with 55kD-NIK-eGFP Schwann cells and 0/7 of the sciatic nerves injected with IRES-GFP Schwann cells (**Figure 20B**). The tumor forming Schwann cells stained positive for GFP and had high levels of RelA and RelB localized to the nucleus (**Figure 21**). This indicated that Schwann cell intrinsic accumulation of active NIK was sufficient to activate both canonical and non-canonical NF-κB signaling and trigger Schwann cells to form tumors. Importantly, GFP positive cells were still present at the site of injection in the mice which received IRES-eGFP Schwann cells. All of the cells were suspended in Matrigel for injection and there is some local tissue disruption observed due the continued presence of the protein gel matrix. However, no histological signs of schwannoma were observed in mice receiving IRES-eGFP transduced cells and the GFP positive cells did not have significant nuclear localization of either RelA or RelB (**Figure 21**).

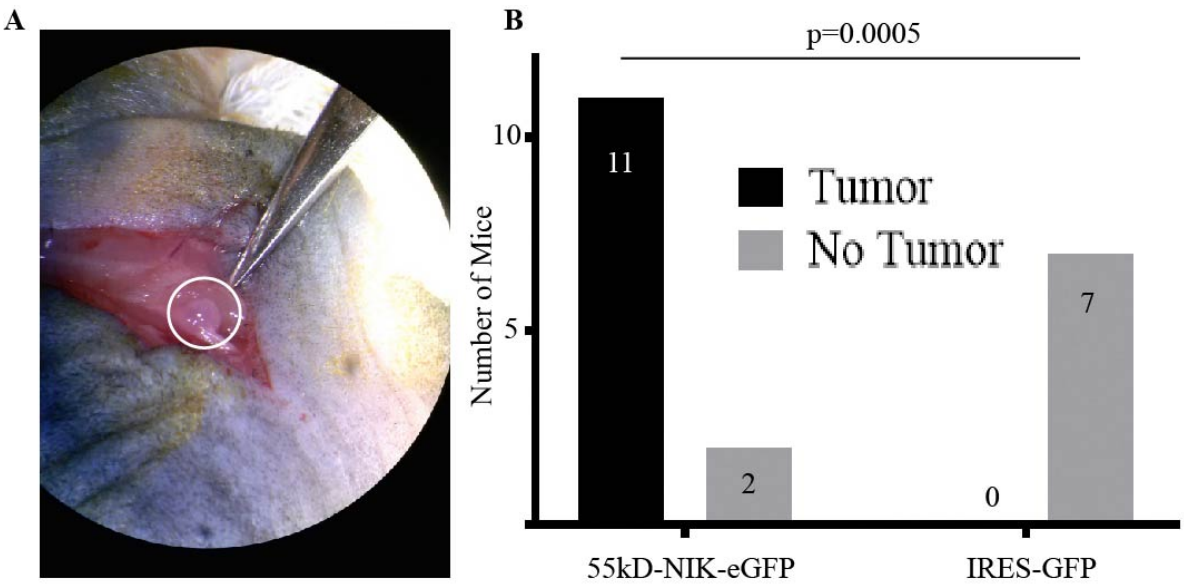

Figure 20. 55kD-NIK-eGFP transduced Schwann cells form tumors *in vivo*. (A) Gross image of sciatic nerve post injection. (**B**) Quantification of tumors 5 months post transplant, p=0.0005, Fisher's exact test.

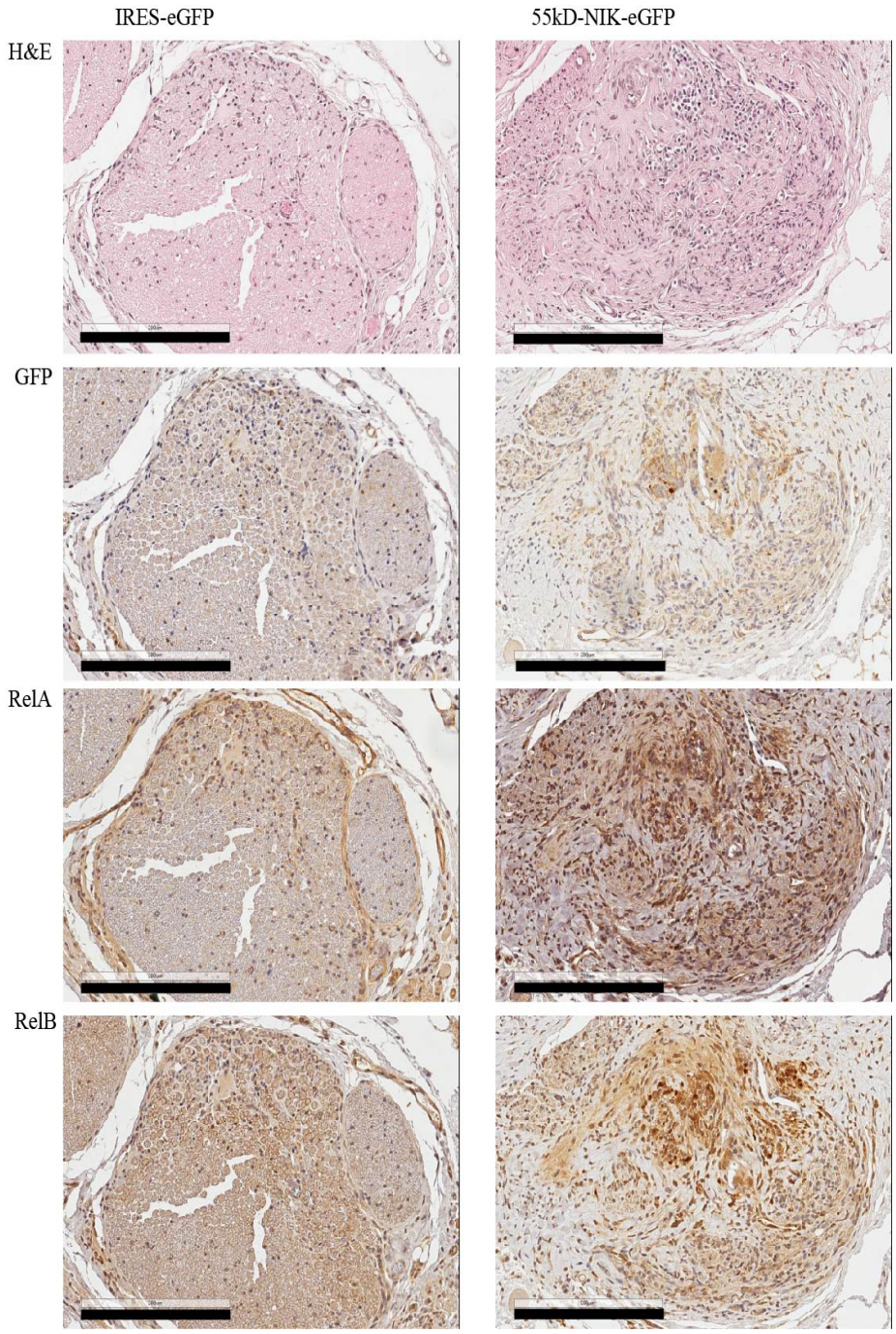

Figure 21. Transferred tumorigenic Schwann cells are GPF, RelA, and RelB triple positive. Representative serial cross sectional images from the sciatic nerves of *Foxn1*^{nu} mice 5 months after Schwann cell transfer. Original magnification 20x, scale bars= 200μm.

Commercially Available NF-κB inhibitors can Reduce Schwannoma Cell Proliferation *in vitro*

Having demonstrated that accumulation of active NIK is sufficient to transform wild type Schwann cells, we wanted to determine if inhibition of NF-κB signaling could slow the growth rate of previously transformed schwannoma cells. None of the NIK specific inhibitors appear to be commercially available so we acquired two less selective NF-κB inhibitors, Bardoxolone Methyl and IKK-16. Bardoxolone Methyl is a reversible, mildly selective IKK/RelA inhibitor and *Nrf2* activator and is the only direct inhibitor of NF-κB with FDA approval where it holds orphan status for the treatment Alport Syndrome. Bardoxolone Methyl has been explored in phase I/II trials for the treatment of chronic kidney disease and refractory late stage solid tumors and lymphoma and has been carried forward into Phase III trials in diabetic kidney disease (NCT03550443) and pulmonary hypertension (NCT03068130) [114,115]. IKK-16 was chosen because it is a potent and significantly more selective NF-κB inhibitor which targets IKKα and IKKβ, blocking both canonical and non canonical signaling [116]. To test these compounds we utilized 3 different murine schwannoma cell lines: the Merlin deficient MS02 cells, MS02 cells in which Merlin expression had been restored via lentiviral transduction, and MS12 cells, a Merlin sufficient Schwann cell line generated by spontaneous transformation of Schwann cells derived from the sciatic nerve of an $Nf2^{flox/flox}$; Cre-negative animal and serially passaged.

In the three Schwann cell lines, Bardoxolone Methyl had an IC_{50} of 0.2 μM which was roughly half of the published IC_{50} of 0.4 μM in HCT-8 human adenocarcinoma cells and 0.32 μM in normal human colonic epithelial cells [117] (**Figure 22A**). Across

multiple experiments Bardoxolone Methyl was found to have a very narrow therapeutic window in Schwann cells where it had no measurable effect at concentrations of 100 nM or less, almost completely blocked proliferation at concentrations around 500 nM and killed cells rapidly at concentrations of 1mM or greater. In the same cell lines, IKK-16 had an IC_{50} of 0.52 μM (**Figure 22B**). At the recommended dosing of 0.75-0.8 μM, IKK-16 inhibited Schwann cell proliferation by greater than 90% and became cytotoxic at concentrations greater than 1 mM [118,119]. Neither compound displayed any significant selectivity against the Merlin deficient Schwann cells over the Merlin sufficient Schwann cells at any concentration tested.

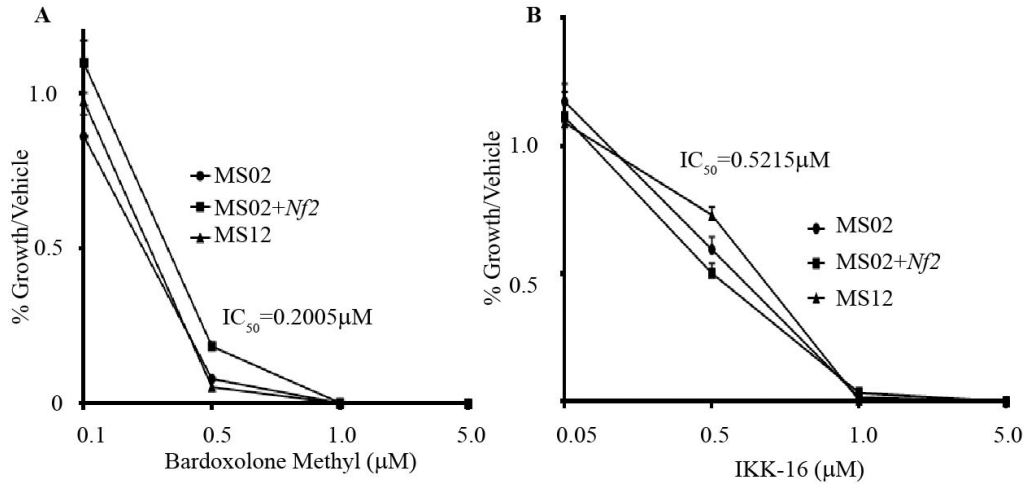

Figure 22. NF-κB inhibitors can inhibit schwannoma cell proliferation *in vitro*. (A) 96 hour CellTiter-Glo assay with Bardoxolone Methyl, IC_{50} = 0.2 μM, error bars represent SEM. (**B**) 96 hour CellTiter-Glo assay with IKK-16, IC_{50} = 0.5 μM, error bars represent SEM. IC_{50} values calculated in GraphPad Prism via the [inhibitor] vs normalized response nonlinear fit algorithm.

Germline Deletion of NIK is Viable in our *Nf2*-cKO Mice but Mice Have a Severely Shortened Lifespan

Consistent with what we observed in the Schwann cells, as a class, broad NF-κB inhibitors have very narrow therapeutic windows and often exhibit profound, pleotropic toxicities *in vivo*. To genetically evaluate how global, selective NIK inhibition could alter the phenotype of our *Nf2*-cKO mice we crossed *Nf2*-cKO animals with *NIK* germline deficient mice. Upon birth, *NIK*$^{-/-}$ mice appeared normal but consistent with the literature, the animals die between 4-6 months of age from a CD4+ T-cell dependent hyper eosinophilic syndrome [120]. These *NIK*$^{-/-}$ mice lack lymph nodes, have abnormal thymic architecture and don't exhibit normal B cell maturation. It is reasonable to suspect that the eosinophilia observed in these animals is a result of a failure in B and T cell development and would not be phenocopied by small molecule inhibition of NIK in animals with an established, mature immune system. Indeed, at least over a 30 day period, complete genetic ablation of *NIK* in mature animals using an inducible tamoxifen-Cre system triggered only a mild reduction in mature B cells and serum IgA levels without an aberrant T cell response [121]. We never detected schwannomas in the *Nf2*$^{flox/flox}$;*NIK*$^{-/-}$;*Postn*-Cre mice but the combination of the systemic inflammation and early mortality significantly limited the definite conclusions we could draw from these mice.

Schwann Cell Expression of *NIK* Appears to be Lost in *Nf2*$^{flox/flox}$;*NIK*$^{flox/flox}$;*Postn*-Cre Animals

To genetically assess how inhibition of Schwann cell intrinsic expression of NIK could alter the NF2 like phenotype in our *Nf2*-cKO mice, we crossed *Nf2*-cKO animals with mice containing loxP recombination sites flanking exon 2 of NIK [121]. *NIK* expression is generally close to or below the limit of detection by qPCR and undetectable by Western blot in Merlin sufficient Schwann cells and non-tumor bearing trigeminal nerves. In the trigeminal nerves of 10 month animals, biallelic disruption of *NIK* in our *Nf2*-cKO animal (*Nf2*$^{flox/flox}$;*NIK*$^{flox/flox}$;*Postn*-Cre, *Nf2*;*NIK*-cDKO), reduced *NIK* mRNA expression down to the levels of Cre-negative animals. Levels of *NIK* mRNA in *NIK* haplosufficient animals (*Nf2*$^{flox/flox}$;*NIK*$^{flox/+}$;*Postn*-Cre, *Nf2* cKO;*NIK*-Het) were similar to those observed in *Nf2*-cKO animals (**Figure 23**).

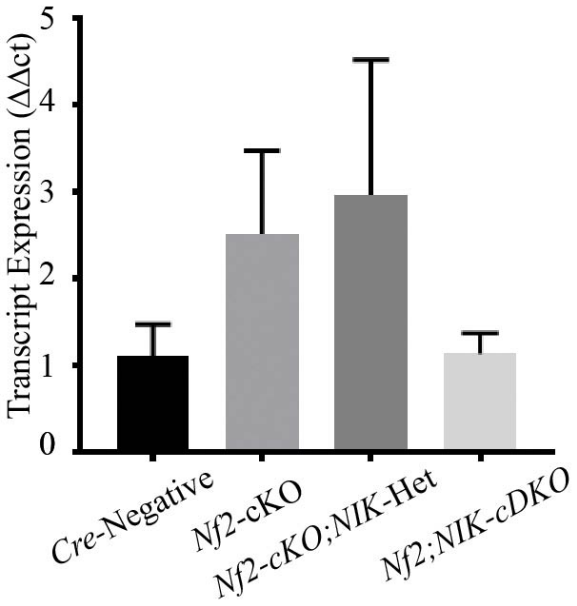

Figure 23. Conditional deletion of *NIK* reduces *NIK* mRNA expression in Schwann cell predominant tissues. NIK expression as measured by RT-qPCR in the trigeminal nerves of 10 month old mice and normalized to the levels in the Cre-negative animals.

NIK Conditional Deletion is Viable in our *Nf2*-cKO Mice and does not Alter the Sensorineural Hearing Loss Phenotype

ABR testing was conducted on cohorts of mice at 6, 8, and 10 months of age. ABR hearing thresholds have been previously well characterized in our *Nf2*-cKO mice wherein elevations in hearing correlate with the presence of tumor [61]. Cre-negative mice have average hearing thresholds around 40dB out to one year of age while a subset of *Nf2*-cKO mice begin to develop sensorineural hearing loss by 6 months of age. A significant difference in average ABR thresholds can be observed by 8 months of age between *Nf2*-cKO animals and Cre-negative controls. Most *Nf2*-cKO mice demonstrate elevated hearing thresholds by 10 months of age. Hearing loss often occurs asymmetrically, developing independently at different times and different rates of progression in each ear so both ears were always tested independently in each mouse.

By 6 months of age, the *Nf2*-cKO;*NIK*-Het had developed significantly elevated hearing thresholds compared with Cre-negative mice. Hearing in the *Nf2*;*NIK*-cDKO was within normal limits (**Figure 24**). This was consistent with trigeminal nerve histology where some of the *Nf2*-cKO;*NIK*-Het displayed significant Schwann cell hyperplasia. Nerves from the *Nf2*;*NIK*-cDKO appeared more normal. By 8 months however, the *Nf2*;*NIK*-cDKO mice demonstrated significantly elevated hearing thresholds compared to Cre-negative animals. These ABR thresholds were similar in magnitude to the *Nf2*-cKO;*NIK*-Het mice ($p=0.37$, Two Way RM ANOVA with multiple comparisons). Neither the progression of sensorineural hearing loss between 8 to 10 months ($p=0.33$, 2 way ANOVA with repeated measures) nor the magnitude of sensorineural hearing loss at 10 months of age ($p=0.14$, Two Way RM ANOVA with multiple comparisons) were

different between *Nf2*;*NIK*-cDKO, and *Nf2*-cKO;*NIK*-Het mice. Genetic deletion of *NIK* therefore appears to have slightly delayed on the onset of sensorineural hearing loss but ultimately neither prevented the development of hearing loss nor reduced the magnitude of hearing loss at 8 or 10 months of age.

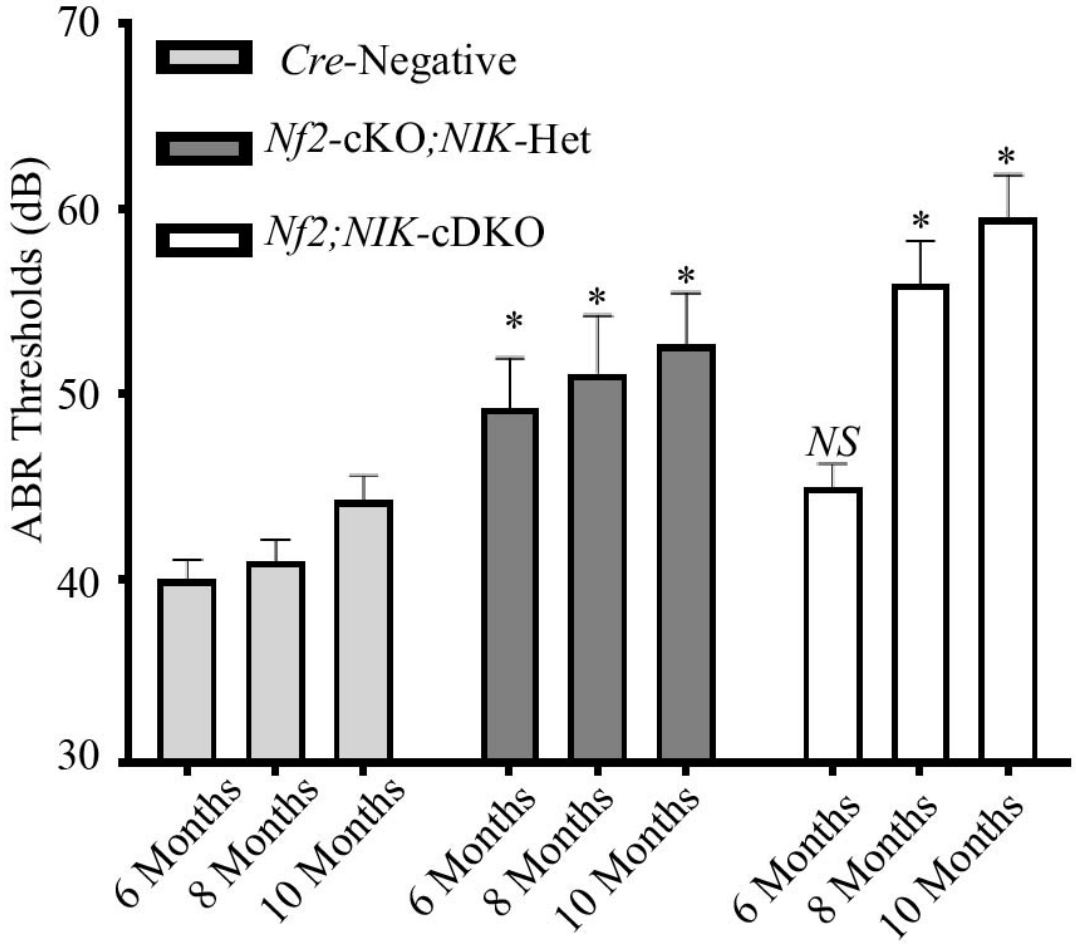

Figure 24. ABR Thresholds in *NIK*-cKO mice. Repeated ABR thresholds in a cohort of mice at 6, 8, and 10 months of age. Tests were conducted independently in each ear. Error bars represent SEM. Cre-negative n=12 mice, *Nf2*-cKO;*NIK*-Het n=13 mice, *Nf2*;*NIK*-cDKO n=21 mice. * represents $p<0.05$ as compared to the age matched Cre-negative control group, 2 way ANOVA with multiple comparisons. Statistics described in text have not been indicated on the figure.

NIK Conditional Deletion Mildly Reduces DRG Volume

At 10 months of age, mice with a conditional NIK deletion were sacrificed and their spinal cords and nerve roots were dissected out. Tumors grow in the spinal DRG with 100% penetrance in our *Nf2*-cKO mice and as the tumors grow in size, the average volume of the DRG expands accordingly. Because the schwannomas grow interspersed with normal nerve tissue is it difficult to precisely quantify tumor size directly so we utilize gross DRG volume as a surrogate for the volume of tumor within each DRG. Normal DRG volume varies with anatomical location. Therefore the same 4 DRG corresponding to nerve roots L3-L6 in the lumbosacral plexus are measured to limit anatomical variability in our measurements (**Figure 25A**). At 10 months of age, the average DRG size of the *Nf2*;*NIK*-cDKO was mildly reduced when compared to the *Nf2*-cKO;*NIK*-Het mice. The average DRG size of the *Nf2*-cKO;*NIK*-Het mice was significantly elevated compared to Cre-negative controls ($p=0.0062$), One Way ANOVA with Tukey's test) while the average size of the *Nf2*;*NIK*-cDKO mice was within normal limits ($p=0.11$, One Way ANOVA with Tukey's test). The largest *Nf2*-cKO;*NIK*-Het DRG of 3.86 has been included in the figure but was excluded from the statistical comparisons in the prior statement as it met criteria for a statistical outlier. (**Figure 25B**). Only one NIK fully sufficient *Nf2*-cKO mouse could be included in the analysis because only one strain matched NIK fully sufficient *Nf2*-cKO mouse survived to 10 months of age. Three mice of the same genotype had to be sacrificed at 6, 8, and 9 months of age per LARC due to the development of large subdermal malignant peripheral nerve sheath tumors (MPNSTs).

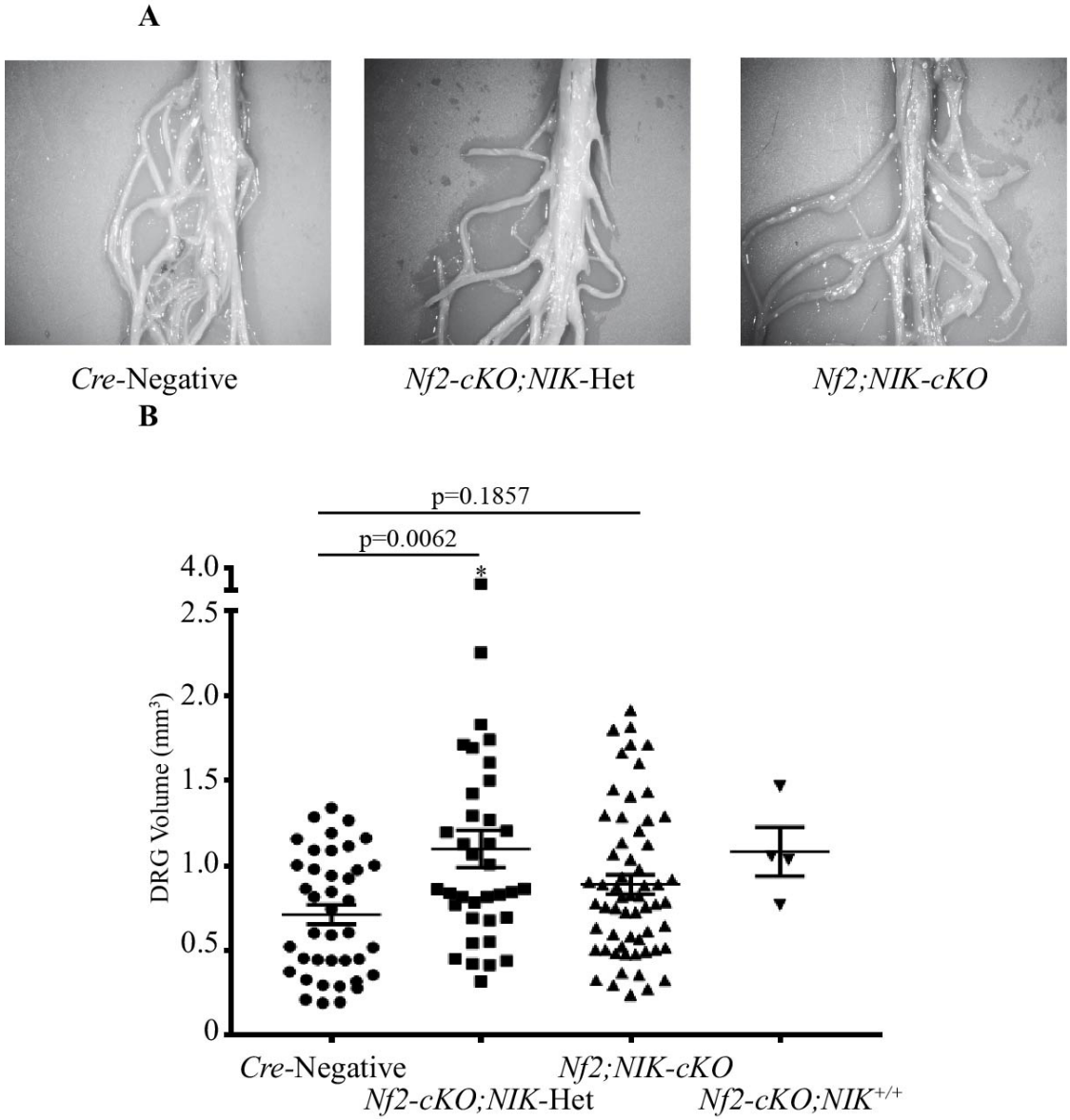

Figure 25. Genetic Deletion of *NIK* reduces average DRG volume in 10 month old *Nf2*-cKO mice. (A) Representative lumbosacral plexi from 10 month old mice, original magnification 1.5x. (**B**) Volume measured in 4 anatomically matched spinal DRG/mouse. Error bars represent SEM. Cre-negative n=10 mice, *Nf2*-cKO;*NIK*-Het n=9 mice, *Nf2*;*NIK*-cDKO n=15 mice, *Nf2*-cDKO;$NIK^{+/+}$ n=1 mouse. p=0.0062, p=0.19 One way ANOVA with Tukey's test. * indicates data point left out of the statistical analysis.

Deletion of *NIK* Alters Tumor Histology and Reduces Activation of NF-κB

Histological sections were taken from DRG and trigeminal nerves (CNV) from 10 month old mice with conditional NIK deletions. Schwannoma was observed in all of the Cre-positive mice. The tumors in the *Nf2*-cKO;*NIK*-Het mice in the DRG and CNV demonstrated Antoni A and Antoni B histology with disorganized whirling Schwann cells (**Figure 26**). Tissues in the *Nf2*;*NIK*-cDKO mice had fewer areas of defined Schwann cells whirls or Verocay bodies but instead had a dense hypercellularity with more cells but less stroma/cell. This histology is consistent with what we observed at earlier time points in our *Nf2*-cKO mice. Tissues that eventually will develop frank schwannoma progress through a precursor lesion or early tumor stage of dense hypercellularity before the classical schwannoma histology develops prominently.

We anticipated that deletion of *NIK* would reduce NF-κB activation in Schwann cells. Western blotting and IHC staining demonstrated a significant reduction in total RelA and RelB levels in the tumor bearing tissues in *Nf2*;*NIK*-cDKO mice (**Figure 27A**). NIK was not detectable in any of the genotypes. There was also a reduction in the nuclear localization of RelA and Rel B in Schwann cells in *Nf2*;*NIK*-cDKO animals compared to *Nf2*-cKO;*NIK*-Het mice indicative that Schwann cell intrinsic loss of NIK had reduced NF-κB activation in the Merlin deficient Schwann cells (**Figure 27B**).

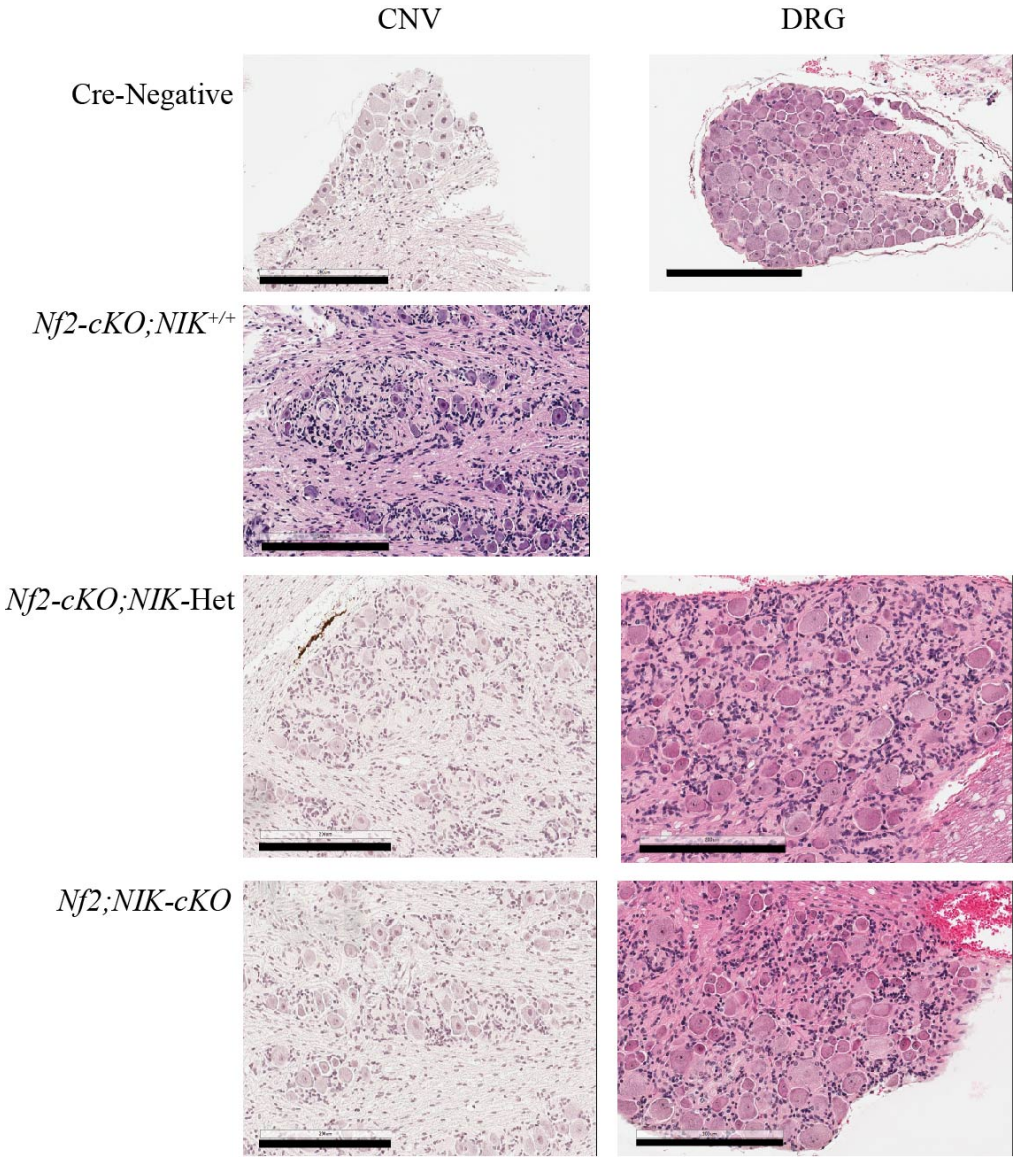

Figure 26. Histology of spinal DRG and CNV in 10 month old mice. Representative H&E stained sections from 10 month old mice. Original magnification 20x. Original magnification 20x, scale bars= 200μm.

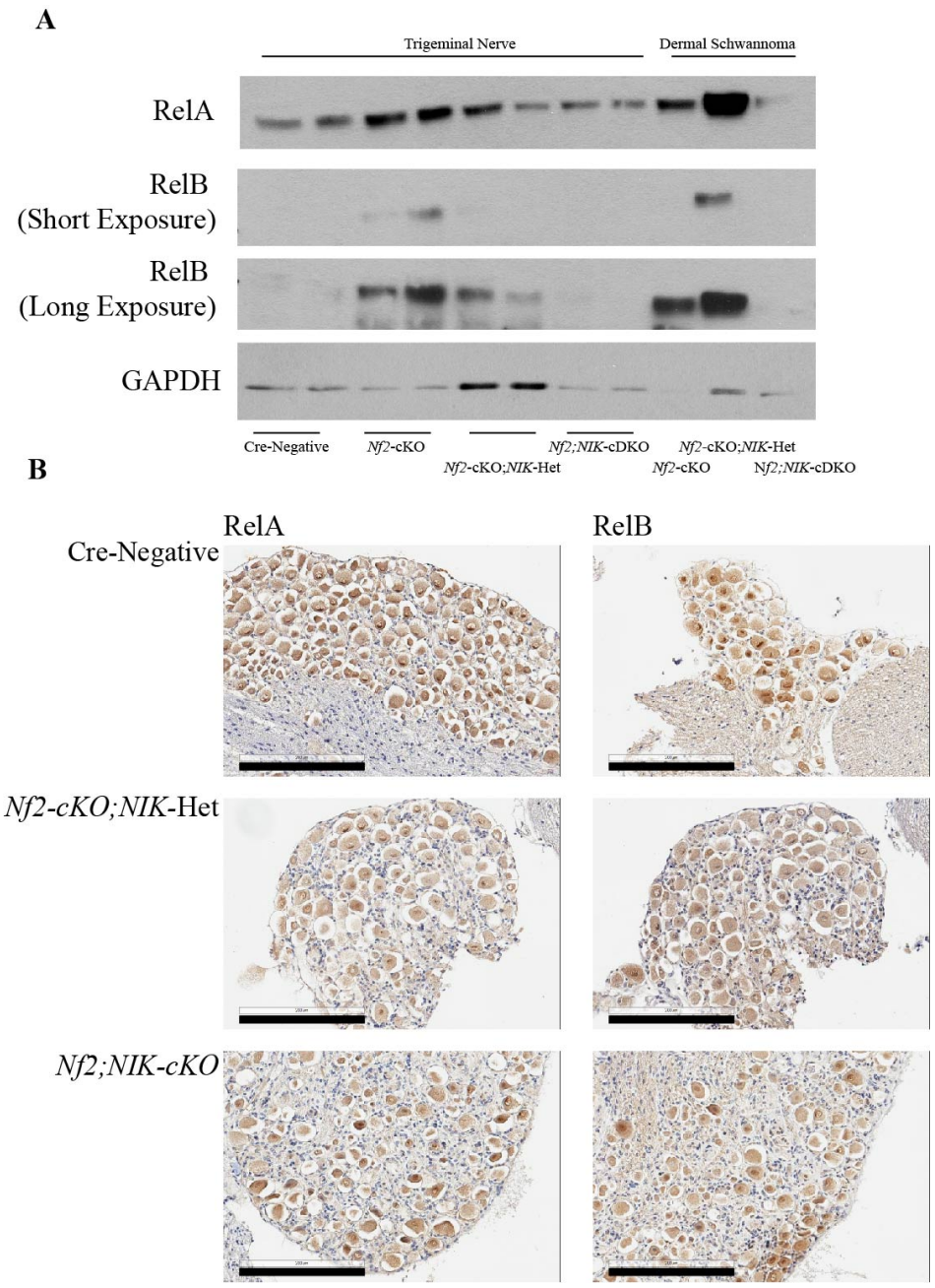

Figure 27. Deletion of *NIK* in Schwann cells reduces NF-κB activation in schwannomas. (A) Western Blot of trigeminal nerve lysates from 10 month old mice and dermal schwannomas from 6-10 month old mice. (**B**) Representative immunohistochemistry from CNV of 10 month old mice. Original magnification 20x, scale bars = 200μm.

Nf2;NIK-cKO Animals Demonstrate non Mendelian Genetics Favoring the Reduction of *NIK* in *Nf2*-cKO Animals

The genetic background of the mice can influence elements of the NF2 like phenotype we observe in our *Nf2*-cKO model. Therefore, when generating the *Nf2;NIK*-cKO mice we first crossed the $Nf2^{flox/flox}$;*Postn*-Cre mice with the $NIK^{flox/flox}$ mice to create an F1 generation that was obligate $Nf2^{flox/+}$;$NIK^{flox/+}$. We intended to generate all the necessary cohorts of mice required to assess the role of *NIK* in schwannoma genesis and growth by setting up breeders from this F1 generation using one Cre-positive male with two Cre-negative female breeders or one Cre-negative male with two Cre-positive female breeders (**Figure 28A**). With this strategy we knew the Cre-mice could only be carrying one Cre-allele. Using this strategy we expected to generate 8-9 *Nf2*-cKO;$NIK^{+/+}$ but in reality we only generated 4 *Nf2*-cKO;$NIK^{+/+}$ mice, 3 of which had to be sacrificed prior to 10 months of age due to the development of MPNSTs as shown in **Figure 29**. That left us with a single *Nf2*-cKO;$NIK^{+/+}$ for our analysis.

Regrouping we decided to set up new breeders utilizing *Nf2*-cKO;*NIK*-Het mice to increase our desired allele frequencies (**Figure 28B**). This would allow for the generation of increased percentages of *Nf2*-cKO;$NIK^{+/+}$ mice with *Nf2*-cKO;*NIK*-Het, and *Nf2;NIK*-cKO littermates to compare with one another. We would be able to compare *Nf2*-cKO;*NIK*-Het, and *Nf2;NIK*-cDKO between the generations to insure the extra generation did not cause a shift in the phenotype. We observed no differences in the phenotypes of the *Nf2*-cKO;*NIK*-Het, and *Nf2;NIK*-cDKO generated from the two different breeding schemes and have been able to generate an additional 5 *Nf2*-

cKO;*NIK*$^{+/+}$ mice, the oldest of which is currently 8 months old. Interestingly, using this breeding schema we see a strong bias against the generation of *Nf2*-cKO;*NIK*$^{+/+}$ mice (p=0.041, Chi square test). This bias against generating *NIK*$^{+/+}$ animals occurs only in *Nf2*$^{flox/flox}$;Cre-positive animals leading us to believe that loss of a single allele of *NIK* is playing a major protective role during embryonic development of the *Nf2*-cKO animals.

A

$Nf2^{flox/+}$; $NIK^{flox/+}$;*Postn*-Cre^{+} Male X $Nf2^{flox/+}$; $NIK^{flox/+}$;*Postn*-Cre^{-} Female

$Nf2^{flox/+}$; $NIK^{flox/+}$;*Postn*-Cre^{-} Female

Generate 278 Mice

	Expect:	Get:
Nf2-cKO Mice:	34.75	29

Cre+	Expect:	Get:
$Nf2^{flox/flox}$; $NIK^{+/+}$ mice:	**8.56**	**4**
$Nf2^{flox/flox}$; $NIK^{flox/+}$ mice:	17.125	18
$Nf2^{flox/flox}$; $NIK^{flox/flox}$ mice:	8.56	7

Cre^{+} Mice	Cre^{-} Mice
Mendelian Genetics 1:2:1	Mendelian Genetics 1:2:1
Chi Square Value: 2.31	Chi Square Value: 2.077
p=0.32	p=0.35

B

$Nf2^{flox/flox}$; $NIK^{flox/+}$;*Postn*-Cre^{+} Male X $Nf2^{flox/flox}$; $NIK^{flox/+}$;*Postn*-Cre^{-} Female

$Nf2^{flox/flox}$; $NIK^{flox/+}$;*Postn*-Cre^{+} Female

Generate 84 Mice

	Expect:	Get:
Nf2-cKO Mice:	52.5	49

Cre+	Expect:	Get:
$Nf2^{flox/flox}$; $NIK^{+/+}$ mice:	**13.125**	**5**
$Nf2^{flox/flox}$; $NIK^{flox/+}$ mice:	26.25	27
$Nf2^{flox/flox}$; $NIK^{flox/flox}$ mice:	13.125	17

Cre^{+} Mice	Cre^{-} Mice
Mendelian Genetics 1:2:1	Mendelian Genetics 1:2:1
Chi Square Value: 6.388	Chi Square Value: 2.086
p=0.041	p=0.35

Figure 28. Loss of *NIK* provides an embryonic survival advantage to *Nf2*-cKO mice. **(A)** Breeding schemas highlighting expected and actual outcomes of mice born with the given genotype from breeding F1 siblings. **(B)** Breeding schemas highlighting expected and actual outcomes of mice born with the given genotype from breeding F1 siblings.

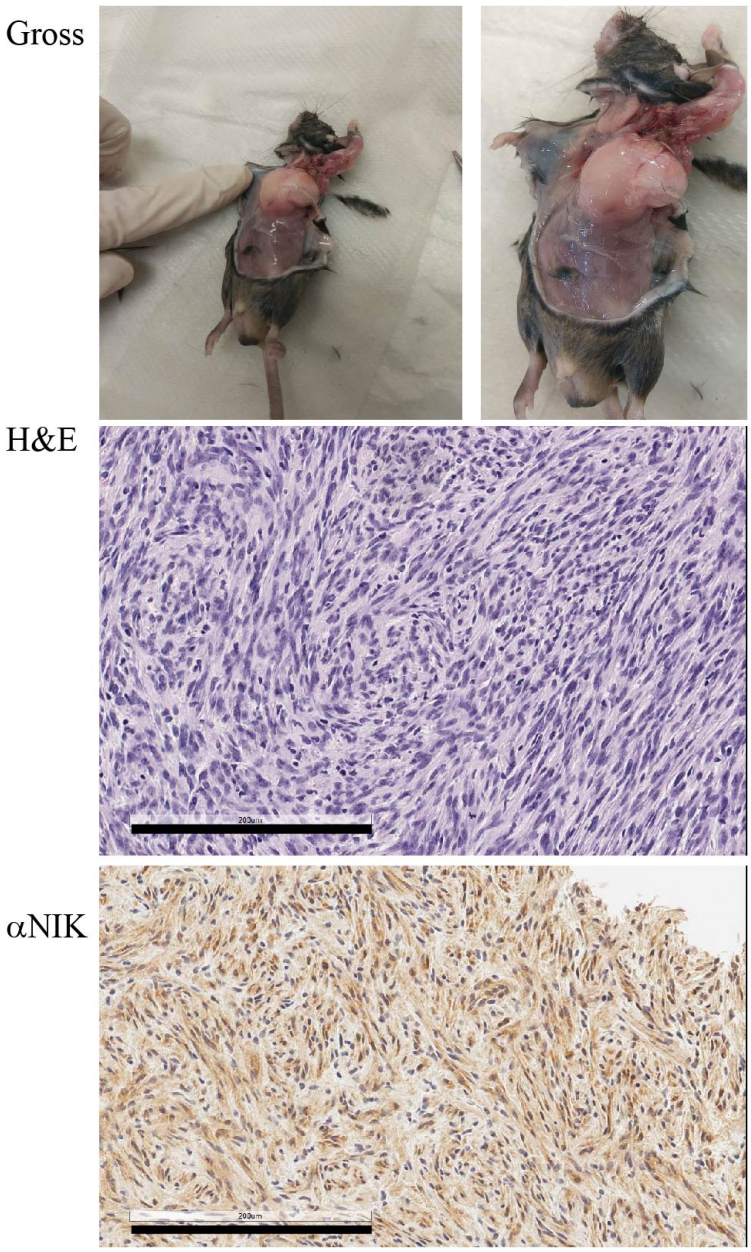

Figure 29. MPNST in 9 month old *Nf2*-cKO;*NIK*$^{+/+}$ mice. Gross images with representative H&E and αNIK IHC sectioning of a mass growing out of the rib cage of a 9 month old animal. Histologic images original magnification 20x, scale bars = 200μM.

Discussion

Having previously recognized activation of the NF-κB pathway to be a universal phenomenon in late state Merlin deficient schwannoma, we attempted pharmacologic and genetic manipulations to increase our knowledge of the precise role of the NF-κB pathway in schwannoma formation and development. Investigating the role of the NF-κB target gene COX-2 seemed to be a logical place to start because there are already potent, well tolerated, FDA approved COX-2 inhibitors that patients use long term for control of arthritis. If overexpression of COX-2 was a major mechanism through which NF-κB activation promoted schwannoma growth then we would have had an easily transferrable therapeutic for our NF2 patients. However, inhibition of COX-2 through the use of Celecoxib demonstrated no inhibitory effects on tumor formation out to 6 months of age.

There is still some hope for the aspirin clinical trial. We didn't test the effects of COX-2 inhibition on the growth of established tumors. Aspirin inhibits both COX-1 and COX-2 so there could also be some role for limiting tumor progression through inhibiting COX-1 in the tumor tissue. Our data do not support the use of COX-2 specific inhibitors as chemopreventative agents but the clinical data may still find a beneficial effect of aspirin as growth inhibitory in large VS.

Trying to treat vestibular schwannomas via targeting one or a small number of NF-κB target genes may be akin to attempting to plug a hole in a dam with your finger. There are hundreds of NF-κB target genes. NIK accumulation be generating a pressure towards tumor formation too strong for inhibition of a single downstream target to halt. So we decided to focus more upstream and try dampen the NF-κB activation directly in

order to relieve pressure behind the dam such that the normal barriers which serve to protect against tumor formation could keep the schwannomas contained.

Of all of the various proteins within the NF-κB pathway that we could target for therapeutic interventions, NF-κB inducing kinase (NIK) seemed the logical first place to start in Merlin deficient schwannoma for three main reasons. First, NIK accumulates in tumorigenic Merlin deficient Schwann cells so we know it is highly expressed in the cells of interest. Second, NIK sits at the headwaters of NF-κB signaling and its accumulation has been shown to play an important role in activation of NF-κB signaling in other tumor types. Whereas many stimuli would be expected to preferentially activate NF-κB through either the canonical or non-canonical pathway, we universally see activation of both in late stage schwannoma. NIK accumulation is one of known mechanisms by which both canonical and non-canonical signaling can be activated simultaneously. Third, NIK is targetable via the use of selective small molecule inhibitors and its inhibition is tolerated *in vivo.* So, if NIK accumulation is essential for schwannoma formation or growth, then there are clear actions that could be taken clinically to translate this information into better care for our patients.

The Schwann cell transfer experiment demonstrated that Schwann cell intrinsic expression of a constitutively active fragment of the NIK kinase domain could activate canonical and non-canonical NF-κB signaling and that expression of that construct was sufficient to cause Schwann cells to form tumors within the sciatic nerve of nude mice. These data argue that the NIK fragment accumulation seen in late stage Merlin deficient schwannoma could play a critical role in the physiology of those tumor. Why loss of Merlin leads to accumulation of NIK is unclear. Thus, it was important to next assess

whether NIK was the critical driver of NF-κB activation and necessary for the formation of Schwann cell tumors *in vivo*.

Schwann cells genetically modified to be dually deficient for Merlin and NIK formed tumors *in vivo*. However, the combination of the slightly delayed onset of hearing loss and the reduction in the percentage of DRG over 1.0 mm^3 in volume at 10 months of age may suggests loss of *NIK* may delay the onset of tumor formation in some Schwann cells. Genetic deletion of *NIK* significantly reduced the levels of RelA and RelB in Schwann cells tumors compared to *NIK* sufficient *Nf2*-cKO animals. By IHC, levels of RelA and RelB in the schwannomas were reduced in *Nf2;NIK*-cDKO animals but still much higher than levels observed in the Schwann cells in Cre-negative animals. This result indicates that there may still be some elevation in NF-κB signaling in these tumors.

Developing a better understanding the pathophysiology of the sensorineural hearing loss has remained a challenge. Clinically, the best predictor of sensorineural loss in NF2 patients is the presence of proteinaceous fluid in the cochlea on MRI [75]. Neither the size nor the growth rate of a patient's vestibular schwannomas has proven to be significantly correlated with the magnitude or progression of their hearing loss. Interestingly, single dose administration of the anti-VEGF humanized monoclonal antibody Bevacizumab has been shown to improve hearing in NF2 patients [122-124]. Treatment with bevacizumab reduces tumor vascular permeability and in the context of NF2, its otoprotective effect is believed to be related to blocking up leaky vasculature, preventing ototoxic tumor secretions from reaching the cochlea [125].

When first conducting whole head sectioning to assess for schwannoma formation in the Vestibular Cochlear nerve (CNVIII) of our *Nf2*-cKO animals we observed

significant pro-inflammatory infiltrates in the cochlea (**Figure 30A-C**). The pathology was at first assessed as otitis media but we see no other evidence of chronic bacterial or viral inner ear infections. Similarly, patient case reports of NF2 patients often describe "recurrent, chronic otitis media" preceding sensorineural hearing loss. In certain cases early hearing loss is attributed to these recurrent "infections" until a more thorough workup reveals a vestibular schwannoma. We can't rule out that NF2 patients could have some underlying sensitivity to recurrent inner ear infections but believe it is more likely that both in our mice and in the NF2 patients, there is chronic sterile inflammation. Clinically, the sterile inflammation would present as an inflammatory immune response in the absence of an infectious agent. As a consequence, sterile inflammation is not readily distinguishable from infectious otitis media making it extremely difficult to properly diagnose without invasive testing. A cytokine analysis of the cochlear fluid lysates found levels of IL-1β to be significantly elevated in our *Nf2*-cKO animals (**Figure 30C**). Transcription of IL-1β is controlled by NF-κB transcription factors [126]. We had hypothesized that genetic disruption of NIK may reduce NF-κB signaling and may therefore reduce levels of IL-1β, providing some protection against the sensorineural hearing loss. Consistent with our findings that deletion of NIK did not lead to sustained protection from hearing loss, deletion of NIK did not reduce levels of proinflammatory cytokines in the inner ears of 11.5 month old mice. Across the four genotypes tested, higher levels of IL-6 and IL-1β did correlate with increased severity of sensorineural hearing loss arguing that inflammation may be a critical component of the hearing loss in our mouse model.

Systemically elevated IL-1β has been previously shown to be a driver of hearing loss in multiple autoimmune related syndromes including Muckle Wells, NOMID, and AIED. In 2014 there was a successful open label Phase I/II sponsored by NIDCD to investigate the efficacy of the IL-1 receptor antagonist, anakinra, in preventing sensorineural hearing loss in AIED [127]. If bevacizumab works by blocking some yet to be determined ototoxic byproduct of the vestibular schwannomas from reaching the cochlea, IL-1β may be that factor.

The direct use of bevacizumab in NF2 patients would be controversial. IL-1β levels are often elevated in cancer patients, particularly those with metastatic disease and high levels of IL-1β are correlated with poor patient prognosis in renal, cervical, and breast carcinomas [128]. Based upon this data, there is an ongoing clinical trial (NCT01802970) investigating the use of anakinra in metastatic breast cancer. But long term use of anakinra as would be necessary for otoprotection in NF2 patients has been associated with a significantly increased incidence of lymphoma and malignant melanoma [129]. The 5-fold increase in malignant melanoma is of particular concern given that NF2 patients already have a greatly increased propensity for the development of neural crest derived tumors. Several independent clinical studies aimed as investigating the potential clinical value of IL-1β inhibition in a variety of solid tumors have measured endogenous levels of IL-1Ra, the IL-1 decoy receptor mimicked by anakinra, in patient serum. Some studies found that IL-1Ra expression correlated with increased severity of colorectal cancer, pancreatic cancer, and breast cancer. Other groups had the exact opposite result and published that IL-1Ra expression correlated with decreased severity of the same cancers in their patients [128]. At minimum there

would be value in assessing anakinra in our *Nf2*-cKO mice to see if IL-1β blockade would affect sensorineural hearing loss progression. Within the Schwann cell tumor, we believe that the pathophysiology of NF2 related and spontaneous vestibular schwannoma are similar. If IL-1β is a primary driver of the hearing loss in spontaneous vestibular schwannoma, anakinra could be a very valuable therapeutic in slowing to preventing hearing loss in these patients.

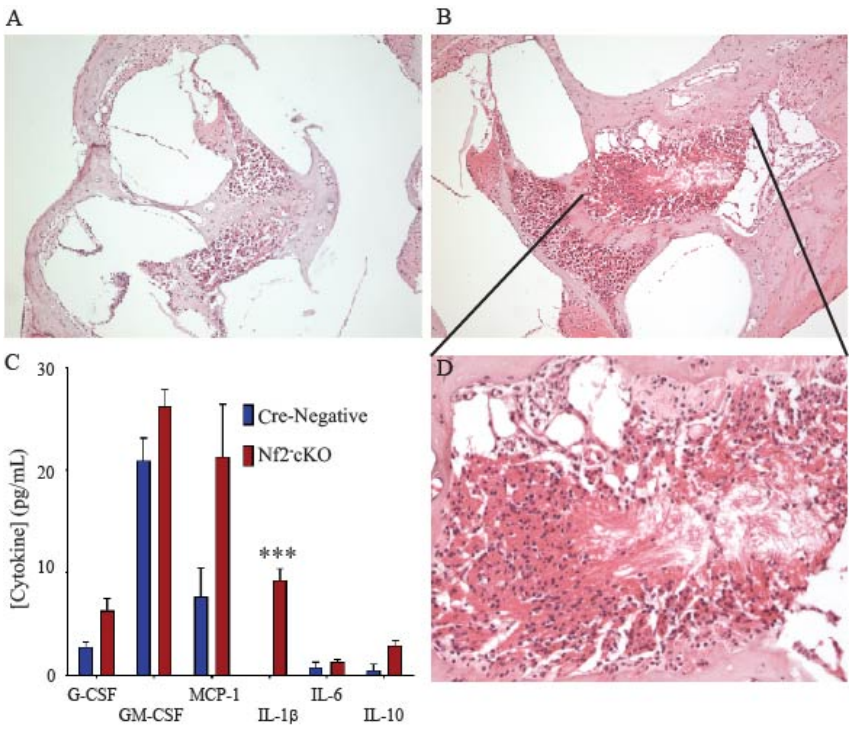

Figure 30. Analysis of cochlea in *Nf2*-cKO mice. (A) Representative H&E mid modialar section from 10 month old Cre-negative animal. Original magnification 10x. **(B)** Representative H&E mid modialar section from 10 month old Cre-positive animal. Original magnification 10x. **(C)** Luminex analysis of cochlear fluid lysates from 10 month old mice. 3 samples/genotype, $p<0.001$, students t-test. **(D)** Digital magnification of (C) highlighting inflammatory infiltrate.

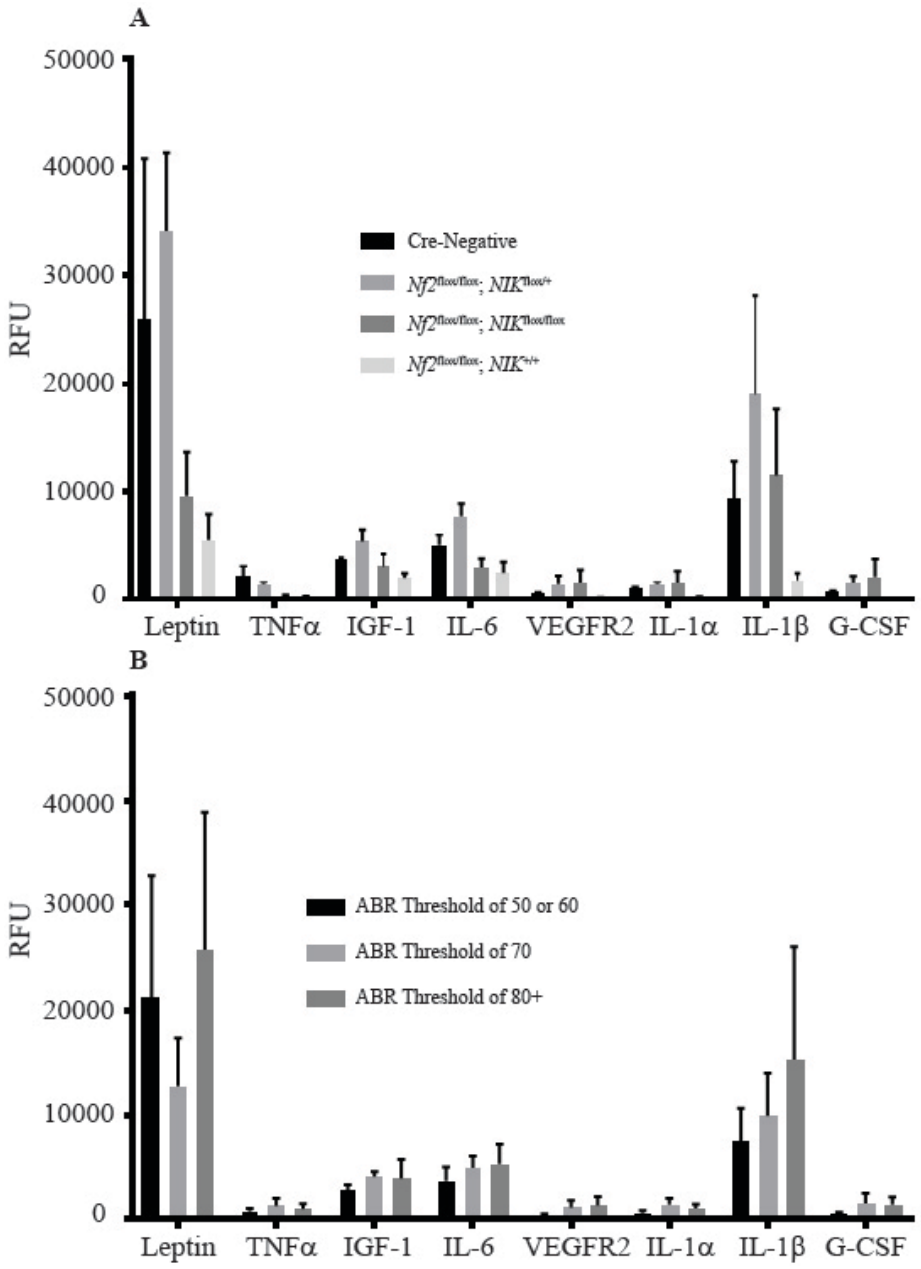

Figure 31. Cytokine analysis of the inner ear in mice with mild, moderate, and severe hearing loss. (A) ELIZA cytokine array of inner ear lysates from 11.5 old mice separated by genotype. 3 mice/genotype, Error bars represent SEM. **(B)** Data from A resorted and grouped by ABR thresholds representing mild, moderate, and severe hearing loss. Error bars represent SEM.

The non Mendelian genetics of the *NIK*-cKO, *Nf2*-cKO intercross was unexpected but provides us with some very interesting new insight into Merlin biology. The lack of sufficient numbers of $NIK^{+/+}$ animals limits any conclusions from the data about the role of *NIK* in schwannoma growth and development. Using the *Nf2*-cKO;*NIK*-Het mice as a positive control, loss of NIK did not appear to dramatically alter the *Nf2*-cKO phenotype.

Looking at the mice at weaning told a different story. At birth our *Nf2*-cKO Cre^+ mice are physically much smaller than their Cre^- littermates and seem to reach sexual maturity later. This developmental delay likely starts very early. When embryonic Schwann cells are harvested (Figure 19) utilizing *Nf2*-cKO mice, the Cre^+ embryos appear at an early developmental stage than the Cre^- embryos in the same uterus. We also observe significantly more degenerate and atrophied embryos in the uteri of animals carrying Cre^+ embryos compared with breedings set up to produce only wild type mice. This result has lead us to hypothesize that the smaller number of Cre^+ embryos carried to term is due to developmental failures of a significant percentage of Cre^+ embryos *in utero*. The embryonic selection pressure against *Nf2*-cKO animals was observed in the F2 intercross of the *Nf2;NIK*-cKO mice. Interestingly, loss of a single allele of *NIK* completely abrogated the selection pressure and restored the numbers of Cre^+:Cre^- embryos/litter to within expected Mendelian ratios. We hypothesize that the embryonic phenotype of the Cre^+ mice is due to the stochastic mechanism upon which the Cre-Lox system is dependent for gene deletion. *Periostin* is expressed in migrating Schwann cells. Some minimal amount of lag time may be required between expression of the endogenous *Periostin* gene and physiological depletion of Merlin to allow for the Schwann cells to migrate to their appropriate anatomical location and mature [130]. If

this is true, then the improved survival of the *NIK*-heterozygous mice argues that failure in Schwann cell development occurring in the mice which lose Merlin early in the stochastic window is driven by activation of NF-κB and that reduction in *NIK* is sufficient to reduce NF-κB activation to a level where normal maturation can occur. As highlighted in the introduction to Chapter 1, mature myelinating Schwann cells don't divide and as schwannomas grow they lose S100 positivity and seem to revert to a more procurer state. The NIK accumulation observed in late stage Schwannoma may be a marker of this progenitor state, aiding in proliferation and preventing differentiation of the tumorigenic cells.

FUTURE DIRECTIONS

The work contained herein offers new insight into the signaling pathways controlling the growth and development of Merlin deficient schwannomas. It also raises many new and important questions worth pursing in the future. As a negative regulator of PAK1, Merlin appears to serve as a critical brake in preventing the development of tumors in a subset of Merlin deficient Schwann cells. As was highlighted in the introduction to Chapter 1, all of the Schwann cells in our *Nf2*-cKO animals are Merlin deficient and only a small minority ever form tumors. In our animals, loss of Merlin appears to be like disengaging the parking brake and PAK1 is the gas pedal. These steps may be necessary for driving the formation of schwannomas but the cells won't begin to move towards a hyper-proliferative state without some other factors starting the engine, shifting the transmission into drive, and then stepping on the gas. This is consistent with what we observe in NF2 patients where despite all of the heterogeneity of different mutations occurring in different cells at different time points, the most common end result is a relatively homogenous phenotype of bilateral vestibular schwannoma with sensorineural hearing loss and vestibular dysfunction. That's not to say that all NF2 patients are the same. When, where, and to what degree Merlin function is lost probably does have a significant impact on the timing and severity of neural crest derived tumor development in these patients. But, the restricted nature of the tumor types and anatomical locations where these tumors develop argues that Merlin only acts as a critical tumor suppressor in very specific physiological conditions in restricted cellular environments.

We are continuing to optimize NVS-PAK1-1 as a potential therapeutic for NF2. However, more work needs to be done to understand what signals activate PAK1 in Schwann cells and neural crest precursors. Loss of negative regulation isn't equivalent to activation and there may be pathways essential for PAK1 activation in Merlin deficient Schwann cells which are easier to target therapeutically than PAK1 directly. The pharmacokinetic and pharmacodynamics barriers associated with achieving durable PAK1 inhibition without PAK2 inhibition are likely surmountable but do render NVS-PAK1-1 suboptimal from a drug development perspective relative to brigatinib, the compound put forth and being developed through the Synodos NF2 Consortium.

Brigatnib is an FDA approved, multi-RTK inhibitor that is used as an ALK inhibitor in ALK positive non-small cell lung carcinoma [131]. We have demonstrated that brigatinib potently reduces tumor size and sensorineural hearing loss in our *Nf2*-cKO animals and a collaborator has shown similar growth inhibitory effects in human Merlin deficient meningioma. These effects can't be attributed to inhibition of ALK because Schwann cells don't express ALK. In Schwann cells, one of the kinases most potently inhibited by brigatinib is FAK. FAK is a potent activator of Rac-1 which in turn is a potent activator of PAK1 [132,133]. So, although brigantinib has not previously been thought of as a PAK1 inhibitor, that may be one of the primary mechanisms through which it has demonstrated great pre-clinical efficacy in multiple independent models of NF2.

The *NIK* data, particularly the increased embryonic survival of *Nf2*-cKO;*NIK*-Het animals leaves many more questions than answers. We know that in our mice, as schwannomas grow, they lose S100 positivity and seem to dedifferentiate into a more

primordial state. The theory of that as cancer cells grow, they lose their differentiation dates back at least as far back as 1974 with Justin Schwind coining the term regressive evolution to describe what he believed was cancer cells shifting away from a phenotype associated with multicellular life and towards a phenotype associated with unicellular life over time [134]. It is possible that NF-κB activation is a maker of this dedifferentiated, more primordial state. This would explain why high levels of NF-κB are commonly observed in a variety of tumors and why we uniformly see NIK accumulation in late stage schwannoma. NF-κB signaling may also reinforce this dedifferentiated state explaining why deletion of one allele of *NIK* protects against the significant embryonic lethality observed in *Nf2*-cKO animals. Targeting NIK directly may not be the best therapeutic approach for the treatment of NF2. Somewhat serendipitously, when we looked for signaling pathways upstream of NIK which activate NF-kB signaling in Schwann cells we came across FAK. In Schwann cells, free myelin basic protein signals through the CR3 receptor to activate FAK, which leads to the degradation of IκBα and nuclear translocation of the RelA/p50 heterodimer [135]. In the *Nf2*-cKO mice, brigatinib significantly reduces NF-κB activation in tumor bearing trigeminal nerve tissue. Schwann cell or nerve damage triggers the release of significant free myelin basic protein. Given the aberrations observed after sciatic nerve injury in $Nf2^{flox/flox}$;P0-Cre mice it would be interesting to see how much of this phenotype could be recapitulated by injection of free myelin basic protein without the injury or whether the pathology requires the mature Merlin deficient Schwann cells to dedifferentiate [136].

When considered as an ALK inhibitor, brigatinib would have seem to have no value in the treatment of NF2. But, the unbiased, omics based approach utilized by

Synodos has demonstrated is efficacious in animal models of NF2 and we now argue that it has a sound mechanism of action for the treatment of NF2 as a FAK inhibitor. Brigatinib already has FDA approval for other indications and we can extrapolate a significant amount of safety data from the multiple Phase I, II, and III trials already published. Therefore, a Phase II clinical trial of brigatinib in adults with NF2 seems like a logical next step in therapeutic development for NF2.

Brigatinib is very unlikely to be a silver bullet in this disease. A review of the previous Phase I/II trials with brigatinib in ALK positive small cell lung cancer reported that 36% of patients developed treatment related grade 3-4 adverse events on a scale where grade 1 is mild and grade 3 is severe and grade 4 is life threatening and or death [137]. For a patient with NF2, we would be likely be treating much healthier patients at a much lower dose but for a much longer time period and so a more selective therapeutic with less toxicity may be greatly preferred. More basic science is needed to understand the precise developmental stage and micro-environmental cues necessary for Merlin deficient schwannoma development. If we can use our *Nf2*-cKO mice to look at precursor lesions and early tumor development we may be able to better define the tumor cell of origin. In doing so we would better understand what cell or cellular cues are best to inhibit, improving our ability for data driven therapeutic development in NF2.

REFERENCES

1. Asthagiri AR, Parry DM, Butman JA, Kim HJ, Tsilou ET, Zhuang Z, Lonser RR. Neurofibromatosis type 2. Lancet. 2009;373(9679):1974-86. Epub 2009/05/30. doi: 10.1016/S0140-6736(09):60259-2. PubMed PMID: 19476995; PMCID: PMC4748851.
2. Evans DG, Huson SM, Donnai D, Neary W, Blair V, Teare D, Newton V, Strachan T, Ramsden R, Harris R. A genetic study of type 2 neurofibromatosis in the United Kingdom. I. Prevalence, mutation rate, fitness, and confirmation of maternal transmission effect on severity. J Med Genet. 1992;29(12):841-6. Epub 1992/12/01. PubMed PMID: 1479598; PMCID: PMC1016198.
3. Evans DG, Huson SM, Donnai D, Neary W, Blair V, Newton V, Harris R. A clinical study of type 2 neurofibromatosis. Q J Med. 1992;84(304):603-18. Epub 1992/08/01. PubMed PMID: 1484939.
4. Kanter WR, Eldridge R, Fabricant R, Allen JC, Koerber T. Central neurofibromatosis with bilateral acoustic neuroma: genetic, clinical and biochemical distinctions from peripheral neurofibromatosis. Neurology. 1980;30(8):851-9. Epub 1980/08/01. PubMed PMID: 6774282.
5. Mautner VF, Lindenau M, Baser ME, Hazim W, Tatagiba M, Haase W, Samii M, Wais R, Pulst SM. The neuroimaging and clinical spectrum of neurofibromatosis 2. Neurosurgery. 1996;38(5):880-5; discussion 5-6. Epub 1996/05/01. PubMed PMID: 8727812.

6. Parry DM, Eldridge R, Kaiser-Kupfer MI, Bouzas EA, Pikus A, Patronas N. Neurofibromatosis 2 (NF2): clinical characteristics of 63 affected individuals and clinical evidence for heterogeneity. Am J Med Genet. 1994;52(4):450-61. Epub 1994/10/01. doi: 10.1002/ajmg.1320520411. PubMed PMID: 7747758.

7. Evans DG. Neurofibromatosis type 2 (NF2): a clinical and molecular review. Orphanet J Rare Dis. 2009;4:16. Epub 2009/06/24. doi: 10.1186/1750-1172-4-16. PubMed PMID: 19545378; PMCID: PMC2708144.

8. Wishard, JH. Case of tumors in the skull, dura mater, and brain. *Edinburgh Med Surg J.* 1822;18(72):393.

9. Hadfield KD, Smith MJ, Urquhart JE, Wallace AJ, Bowers NL, King AT, Rutherford SA, Trump D, Newman WG, Evans DG. Rates of loss of heterozygosity and mitotic recombination in NF2 schwannomas, sporadic vestibular schwannomas and schwannomatosis schwannomas. Oncogene. 2010;29(47):6216-21. Epub 2010/08/24. doi: 10.1038/onc.2010.363. PubMed PMID: 20729918.

10. RM DEC, C DECSA, Pinto GR, Paschoal EHA, Tuji FM, B DONB, Soares PC, Junior AGF, Rey JA, Chaves LCL, Burbano RR. Frequency of the Loss of Heterozygosity of the NF2 Gene in Sporadic Spinal Schwannomas. Anticancer Res. 2018;38(4):2149-54. Epub 2018/03/31. doi: 10.21873/anticanres.12455. PubMed PMID: 29599333.

11. Kshettry VR, Hsieh JK, Ostrom QT, Kruchko C, Barnholtz-Sloan JS. Incidence of vestibular schwannomas in the United States. J Neurooncol. 2015;124(2):223-8. Epub 2015/05/31. doi: 10.1007/s11060-015-1827-9. PubMed PMID: 26024654.

12. Murphy ES, Suh JH. Radiotherapy for vestibular schwannomas: a critical review. Int J Radiat Oncol Biol Phys. 2011;79(4):985-97. Epub 2011/03/01. doi: 10.1016/j.ijrobp.2010.10.010. PubMed PMID: 21353158.

13. Narod SA, Parry DM, Parboosingh J, Lenoir GM, Ruttledge M, Fischer G, Eldridge R, Martuza RL, Frontali M, Haines J, et al. Neurofibromatosis type 2 appears to be a genetically homogeneous disease. Am J Hum Genet. 1992;51(3):486-96. Epub 1992/09/01. PubMed PMID: 1496982; PMCID: PMC1682700.

14. Rouleau GA, Merel P, Lutchman M, Sanson M, Zucman J, Marineau C, Hoang-Xuan K, Demczuk S, Desmaze C, Plougastel B, et al. Alteration in a new gene encoding a putative membrane-organizing protein causes neuro-fibromatosis type 2. Nature. 1993;363(6429):515-21. Epub 1993/06/10. doi: 10.1038/363515a0. PubMed PMID: 8379998.

15. Trofatter JA, MacCollin MM, Rutter JL, Murrell JR, Duyao MP, Parry DM, Eldridge R, Kley N, Menon AG, Pulaski K, et al. A novel moesin-, ezrin-, radixin-like gene is a candidate for the neurofibromatosis 2 tumor suppressor. Cell. 1993;72(5):791-800. Epub 1993/03/12. PubMed PMID: 8453669.

16. Cooper J, Giancotti FG. Molecular insights into NF2/Merlin tumor suppressor function. FEBS Lett. 2014;588(16):2743-52. Epub 2014/04/15. doi: 10.1016/j.febslet.2014.04.001. PubMed PMID: 24726726; PMCID: PMC4111995.

17. Sher I, Hanemann CO, Karplus PA, Bretscher A. The tumor suppressor merlin controls growth in its open state, and phosphorylation converts it to a less-active

more-closed state. Dev Cell. 2012;22(4):703-5. Epub 2012/04/21. doi: 10.1016/j.devcel.2012.03.008. PubMed PMID: 22516197; PMCID: PMC3725555.

18. Lallemand D, Saint-Amaux AL, Giovannini M. Tumor-suppression functions of merlin are independent of its role as an organizer of the actin cytoskeleton in Schwann cells. J Cell Sci. 2009;122(Pt 22):4141-9. Epub 2009/11/17. doi: 10.1242/jcs.045914. PubMed PMID: 19910496.

19. Xu HM, Gutmann DH. Merlin differentially associates with the microtubule and actin cytoskeleton. J Neurosci Res. 1998;51(3):403-15. Epub 1998/03/05. doi: 10.1002/(SICI)1097-4547(19980201)51:3<403::AID-JNR13>3.0.CO;2-7. PubMed PMID: 9486775.

20. Petrilli AM, Fernandez-Valle C. Role of Merlin/NF2 inactivation in tumor biology. Oncogene. 2016;35(5):537-48. Epub 2015/04/22. doi: 10.1038/onc.2015.125. PubMed PMID: 25893302; PMCID: PMC4615258.

21. Rong R, Surace EI, Haipek CA, Gutmann DH, Ye K. Serine 518 phosphorylation modulates merlin intramolecular association and binding to critical effectors important for NF2 growth suppression. Oncogene. 2004;23(52):8447-54. Epub 2004/09/21. doi: 10.1038/sj.onc.1207794. PubMed PMID: 15378014.

22. Shaw RJ, McClatchey AI, Jacks T. Regulation of the neurofibromatosis type 2 tumor suppressor protein, merlin, by adhesion and growth arrest stimuli. J Biol Chem. 1998;273(13):7757-64. Epub 1998/04/29. PubMed PMID: 9516485.

23. Morrison H, Sherman LS, Legg J, Banine F, Isacke C, Haipek CA, Gutmann DH, Ponta H, Herrlich P. The NF2 tumor suppressor gene product, merlin, mediates

contact inhibition of growth through interactions with CD44. Genes Dev. 2001;15(8):968-80. Epub 2001/04/24. doi: 10.1101/gad.189601. PubMed PMID: 11316791; PMCID: PMC312675.

24. Okada T, Lopez-Lago M, Giancotti FG. Merlin/NF-2 mediates contact inhibition of growth by suppressing recruitment of Rac to the plasma membrane. J Cell Biol. 2005;171(2):361-71. Epub 2005/10/26. doi: 10.1083/jcb.200503165. PubMed PMID: 16247032; PMCID: PMC2171182.

25. Chong C, Tan L, Lim L, Manser E. The mechanism of PAK activation. Autophosphorylation events in both regulatory and kinase domains control activity. J Biol Chem. 2001;276(20):17347-53. Epub 2001/03/30. doi: 10.1074/jbc.M009316200. PubMed PMID: 11278486.

26. Kissil JL, Wilker EW, Johnson KC, Eckman MS, Yaffe MB, Jacks T. Merlin, the product of the Nf2 tumor suppressor gene, is an inhibitor of the p21-activated kinase, Pak1. Mol Cell. 2003;12(4):841-9. Epub 2003/10/29. PubMed PMID: 14580336.

27. Ammoun S, Cunliffe CH, Allen JC, Chiriboga L, Giancotti FG, Zagzag D, Hanemann CO, Karajannis MA. ErbB/HER receptor activation and preclinical efficacy of lapatinib in vestibular schwannoma. Neuro Oncol. 2010;12(8):834-43. Epub 2010/06/01. doi: 10.1093/neuonc/noq012. PubMed PMID: 20511180; PMCID: PMC2940674.

28. Zhou L, Ercolano E, Ammoun S, Schmid MC, Barczyk MA, Hanemann CO. Merlin-deficient human tumors show loss of contact inhibition and activation of Wnt/beta-catenin signaling linked to the PDGFR/Src and Rac/PAK pathways.

Neoplasia. 2011;13(12):1101-12. Epub 2012/01/17. PubMed PMID: 22247700; PMCID: PMC3257450.

29. Ammoun S, Provenzano L, Zhou L, Barczyk M, Evans K, Hilton DA, Hafizi S, Hanemann CO. Axl/Gas6/NFkappaB signalling in schwannoma pathological proliferation, adhesion and survival. Oncogene. 2014;33(3):336-46. Epub 2013/01/16. doi: 10.1038/onc.2012.587. PubMed PMID: 23318455.

30. James MF, Han S, Polizzano C, Plotkin SR, Manning BD, Stemmer-Rachamimov AO, Gusella JF, Ramesh V. NF2/merlin is a novel negative regulator of mTOR complex 1, and activation of mTORC1 is associated with meningioma and schwannoma growth. Mol Cell Biol. 2009;29(15):4250-61. Epub 2009/05/20. doi: 10.1128/MCB.01581-08. PubMed PMID: 19451225; PMCID: PMC2715803.

31. Zhang N, Bai H, David KK, Dong J, Zheng Y, Cai J, Giovannini M, Liu P, Anders RA, Pan D. The Merlin/NF2 tumor suppressor functions through the YAP oncoprotein to regulate tissue homeostasis in mammals. Dev Cell. 2010;19(1):27-38. Epub 2010/07/21. doi: 10.1016/j.devcel.2010.06.015. PubMed PMID: 20643348; PMCID: PMC2925178.

32. Jacob A, Lee TX, Neff BA, Miller S, Welling B, Chang LS. Phosphatidylinositol 3-kinase/AKT pathway activation in human vestibular schwannoma. Otol Neurotol. 2008;29(1):58-68. Epub 2008/01/18. doi: 10.1097/mao.0b013e31816021f7. PubMed PMID: 18199958.

33. Bagrodia S, Taylor SJ, Creasy CL, Chernoff J, Cerione RA. Identification of a mouse p21Cdc42/Rac activated kinase. J Biol Chem. 1995;270(39):22731-7. Epub 1995/09/29. PubMed PMID: 7559398.

34. Knaus UG, Morris S, Dong HJ, Chernoff J, Bokoch GM. Regulation of human leukocyte p21-activated kinases through G protein--coupled receptors. Science. 1995;269(5221):221-3. Epub 1995/07/14. PubMed PMID: 7618083.

35. Kumar R, Li DQ. PAKs in Human Cancer Progression: From Inception to Cancer Therapeutic to Future Oncobiology. Adv Cancer Res. 2016;130:137-209. Epub 2016/04/03. doi: 10.1016/bs.acr.2016.01.002. PubMed PMID: 27037753.

36. Parrini MC, Lei M, Harrison SC, Mayer BJ. Pak1 kinase homodimers are autoinhibited in trans and dissociated upon activation by Cdc42 and Rac1. Mol Cell. 2002;9(1):73-83. Epub 2002/01/24. PubMed PMID: 11804587.

37. Mayhew MW, Jeffery ED, Sherman NE, Nelson K, Polefrone JM, Pratt SJ, Shabanowitz J, Parsons JT, Fox JW, Hunt DF, Horwitz AF. Identification of phosphorylation sites in betaPIX and PAK1. J Cell Sci. 2007;120(Pt 22):3911-8. Epub 2007/11/09. doi: 10.1242/jcs.008177. PubMed PMID: 17989089; PMCID: PMC4627702.

38. Uhlen M, Fagerberg L, Hallstrom BM, Lindskog C, Oksvold P, Mardinoglu A, Sivertsson A, Kampf C, Sjostedt E, Asplund A, Olsson I, Edlund K, Lundberg E, Navani S, Szigyarto CA, Odeberg J, Djureinovic D, Takanen JO, Hober S, Alm T, Edqvist PH, Berling H, Tegel H, Mulder J, Rockberg J, Nilsson P, Schwenk JM, Hamsten M, von Feilitzen K, Forsberg M, Persson L, Johansson F, Zwahlen M, von Heijne G, Nielsen J, Ponten F. Proteomics. Tissue-based map of the human proteome. Science. 2015;347(6220):1260419. Epub 2015/01/24. doi: 10.1126/science.1260419. PubMed PMID: 25613900.

39. Ye DZ, Field J. PAK signaling in cancer. Cell Logist. 2012;2(2):105-16. Epub 2012/11/20. doi: 10.4161/cl.21882. PubMed PMID: 23162742; PMCID: PMC3490961.

40. Eswaran J, Li DQ, Shah A, Kumar R. Molecular pathways: targeting p21-activated kinase 1 signaling in cancer--opportunities, challenges, and limitations. Clin Cancer Res. 2012;18(14):3743-9. Epub 2012/05/19. doi: 10.1158/1078-0432.CCR-11-1952. PubMed PMID: 22595609; PMCID: PMC3399091.

41. Shrestha Y, Schafer EJ, Boehm JS, Thomas SR, He F, Du J, Wang S, Barretina J, Weir BA, Zhao JJ, Polyak K, Golub TR, Beroukhim R, Hahn WC. PAK1 is a breast cancer oncogene that coordinately activates MAPK and MET signaling. Oncogene. 2012;31(29):3397-408. Epub 2011/11/23. doi: 10.1038/onc.2011.515. PubMed PMID: 22105362; PMCID: PMC3291810.

42. Motwani M, Li DQ, Horvath A, Kumar R. Identification of novel gene targets and functions of p21-activated kinase 1 during DNA damage by gene expression profiling. PLoS One. 2013;8(8):e66585. Epub 2013/08/21. doi: 10.1371/journal.pone.0066585. PubMed PMID: 23950862; PMCID: PMC3741304.

43. Beeser A, Jaffer ZM, Hofmann C, Chernoff J. Role of group A p21-activated kinases in activation of extracellular-regulated kinase by growth factors. J Biol Chem. 2005;280(44):36609-15. Epub 2005/09/01. doi: 10.1074/jbc.M502306200. PubMed PMID: 16129686.

44. Acconcia F, Barnes CJ, Singh RR, Talukder AH, Kumar R. Phosphorylation-dependent regulation of nuclear localization and functions of integrin-linked

kinase. Proc Natl Acad Sci U S A. 2007;104(16):6782-7. Epub 2007/04/11. doi: 10.1073/pnas.0701999104. PubMed PMID: 17420447; PMCID: PMC1871862.

45. Maroto B, Ye MB, von Lohneysen K, Schnelzer A, Knaus UG. P21-activated kinase is required for mitotic progression and regulates Plk1. Oncogene. 2008;27(36):4900-8. Epub 2008/04/23. doi: 10.1038/onc.2008.131. PubMed PMID: 18427546.

46. Yang Z, Rayala S, Nguyen D, Vadlamudi RK, Chen S, Kumar R. Pak1 phosphorylation of snail, a master regulator of epithelial-to-mesenchyme transition, modulates snail's subcellular localization and functions. Cancer Res. 2005;65(8):3179-84. Epub 2005/04/19. doi: 10.1158/0008-5472.CAN-04-3480. PubMed PMID: 15833848.

47. Kissil JL, Johnson KC, Eckman MS, Jacks T. Merlin phosphorylation by p21-activated kinase 2 and effects of phosphorylation on merlin localization. J Biol Chem. 2002;277(12):10394-9. Epub 2002/01/10. doi: 10.1074/jbc.M200083200. PubMed PMID: 11782491.

48. Kidd GJ, Ohno N, Trapp BD. Biology of Schwann cells. Handb Clin Neurol. 2013;115:55-79. Epub 2013/08/13. doi: 10.1016/B978-0-444-52902-2.00005-9. PubMed PMID: 23931775.

49. Jessen KR, Mirsky R. The repair Schwann cell and its function in regenerating nerves. J Physiol. 2016;594(13):3521-31. Epub 2016/02/13. doi: 10.1113/JP270874. PubMed PMID: 26864683; PMCID: PMC4929314.

50. Hung G, Colton J, Fisher L, Oppenheimer M, Faudoa R, Slattery W, Linthicum F. Immunohistochemistry study of human vestibular nerve schwannoma

differentiation. Glia. 2002;38(4):363-70. Epub 2002/05/15. doi: 10.1002/glia.10077. PubMed PMID: 12007148.

51. Giovannini M, Robanus-Maandag E, van der Valk M, Niwa-Kawakita M, Abramowski V, Goutebroze L, Woodruff JM, Berns A, Thomas G. Conditional biallelic Nf2 mutation in the mouse promotes manifestations of human neurofibromatosis type 2. Genes Dev. 2000;14(13):1617-30. Epub 2000/07/11. PubMed PMID: 10887156; PMCID: PMC316733.

52. Mindos T, Dun XP, North K, Doddrell RD, Schulz A, Edwards P, Russell J, Gray B, Roberts SL, Shivane A, Mortimer G, Pirie M, Zhang N, Pan D, Morrison H, Parkinson DB. Merlin controls the repair capacity of Schwann cells after injury by regulating Hippo/YAP activity. J Cell Biol. 2017;216(2):495-510. Epub 2017/02/01. doi: 10.1083/jcb.201606052. PubMed PMID: 28137778; PMCID: PMC5294779.

53. Hung G, Li X, Faudoa R, Xeu Z, Kluwe L, Rhim JS, Slattery W, Lim D. Establishment and characterization of a schwannoma cell line from a patient with neurofibromatosis 2. Int J Oncol. 2002;20(3):475-82. Epub 2002/02/12. PubMed PMID: 11836557.

54. Lepont P, Stickney JT, Foster LA, Meng JJ, Hennigan RF, Ip W. Point mutation in the NF2 gene of HEI-193 human schwannoma cells results in the expression of a merlin isoform with attenuated growth suppressive activity. Mutat Res. 2008;637(1-2):142-51. Epub 2007/09/18. doi: 10.1016/j.mrfmmm.2007.07.015. PubMed PMID: 17868749; PMCID: PMC2233940.

55. Synodos for NFC, Allaway R, Angus SP, Beauchamp RL, Blakeley JO, Bott M, Burns SS, Carlstedt A, Chang LS, Chen X, Clapp DW, Desouza PA, Erdin S, Fernandez-Valle C, Guinney J, Gusella JF, Haggarty SJ, Johnson GL, La Rosa S, Morrison H, Petrilli AM, Plotkin SR, Pratap A, Ramesh V, Sciaky N, Stemmer-Rachamimov A, Stuhlmiller TJ, Talkowski ME, Welling DB, Yates CW, Zawistowski JS, Zhao WN. Traditional and systems biology based drug discovery for the rare tumor syndrome neurofibromatosis type 2. PLoS One. 2018;13(6):e0197350. Epub 2018/06/14. doi: 10.1371/journal.pone.0197350. PubMed PMID: 29897904; PMCID: PMC5999111.

56. Kapalczynska M, Kolenda T, Przybyla W, Zajaczkowska M, Teresiak A, Filas V, Ibbs M, Blizniak R, Luczewski L, Lamperska K. 2D and 3D cell cultures - a comparison of different types of cancer cell cultures. Arch Med Sci. 2018;14(4):910-9. Epub 2018/07/14. doi: 10.5114/aoms.2016.63743. PubMed PMID: 30002710; PMCID: PMC6040128.

57. McClatchey AI, Saotome I, Ramesh V, Gusella JF, Jacks T. The Nf2 tumor suppressor gene product is essential for extraembryonic development immediately prior to gastrulation. Genes Dev. 1997;11(10):1253-65. Epub 1997/05/15. PubMed PMID: 9171370.

58. McClatchey AI, Saotome I, Mercer K, Crowley D, Gusella JF, Bronson RT, Jacks T. Mice heterozygous for a mutation at the Nf2 tumor suppressor locus develop a range of highly metastatic tumors. Genes Dev. 1998;12(8):1121-33. Epub 1998/05/30. PubMed PMID: 9553042; PMCID: PMC316711.

59. Messing A, Behringer RR, Hammang JP, Palmiter RD, Brinster RL, Lemke G. P0 promoter directs expression of reporter and toxin genes to Schwann cells of transgenic mice. Neuron. 1992;8(3):507-20. Epub 1992/03/01. PubMed PMID: 1372510.

60. Lindsley A, Snider P, Zhou H, Rogers R, Wang J, Olaopa M, Kruzynska-Frejtag A, Koushik SV, Lilly B, Burch JB, Firulli AB, Conway SJ. Identification and characterization of a novel Schwann and outflow tract endocardial cushion lineage-restricted periostin enhancer. Dev Biol. 2007;307(2):340-55. Epub 2007/06/02. doi: 10.1016/j.ydbio.2007.04.041. PubMed PMID: 17540359; PMCID: PMC1995123.

61. Gehlhausen JR, Park SJ, Hickox AE, Shew M, Staser K, Rhodes SD, Menon K, Lajiness JD, Mwanthi M, Yang X, Yuan J, Territo P, Hutchins G, Nalepa G, Yang FC, Conway SJ, Heinz MG, Stemmer-Rachamimov A, Yates CW, Wade Clapp D. A murine model of neurofibromatosis type 2 that accurately phenocopies human schwannoma formation. Hum Mol Genet. 2015;24(1):1-8. Epub 2014/08/13. doi: 10.1093/hmg/ddu414. PubMed PMID: 25113746; PMCID: PMC4262489.

62. Koval AB, Wuest WM. An optimized synthesis of the potent and selective Pak1 inhibitor FRAX-1036. Tetrahedron Lett. 2016;57(3):449-51. doi: 10.1016/j.tetlet.2015.12.059. PubMed PMID: WOS:000369556900054.

63. Prudnikova TY, Chernoff J. The Group I Pak inhibitor Frax-1036 sensitizes 11q13-amplified ovarian cancer cells to the cytotoxic effects of Rottlerin. Small GTPases. 2017;8(4):193-8. Epub 2016/07/19. doi:

10.1080/21541248.2016.1213089. PubMed PMID: 27427770; PMCID: PMC5680705.

64. Ndubaku CO, Crawford JJ, Drobnick J, Aliagas I, Campbell D, Dong P, Dornan LM, Duron S, Epler J, Gazzard L, Heise CE, Hoeflich KP, Jakubiak D, La H, Lee W, Lin B, Lyssikatos JP, Maksimoska J, Marmorstein R, Murray LJ, O'Brien T, Oh A, Ramaswamy S, Wang W, Zhao X, Zhong Y, Blackwood E, Rudolph J. Design of Selective PAK1 Inhibitor G-5555: Improving Properties by Employing an Unorthodox Low-pK a Polar Moiety. ACS Med Chem Lett. 2015;6(12):1241-6. Epub 2015/12/30. doi: 10.1021/acsmedchemlett.5b00398. PubMed PMID: 26713112; PMCID: PMC4677365.

65. Allen JD, Jaffer ZM, Park SJ, Burgin S, Hofmann C, Sells MA, Chen S, Derr-Yellin E, Michels EG, McDaniel A, Bessler WK, Ingram DA, Atkinson SJ, Travers JB, Chernoff J, Clapp DW. p21-activated kinase regulates mast cell degranulation via effects on calcium mobilization and cytoskeletal dynamics. Blood. 2009;113(12):2695-705. Epub 2009/01/07. doi: 10.1182/blood-2008-06-160861. PubMed PMID: 19124833; PMCID: PMC2661857

66. Radu M, Lyle K, Hoeflich KP, Villamar-Cruz O, Koeppen H, Chernoff J. p21-Activated Kinase 2 Regulates Endothelial Development and Function through the Bmk1/Erk5 Pathway. Mol Cell Biol. 2015;35(23):3990-4005. Epub 2015/09/24. doi: 10.1128/MCB.00630-15. PubMed PMID: 26391956; PMCID: PMC4628059.

67. Kosoff R, Chow HY, Radu M, Chernoff J. Pak2 kinase restrains mast cell FcepsilonRI receptor signaling through modulation of Rho protein guanine nucleotide exchange factor (GEF) activity. J Biol Chem. 2013;288(2):974-83.

Epub 2012/12/04. doi: 10.1074/jbc.M112.422295. PubMed PMID: 23204526; PMCID: PMC3543047.

68. Karpov AS, Amiri P, Bellamacina C, Bellance MH, Breitenstein W, Daniel D, Denay R, Fabbro D, Fernandez C, Galuba I, Guerro-Lagasse S, Gutmann S, Hinh L, Jahnke W, Klopp J, Lai A, Lindvall MK, Ma S, Mobitz H, Pecchi S, Rummel G, Shoemaker K, Trappe J, Voliva C, Cowan-Jacob SW, Marzinzik AL. Optimization of a Dibenzodiazepine Hit to a Potent and Selective Allosteric PAK1 Inhibitor. ACS Med Chem Lett. 2015;6(7):776-81. Epub 2015/07/21. doi: 10.1021/acsmedchemlett.5b00102. PubMed PMID: 26191365; PMCID: PMC4499825.

69. Griffin CE, 3rd, Kaye AM, Bueno FR, Kaye AD. Benzodiazepine pharmacology and central nervous system-mediated effects. Ochsner J. 2013;13(2):214-23. Epub 2013/06/22. PubMed PMID: 23789008; PMCID: PMC3684331.

70. Mizuno K, Katoh M, Okumura H, Nakagawa N, Negishi T, Hashizume T, Nakajima M, Yokoi T. Metabolic activation of benzodiazepines by CYP3A4. Drug Metab Dispos. 2009;37(2):345-51. Epub 2008/11/14. doi: 10.1124/dmd.108.024521. PubMed PMID: 19005028.

71. Hsu A, Granneman GR, Bertz RJ. Ritonavir. Clinical pharmacokinetics and interactions with other anti-HIV agents. Clin Pharmacokinet. 1998;35(4):275-91. Epub 1998/11/13. doi: 10.2165/00003088-199835040-00002. PubMed PMID: 9812178.

72. Nelson DR, Zeldin DC, Hoffman SM, Maltais LJ, Wain HM, Nebert DW. Comparison of cytochrome P450 (CYP) genes from the mouse and human

genomes, including nomenclature recommendations for genes, pseudogenes and alternative-splice variants. Pharmacogenetics. 2004;14(1):1-18. Epub 2004/05/07. PubMed PMID: 15128046.

73. Li Y, Ross-Viola JS, Shay NF, Moore DD, Ricketts ML. Human CYP3A4 and murine Cyp3A11 are regulated by equol and genistein via the pregnane X receptor in a species-specific manner. J Nutr. 2009;139(5):898-904. Epub 2009/03/20. doi: 10.3945/jn.108.103572. PubMed PMID: 19297428; PMCID: PMC2714390.

74. Balani SK, Li P, Nguyen J, Cardoza K, Zeng H, Mu DX, Wu JT, Gan LS, Lee FW. Effective dosing regimen of 1-aminobenzotriazole for inhibition of antipyrine clearance in guinea pigs and mice using serial sampling. Drug Metab Dispos. 2004;32(10):1092-5. Epub 2004/06/26. doi: 10.1124/dmd.104.000349. PubMed PMID: 15217988.

75. Asthagiri AR, Vasquez RA, Butman JA, Wu T, Morgan K, Brewer CC, King K, Zalewski C, Kim HJ, Lonser RR. Mechanisms of hearing loss in neurofibromatosis type 2. PLoS One. 2012;7(9):e46132. Epub 2012/10/11. doi: 10.1371/journal.pone.0046132. PubMed PMID: 23049959; PMCID: PMC3458837.

76. Sen R, Baltimore D. Multiple nuclear factors interact with the immunoglobulin enhancer sequences. Cell. 1986;46(5):705-16. Epub 1986/08/29. PubMed PMID: 3091258.

77. Liu T, Zhang L, Joo D, Sun SC. NF-kappaB signaling in inflammation. Signal Transduct Target Ther. 2017;2. Epub 2017/11/22. doi: 10.1038/sigtrans.2017.23. PubMed PMID: 29158945; PMCID: PMC5661633.

78. Okin D, Medzhitov R. Evolution of inflammatory diseases. Curr Biol. 2012;22(17):R733-40. Epub 2012/09/15. doi: 10.1016/j.cub.2012.07.029. PubMed PMID: 22975004; PMCID: PMC3601794.

79. Zhang Q, Lenardo MJ, Baltimore D. 30 Years of NF-kappaB: A Blossoming of Relevance to Human Pathobiology. Cell. 2017;168(1-2):37-57. Epub 2017/01/14. doi: 10.1016/j.cell.2016.12.012. PubMed PMID: 28086098; PMCID: PMC5268070.

80. Hayden MS, Ghosh S. NF-kappaB, the first quarter-century: remarkable progress and outstanding questions. Genes Dev. 2012;26(3):203-34. Epub 2012/02/04. doi: 10.1101/gad.183434.111. PubMed PMID: 22302935; PMCID: PMC3278889.

81. Napetschnig J, Wu H. Molecular basis of NF-kappaB signaling. Annu Rev Biophys. 2013;42:443-68. Epub 2013/03/19. doi: 10.1146/annurev-biophys-083012-130338. PubMed PMID: 23495970; PMCID: PMC3678348.

82. Pahl HL. Activators and target genes of Rel/NF-kappaB transcription factors. Oncogene. 1999;18(49):6853-66. Epub 1999/12/22. doi: 10.1038/sj.onc.1203239. PubMed PMID: 10602461.

83. Carswell EA, Old LJ, Kassel RL, Green S, Fiore N, Williamson B. An endotoxin-induced serum factor that causes necrosis of tumors. Proc Natl Acad Sci U S A. 1975;72(9):3666-70. Epub 1975/09/01. PubMed PMID: 1103152; PMCID: PMC433057.

84. Podleska LE, Funk K, Umutlu L, Grabellus F, Taeger G, de Groot H. TNF-alpha and melphalan-based isolated limb perfusion: no evidence supporting the early destruction of tumour vasculature. Br J Cancer. 2015;113(4):645-52. Epub 2015/07/15. doi: 10.1038/bjc.2015.246. PubMed PMID: 26171939; PMCID: PMC4647687.

85. van Horssen R, Ten Hagen TL, Eggermont AM. TNF-alpha in cancer treatment: molecular insights, antitumor effects, and clinical utility. Oncologist. 2006;11(4):397-408. Epub 2006/04/15. doi: 10.1634/theoncologist.11-4-397. PubMed PMID: 16614236.

86. Wang X, Lin Y. Tumor necrosis factor and cancer, buddies or foes? Acta Pharmacol Sin. 2008;29(11):1275-1288.Epub 2009/09/01. doi: 10.1111/j.1745-7254.2008.00889.x. PubMed PMID: 18954521; PMCID:PMC2631033.

87. Jing Y, Ma N, Fan T, Wang C, Bu X, Jiang G, Li R, Gao L, Li D, Wu M, Wei L. Tumor necrosis factor alpha promotes tumor growth by inducing vascular endothelial growth factor. Cancer Invest. 2011;29(7):485-93. Epub 2011/07/08. doi: 10.2109/07357907.2011.597812. PubMed PMID: 21740086.

88. Li B, Vincent A, Cates J, Brantley-Sieders DM, Polk DB, Young PP. Low levels of tumor necrosis factor a increase tumor growth by inducing an endothelial phenotype of monocytes recruited to the tumor site. Cancer Res. 2009;69(1):338-348. Epub 2010/01/01. doi: 10.1158/0008-5472.CAN-08-1565. PubMed PMID: 19118019; PMCID: PMC2651676.

89. Terzic J, Grivennikov S, Karin E, Karin M. Inflammation and colon cancer. Gastroenterology. 2010;138(6):2101-14 e5. Epub 2010/04/28. doi: 10.1053/j.gastro.2010.01.058. PubMed PMID: 20420949.

90. Hoesel B, Schmid JA. The complexity of NF-kappaB signaling in inflammation and cancer. Mol Cancer. 2013;12:86. Epub 2013/08/07. doi: 10.1186/1476-4598-12-86. PubMed PMID: 23915189; PMCID: PMC3750319.

91. Gerondakis S, Siebenlist U. Roles of the NF-kappaB pathway in lymphocyte development and function. Cold Spring Harb Perspect Biol. 2010;2(5):a000182. Epub 2010/05/11. doi: 10.1101/cshperspect.a000182. PubMed PMID: 20452952; PMCID: PMC2857169.

92. Park MH, Hong JT. Roles of NF-kappaB in Cancer and Inflammatory Diseases and Their Therapeutic Approaches. Cells. 2016;5(2). Epub 2016/04/05. doi: 10.3390/cells5020015. PubMed PMID: 27043634; PMCID: PMC4931664.

93. Walsby E, Pearce L, Burnett AK, Fegan C, Pepper C. The Hsp90 inhibitor NVP-AUY922-AG inhibits NF-kappaB signaling, overcomes microenvironmental cytoprotection and is highly synergistic with fludarabine in primary CLL cells. Oncotarget. 2012;3(5):525-34. Epub 2012/05/24. doi: 10.18632/oncotarget.491. PubMed PMID: 22619113; PMCID: PMC3388182.

94. Buontempo F, Chiarini F, Bressanin D, Tabellini G, Melchionda F, Pession A, Fini M, Neri LM, McCubrey JA, Martelli AM. Activity of the selective IkappaB kinase inhibitor BMS-345541 against T-cell acute lymphoblastic leukemia: involvement of FOXO3a. Cell Cycle. 2012;11(13):2467-75. Epub 2012/06/21. doi: 10.4161/cc.20859. PubMed PMID: 22713244.

95. Gupta SC, Sundaram C, Reuter S, Aggarwal BB. Inhibiting NF-kappaB activation by small molecules as a therapeutic strategy. Biochim Biophys Acta. 2010;1799(10-12):775-87. Epub 2010/05/25. doi: 10.1016/j.bbagrm.2010.05.004. PubMed PMID: 20493977; PMCID: PMC2955987.

96. Gehlhausen JR, Hawley E, Wahle BM, He Y, Edwards D, Rhodes SD, Lajiness JD, Staser K, Chen S, Yang X, Yuan J, Li X, Jiang L, Smith A, Bessler W, Sandusky G, Stemmer-Rachamimov A, Stuhlmiller TJ, Angus SP, Johnson GL, Nalepa G, Yates CW, Wade Clapp D, Park SJ. A proteasome-resistant fragment of NIK mediates oncogenic NF-kappaB signaling in schwannomas. Hum Mol Genet. 2018. Epub 2018/10/20. doi: 10.1093/hmg/ddy361. PubMed PMID: 30335132.

97. Kim JY, Kim H, Jeun SS, Rha SJ, Kim YH, Ko YJ, Won J, Lee KH, Rha HK, Wang YP. Inhibition of NF-kappaB activation by merlin. Biochem Biophys Res Commun. 2002;296(5):1295-302. Epub 2002/09/05. PubMed PMID: 12207915.

98. Foryst-Ludwig A, Naumann M. p21-activated kinase 1 activates the nuclear factor kappa B (NF-kappa B)-inducing kinase-Ikappa B kinases NF-kappa B pathway and proinflammatory cytokines in Helicobacter pylori infection. J Biol Chem. 2000;275(50):39779-85. Epub 2000/10/04. doi: 10.1074/jbc.M007617200. PubMed PMID: 11016939.

99. Rosebeck S, Madden L, Jin X, Gu S, Apel IJ, Appert A, Hamoudi RA, Noels H, Sagaert X, Van Loo P, Baens M, Du MQ, Lucas PC, McAllister-Lucas LM. Cleavage of NIK by the API2-MALT1 fusion oncoprotein leads to noncanonical

NF-kappaB activation. Science. 2011;331(6016):468-72. Epub 2011/01/29. doi: 10.1126/science.1198946. PubMed PMID: 21273489; PMCID: PMC3124150.

100. Takeda K, Takeuchi O, Tsujimura T, Itami S, Adachi O, Kawai T, Sanjo H, Yoshikawa K, Terada N, Akira S. Limb and skin abnormalities in mice lacking IKKalpha. Science. 1999;284(5412):313-6. Epub 1999/04/09. PubMed PMID: 10195895.

101. Li ZW, Chu W, Hu Y, Delhase M, Deerinck T, Ellisman M, Johnson R, Karin M. The IKKbeta subunit of IkappaB kinase (IKK) is essential for nuclear factor kappaB activation and prevention of apoptosis. J Exp Med. 1999;189(11):1839-45. Epub 1999/06/08. PubMed PMID: 10359587; PMCID: PMC2193082.

102. Schmidt-Supprian M, Bloch W, Courtois G, Addicks K, Israel A, Rajewsky K, Pasparakis M. NEMO/IKK gamma-deficient mice model incontinentia pigmenti. Mol Cell. 2000;5(6):981-92. Epub 2000/07/27. PubMed PMID: 10911992.

103. Yin L, Wu L, Wesche H, Arthur CD, White JM, Goeddel DV, Schreiber RD. Defective lymphotoxin-beta receptor-induced NF-kappaB transcriptional activity in NIK-deficient mice. Science. 2001;291(5511):2162-5. Epub 2001/03/17. doi: 10.1126/science.1058453. PubMed PMID: 11251123.

104. Willmann KL, Klaver S, Dogu F, Santos-Valente E, Garncarz W, Bilic I, Mace E, Salzer E, Conde CD, Sic H, Majek P, Banerjee PP, Vladimer GI, Haskologlu S, Bolkent MG, Kupesiz A, Condino-Neto A, Colinge J, Superti-Furga G, Pickl WF, van Zelm MC, Eibel H, Orange JS, Ikinciogullari A, Boztug K. Biallelic loss-of-function mutation in NIK causes a primary immunodeficiency with multifaceted

aberrant lymphoid immunity. Nat Commun. 2014;5:5360. Epub 2014/11/20. doi: 10.1038/ncomms6360. PubMed PMID: 25406581; PMCID: PMC4263125.

105. Castanedo GM, Blaquiere N, Beresini M, Bravo B, Brightbill H, Chen J, Cui HF, Eigenbrot C, Everett C, Feng J, Godemann R, Gogol E, Hymowitz S, Johnson A, Kayagaki N, Kohli PB, Knuppel K, Kraemer J, Kruger S, Loke P, McEwan P, Montalbetti C, Roberts DA, Smith M, Steinbacher S, Sujatha-Bhaskar S, Takahashi R, Wang X, Wu LC, Zhang Y, Staben ST. Structure-Based Design of Tricyclic NF-kappaB Inducing Kinase (NIK) Inhibitors That Have High Selectivity over Phosphoinositide-3-kinase (PI3K). J Med Chem. 2017;60(2):627-40. Epub 2016/12/23. doi: 10.1021/acs.jmedchem.6b01363. PubMed PMID: 28005357.

106. Brightbill HD, Suto E, Blaquiere N, Ramamoorthi N, Sujatha-Bhaskar S, Gogol EB, Castanedo GM, Jackson BT, Kwon YC, Haller S, Lesch J, Bents K, Everett C, Kohli PB, Linge S, Christian L, Barrett K, Jaochico A, Berezhkovskiy LM, Fan PW, Modrusan Z, Veliz K, Townsend MJ, DeVoss J, Johnson AR, Godemann R, Lee WP, Austin CD, McKenzie BS, Hackney JA, Crawford JJ, Staben ST, Alaoui Ismaili MH, Wu LC, Ghilardi N. NF-kappaB inducing kinase is a therapeutic target for systemic lupus erythematosus. Nat Commun. 2018;9(1):179. Epub 2018/01/14. doi: 10.1038/s41467-017-02672-0. PubMed PMID: 29330524; PMCID: PMC5766581.

107. Kandathil CK, Dilwali S, Wu CC, Ibrahimov M, McKenna MJ, Lee H, Stankovic KM. Aspirin intake correlates with halted growth of sporadic vestibular

schwannoma in vivo. Otol Neurotol. 2014;35(2):353-7. Epub 2014/01/23. doi: 10.1097/MAO.0000000000000189. PubMed PMID: 24448296.

108. Kang YJ, Mbonye UR, DeLong CJ, Wada M, Smith WL. Regulation of intracellular cyclooxygenase levels by gene transcription and protein degradation. Prog Lipid Res. 2007;46(2):108-25. Epub 2007/02/24. doi: 10.1016/j.plipres.2007.01.001. PubMed PMID: 17316818; PMCID: PMC3253738.

109. Hong B, Krusche CA, Schwabe K, Friedrich S, Klein R, Krauss JK, Nakamura M. Cyclooxygenase-2 supports tumor proliferation in vestibular schwannomas. Neurosurgery. 2011;68(4):1112-7. Epub 2011/01/12. doi: 10.1227/NEU.0b013e318208f5c7. PubMed PMID: 21221032.

110. Wahle BM, Hawley ET, He Y, Smith AE, Yuan J, Masters AR, Jones DR, Gehlhausen JR, Park SJ, Conway SJ, Clapp DW, Yates CW. Chemopreventative celecoxib fails to prevent schwannoma formation or sensorineural hearing loss in genetically engineered murine model of neurofibromatosis type 2. Oncotarget. 2018;9(1):718-25. Epub 2018/02/09. doi: 10.18632/oncotarget.22002. PubMed PMID: 29416648; PMCID: PMC5787503.

111. Ling L, Cao Z, Goeddel DV. NF-kappaB-inducing kinase activates IKK-alpha by phosphorylation of Ser-176. Proc Natl Acad Sci U S A. 1998;95(7):3792-7. Epub 1998/05/09. PubMed PMID: 9520446; PMCID: PMC19916.

112. Zarnegar B, Yamazaki S, He JQ, Cheng G. Control of canonical NF-kappaB activation through the NIK-IKK complex pathway. Proc Natl Acad Sci U S A.

2008;105(9):3503-8. Epub 2008/02/23. doi: 10.1073/pnas.0707959105. PubMed PMID: 18292232; PMCID: PMC2265190.

113. O'Mahony A, Lin X, Geleziunas R, Greene WC. Activation of the heterodimeric IkappaB kinase alpha (IKKalpha)-IKKbeta complex is directional: IKKalpha regulates IKKbeta under both basal and stimulated conditions. Mol Cell Biol. 2000;20(4):1170-8. Epub 2000/01/29. PubMed PMID: 10648602; PMCID: PMC85235.

114. Chin MP, Bakris GL, Block GA, Chertow GM, Goldsberry A, Inker LA, Heerspink HJL, O'Grady M, Pergola PE, Wanner C, Warnock DG, Meyer CJ. Bardoxolone Methyl Improves Kidney Function in Patients with Chronic Kidney Disease Stage 4 and Type 2 Diabetes: Post-Hoc Analyses from Bardoxolone Methyl Evaluation in Patients with Chronic Kidney Disease and Type 2 Diabetes Study. Am J Nephrol. 2018;47(1):40-7. Epub 2018/02/07. doi: 10.1159/000486398. PubMed PMID: 29402767; PMCID: PMC5841134.

115. Hong DS, Kurzrock R, Supko JG, He X, Naing A, Wheler J, Lawrence D, Eder JP, Meyer CJ, Ferguson DA, Mier J, Konopleva M, Konoplev S, Andreeff M, Kufe D, Lazarus H, Shapiro GI, Dezube BJ. A phase I first-in-human trial of bardoxolone methyl in patients with advanced solid tumors and lymphomas. Clin Cancer Res. 2012;18(12):3396-406. Epub 2012/05/29. doi: 10.1158/1078-0432.CCR-11-2703. PubMed PMID: 22634319; PMCID: PMC4494099.

116. Waelchli R, Bollbuck B, Bruns C, Buhl T, Eder J, Feifel R, Hersperger R, Janser P, Revesz L, Zerwes HG, Schlapbach A. Design and preparation of 2-benzamido-

pyrimidines as inhibitors of IKK. Bioorg Med Chem Lett. 2006;16(1):108-12. Epub 2005/10/21. doi: 10.1016/j.bmcl.2005.09.035. PubMed PMID: 16236504.

117. Ai Y, Kang F, Huang Z, Xue X, Lai Y, Peng S, Tian J, Zhang Y. Synthesis of CDDO-amino acid-nitric oxide donor trihybrids as potential antitumor agents against both drug-sensitive and drug-resistant colon cancer. J Med Chem. 2015;58(5):2452-64. Epub 2015/02/13. doi: 10.1021/jm5019302. PubMed PMID: 25675144.

118. Tse AK, Chen YJ, Fu XQ, Su T, Li T, Guo H, Zhu PL, Kwan HY, Cheng BC, Cao HH, Lee SK, Fong WF, Yu ZL. Sensitization of melanoma cells to alkylating agent-induced DNA damage and cell death via orchestrating oxidative stress and IKKbeta inhibition. Redox Biol. 2017;11:562-76. Epub 2017/01/21. doi: 10.1016/j.redox.2017.01.010. PubMed PMID: 28107677; PMCID: PMC5247288.

119. Cataldi M, Shah NR, Felt SA, Grdzelishvili VZ. Breaking resistance of pancreatic cancer cells to an attenuated vesicular stomatitis virus through a novel activity of IKK inhibitor TPCA-1. Virology. 2015;485:340-54. Epub 2015/09/04. doi: 10.1016/j.virol.2015.08.003. PubMed PMID: 26331681; PMCID: PMC4619123.

120. Hacker H, Chi L, Rehg JE, Redecke V. NIK prevents the development of hypereosinophilic syndrome-like disease in mice independent of IKKalpha activation. J Immunol. 2012;188(9):4602-10. Epub 2012/04/05. doi: 10.4049/jimmunol.1200021. PubMed PMID: 22474019; PMCID: PMC3532048.

121. Brightbill HD, Jackman JK, Suto E, Kennedy H, Jones C, 3rd, Chalasani S, Lin Z, Tam L, Roose-Girma M, Balazs M, Austin CD, Lee WP, Wu LC. Conditional Deletion of NF-kappaB-Inducing Kinase (NIK) in Adult Mice Disrupts Mature B

Cell Survival and Activation. J Immunol. 2015;195(3):953-64. Epub 2015/06/28. doi: 10.4049/jimmunol.1401514. PubMed PMID: 26116508.

122. Plotkin SR, Merker VL, Halpin C, Jennings D, McKenna MJ, Harris GJ, Barker FG, 2nd. Bevacizumab for progressive vestibular schwannoma in neurofibromatosis type 2: a retrospective review of 31 patients. Otol Neurotol. 2012;33(6):1046-52. Epub 2012/07/19. doi: 10.1097/MAO.0b013e31825e73f5. PubMed PMID: 22805104.

123. Mautner VF, Nguyen R, Kutta H, Fuensterer C, Bokemeyer C, Hagel C, Friedrich RE, Panse J. Bevacizumab induces regression of vestibular schwannomas in patients with neurofibromatosis type 2. Neuro Oncol. 2010;12(1):14-8. Epub 2010/02/13. doi: 10.1093/neuonc/nop010. PubMed PMID: 20150363; PMCID: PMC2940556.

124. Eminowicz GK, Raman R, Conibear J, Plowman PN. Bevacizumab treatment for vestibular schwannomas in neurofibromatosis type two: report of two cases, including responses after prior gamma knife and vascular endothelial growth factor inhibition therapy. J Laryngol Otol. 2012;126(1):79-82. Epub 2011/10/19. doi: 10.1017/S0022215111002805. PubMed PMID: 22004800.

125. London NR, Gurgel RK. The role of vascular endothelial growth factor and vascular stability in diseases of the ear. Laryngoscope. 2014;124(8):E340-6. Epub 2013/12/19. doi: 10.1002/lary.24564. PubMed PMID: 24347479.

126. Cogswell JP, Godlevski MM, Wisely GB, Clay WC, Leesnitzer LM, Ways JP, Gray JG. NF-kappa B regulates IL-1 beta transcription through a consensus NF-

kappa B binding site and a nonconsensus CRE-like site. J Immunol. 1994;153(2):712-23. Epub 1994/07/15. PubMed PMID: 8021507.

127. Vambutas A, Lesser M, Mullooly V, Pathak S, Zahtz G, Rosen L, Goldofsky E. Early efficacy trial of anakinra in corticosteroid-resistant autoimmune inner ear disease. J Clin Invest. 2014;124(9):4115-22. Epub 2014/08/19. doi: 10.1172/JCI76503. PubMed PMID: 25133431; PMCID: PMC4160092.

128. Dinarello CA. Why not treat human cancer with interleukin-1 blockade? Cancer Metastasis Rev. 2010;29(2):317-29. Epub 2010/04/28. doi: 10.1007/s10555-010-9229-0. PubMed PMID: 20422276; PMCID: PMC2865633.

129. Fleischmann RM, Tesser J, Schiff MH, Schechtman J, Burmester GR, Bennett R, Modafferi D, Zhou L, Bell D, Appleton B. Safety of extended treatment with anakinra in patients with rheumatoid arthritis. Ann Rheum Dis. 2006;65(8):1006-12. Epub 2006/01/07. doi: 10.1136/ard.2005.048371. PubMed PMID: 16396977; PMCID: PMC1798263.

130. Sonnenberg-Riethmacher E, Miehe M, Riethmacher D. Promotion of periostin expression contributes to the migration of Schwann cells. J Cell Sci. 2015;128(17):3345-55. Epub 2015/07/19. doi: 10.1242/jcs.174177. PubMed PMID: 26187852.

131. Kim DW, Tiseo M, Ahn MJ, Reckamp KL, Hansen KH, Kim SW, Huber RM, West HL, Groen HJM, Hochmair MJ, Leighl NB, Gettinger SN, Langer CJ, Paz-Ares Rodriguez LG, Smit EF, Kim ES, Reichmann W, Haluska FG, Kerstein D, Camidge DR. Brigatinib in Patients With Crizotinib-Refractory Anaplastic Lymphoma Kinase-Positive Non-Small-Cell Lung Cancer: A Randomized,

Multicenter Phase II Trial. J Clin Oncol. 2017;35(22):2490-8. Epub 2017/05/06. doi: 10.1200/JCO.2016.71.5904. PubMed PMID: 28475456.

132. Chang F, Lemmon CA, Park D, Romer LH. FAK potentiates Rac1 activation and localization to matrix adhesion sites: a role for betaPIX. Mol Biol Cell. 2007;18(1):253-64. Epub 2006/11/10. doi: 10.1091/mbc.e06-03-0207. PubMed PMID: 17093062; PMCID: PMC1751318.

133. ten Klooster JP, Jaffer ZM, Chernoff J, Hordijk PL. Targeting and activation of Rac1 are mediated by the exchange factor beta-Pix. J Cell Biol. 2006;172(5):759-69. Epub 2006/02/24. doi: 10.1083/jcb.200509096. PubMed PMID: 16492808; PMCID: PMC2063707.

134. Schwind JV. Cancer: regressive evolution? Preliminary report of a new hypothesis. Oncology. 1974;29(2):172-80. Epub 1974/01/01. doi: 10.1159/000224899. PubMed PMID: 4836678.

135. Sun X, Wang X, Chen T, Li T, Cao K, Lu A, Chen Y, Sun D, Luo J, Fan J, Young W, Ren Y. Myelin activates FAK/Akt/NF-kappaB pathways and provokes CR3-dependent inflammatory response in murine system. PLoS One. 2010;5(2):e9380. Epub 2010/02/27. doi: 10.1371/journal.pone.0009380. PubMed PMID: 20186338; PMCID: PMC2826415.

136. Schulz A, Buttner R, Hagel C, Baader SL, Kluwe L, Salamon J, Mautner VF, Mindos T, Parkinson DB, Gehlhausen JR, Clapp DW, Morrison H. The importance of nerve microenvironment for schwannoma development. Acta Neuropathol. 2016;132(2):289-307. Epub 2016/05/30. doi: 10.1007/s00401-016-1583-8. PubMed PMID: 27236462; PMCID: PMC4947119.

137. Sabari JK, Santini FC, Schram AM, Bergagnini I, Chen R, Mrad C, Lai WV, Arbour KC, Drilon A. The activity, safety, and evolving role of brigatinib in patients with ALK-rearranged non-small cell lung cancers. Onco Targets Ther. 2017;10:1983-92. Epub 2017/04/25. doi: 10.2147/OTT.S109295. PubMed PMID: 28435288; PMCID: PMC5388194.

CURRICULUM VITAE

Eric Thomas Hawley

Education

2013-present: MSTP (MD/PhD) Student, Indiana University School of Medicine, Indianapolis, IN

2015-2019: Ph.D., Biochemistry and Molecular Biology, Indiana University, Indianapolis, IN

2007-2011: B.A. Biology, DePauw University, Greencastle, IN

Academic and Professional Honors

2017: 3rd Place for Best Poster at IUSCC Cancer Day

2017: Jack David Award Winner for best seminar by a graduate student, IUSM Biochemistry Department

2017: Honorable Mention in Annual Biochemistry Research Day Poster Competition, IUSM Biochemistry Department

2012: Outstanding Post-Bacc presentation, NIH

2008-2009: Academic all- American, NCAA

2007-2011: Presidential Scholarship, DePauw University

Research Experience

2015-2019: Graduate student, Lab of Dr. Wade Clapp, Dept. of Biochemistry, Indiana University School of Medicine, Indianapolis, IN.

2011-2013: IRTA Post-Bacc, Lab of Dr. Richard Siegel, NIAMS, NIH, Bethesda, MD.

2011: Undergraduate researcher, Lab of Dr. John Stegeman, Woods Hole Oceanographic Institute, Woods Hole, MA

2010: Undergraduate researcher, Lab of Dr. David Roos, University of Pennsylvania, Philadelphia, PA.

2009: REU Fellow, Lab of Dr. Kristin Hager, University of Notre Dame, South Bend, IN

2008: Undergraduate researcher, Lab of Dr. Henning Schneider, DePauw University, Greencastle, IN.

Clinical Experience

2016-Present: Volunteer, Good Samaritan Health Clinic, Indianapolis, IN

2013-2016: Volunteer, IUSM Student Outreach Clinic, Indianapolis, IN

2009: EMT-B, Care Ambulance Service, Indianapolis, IN

Positions and Employment

2015-2016: Internal Medicine SIG Research Chair, IUSM

2014-2016: Student Research Committee Student Representative, IUSM Deans Committee

2014-2015: Internal Medicine SIG Recruitment Chair, IUSM

Professional Societies

2018-Present: Associate Member, American Association of Cancer Research

2013-Present: Member, American Physician Scientists Association

2013-Present: Student member, American College of Physicians

Training Grants and Fellowships

2018-Present: NIH/NIDCD NRSA F31 5F31DC016528-02

2016-2017: IU Simon Cancer Center Cancer Biology Training Program Fellowship

2014-2016: NIH/NIGMS, T31 5T32GM077229-05, (PI: Dr. Raghu Mirmira)

2011-2013: Postbac IRTA, NIH/NIAMS

2007-2011: Science Research Fellowship, DePauw University

2011: Woods Hole Summer Student Fellowship

2009: NIH REU Fellowship

First Author Posters

1. Genetic Ablation of Pak1 Extends the Lifespan and Reduces the Size of Tumor Bearing Tissue in a Genetically Engineered Mouse Model of Neurofibromatosis Type 2 (NF2). Hawley ET, Park SJ, Lang L, Chernoff J, Clapp DW. Joint Global Neurofibromatosis Conference. Paris France (November 2018).
2. Genetic Ablation of Pak1 Extends the Lifespan and Reduces the Size of Tumor Bearing Tissue in a Genetically Engineered Mouse Model of Neurofibromatosis Type 2 (NF2). Hawley ET, Park SJ, Lang L, Chernoff J, Clapp DW. Biochemistry Research Day. Indianapolis, IN (October 2018).
3. PAK1 Inhibition Reduces Tumor Size and Extends the Lifespan of Animals in a Genetically Engineered Mouse Model of Neurofibromatosis Type 2 (NF2). Hawley ET, Park SJ, Bessler W, Masters A, Lang L, Gehlhausen J, Burks C, Paini C, Jones D, Clapp DW. IUSCC Cancer Research Day. Indianapolis, IN (May 2018).
4. Targeting NF-kB Signaling in Neurofibromatosis Type 2 (NF2). Hawley ET, Gehlhausen J, Wahle B, He Y, Clapp DW. Biochemistry Research Day. Indianapolis, IN (October 2017).
5. NF-kB Inducing Kinase- A Novel Driver of Schwann Cell Transformation in Neurofibromatosis Type 2. Hawley ET, Gehlhausen J, Wahle B, He Y, Park SJ, Clapp DW. IUSCC Cancer Research Day. Indianapolis, IN (May 2017).

6. NF-kB Inducing Kinase- A Novel Driver of Schwann Cell Transformation in Neurofibromatosis Type 2. Hawley ET, Wahle B, Gehlhausen J, He Y, Clapp DW. IUSCC Cancer Research Day. Indianapolis, IN (May 2016).
7. The TL1A-IL13 Axis: A Novel Pathway for Type 2 Immunity Mediated Independently of Commensal Flora and Nematode Infection. Hawley ET, Meylan F, Barron L, Richard AC, Bradley N, Barlow J, Paul WE, McKenzie A, Wynn T, and Siegel RM. NIH Spring Research Festival. Bethesda, MD (April 2012).
8. The TL1A-IL13 Axis: A Novel Pathway for Type 2 Immunity Mediated Independently of Commensal Flora and Nematode Infection. Hawley ET, Meylan F, Barron L, Richard AC, Bradley N, Barlow J, Paul WE, McKenzie A, Wynn T, and Siegel RM. Keystone Biology of Cytokines. Keystone, CO (February 2012).
9. Computational Approaches to Virulence and Ligand Identification in Apicomplexans. Hawley ET, Tripathi A, Emrich S, and Hager KM. Molecular Parasitology Meeting. Woods Hole, MA (September 2009).

Oral Presentations

1. Small Molecule to Mouse and Back: Targeting PAK1 in Neurofibromatosis Type 2. Biochemistry Student Seminar Series. Indianapolis, IN (October 2018).

2. Connecting NF-kB Signaling to Loss of Merlin in Neurofibromatosis Type 2. Biochemistry Student Seminar Series. Indianapolis, IN (January 2017).
3. A Novel Approach to Treating Sensorineural Hearing Loss in Neurofibromatosis Type 2. Biochemistry Student Seminar Series. Indianapolis, IN (November 2017).
4. NF-kB Signaling Drives Oncogenic Transformation in a Murine Model of Neurofibromatosis Type 2. Biochemistry Student Seminar Series. Indianapolis, IN (February 2016).
5. The TNF Family Cytokine TL1A in Disease: An Investigation into the role of TL1A in Autoinflammatory Disease. NIAMS Branch Meeting, Bethesda MD. (April 2013).

Publications

1. Gehlhausen JR, Hawley E, Wahle BM, He Y, Edwards D, Rhodes SD, Lajiness JD, Staser K, Chen S, Yang X, Yuan J, Li X, Jiang L, Smith A, Bessler W, Sandusky G, Stemmer-Rachamimov A, Stuhlmiller TJ, Angus SP, Johnson GL, Nalepa G, Yates CW, Wade Clapp D, Park SJ. A proteasome-resistant fragment of NIK mediates oncogenic NF-kappaB signaling in schwannomas. Hum Mol Genet. 2018. Epub 2018/10/20. doi: 10.1093/hmg/ddy361. PubMed PMID: 30335132.
2. Wahle BM, Hawley ET, He Y, Smith AE, Yuan J, Masters AR, Jones DR, Gehlhausen JR, Park SJ, Conway SJ, Clapp DW, Yates CW.

Chemopreventative celecoxib fails to prevent schwannoma formation or sensorineural hearing loss in genetically engineered murine model of neurofibromatosis type 2. Oncotarget. 2018;9(1):718-25. Epub 2018/02/09. doi: 10.18632/oncotarget.22002. PubMed PMID: 29416648; PMCID: PMC5787503.

3. Richard AC, Peters JE, Savinykh N, Lee JC, Hawley ET, Meylan F, Siegel RM, Lyons PA, Smith KGC. Reduced monocyte and macrophage TNFSF15/TL1A expression is associated with susceptibility to inflammatory bowel disease. PLoS Genet. 2018;14(9):e1007458. Epub 2018/09/11. doi: 10.1371/journal.pgen.1007458. PubMed PMID: 30199539; PMCID: PMC6130856 "Antibodies that bind to TL1A and methods of treating inflammatory or autoimmune disease comprising administering such antibodies.".

4. Richard AC, Tan C, Hawley ET, Gomez-Rodriguez J, Goswami R, Yang XP, Cruz AC, Penumetcha P, Hayes ET, Pelletier M, Gabay O, Walsh M, Ferdinand JR, Keane-Myers A, Choi Y, O'Shea JJ, Al-Shamkhani A, Kaplan MH, Gery I, Siegel RM, Meylan F. The TNF-family ligand TL1A and its receptor DR3 promote T cell-mediated allergic immunopathology by enhancing differentiation and pathogenicity of IL-9-producing T cells. J Immunol. 2015;194(8):3567-82. Epub 2015/03/20. doi: 10.4049/jimmunol.1401220. PubMed PMID: 25786692; PMCID: PMC5112176.

5. Meylan F, Hawley ET, Barron L, Barlow JL, Penumetcha P, Pelletier M, Sciume G, Richard AC, Hayes ET, Gomez-Rodriguez J, Chen X, Paul WE, Wynn TA, McKenzie AN, Siegel RM. The TNF-family cytokine TL1A promotes allergic immunopathology through group 2 innate lymphoid cells. Mucosal Immunol. 2014;7(4):958-68. Epub 2013/12/26. doi: 10.1038/mi.2013.114. PubMed PMID: 24368564; PMCID: PMC4165592.

6. Schneider H, Fritzky L, Williams J, Heumann C, Yochum M, Pattar K, Noppert G, Mock V, Hawley E. Cloning and expression of a zebrafish 5-HT(2C) receptor gene. Gene. 2012;502(2):108-17. Epub 2012/04/24. doi: 10.1016/j.gene.2012.03.070. PubMed PMID: 22521866.